THE HYPERSONIC LAMINAR BOUNDARY LAYER NEAR A SHARP EXPANSION CORNER

Thesis by

Keith Jordis Victoria

In Partial Fulfillment of the Requirements

For the Degree of

Doctor of Philosophy

California Institute of Technology

Pasadena, California

1969

(Submitted May 29, 1969)

ACKNOWLEDGMENTS

My education at the California Institute of Technology has been made possible through the efforts of many individuals who have contributed in both a personal and a technical way. To all of these I wish to express my sincere gratitude.

I feel a deep sense of gratitude to Professor Toshi Kubota who, through his broad understanding and continued guidance, contributed significantly to the completion of this research. I also want to express my appreciation to Professor Lester Lees whose interest, guidance and personal encouragement have been invaluable to me through the course of my graduate education.

Special appreciation and thanks are also due to Mrs. Truus Van Harreveld for her unrelenting care in the reduction of the experimental data and the preparation of many of the figures; to Mrs. Virginia Conner for her patience and skill in the typing of this manuscript; to the staff of the GALCIT Hypersonic Wind Tunnel, P. Baloga, S. Roman, G. Van Halewyn, J. Van Dijk and H. Mazurowski for their able assistance in conducting the wind tunnel tests; and to the staff of the Aeronautics Shop, particularly G. Carlson and H. McDonald for their skill in the construction of the experimental equipment.

I wish to acknowledge, with much appreciation, the financial support provided me by the California Institute of Technology throughout my graduate education, by the National Aeronautics and Space Administration for the years 1964-1967 and by the Rand Corporation for the academic year 1967-1968. This investigation was carried out under the sponsorship and with the financial support of the U. S. Army

Research Office and the Advanced Research Projects Agency under Contract No. DA-31-124-ARO(D)-33.

Finally, I would like to acknowledge the encouragement given to me by all of my family. To my wife Barbara and to my children Karin and Jonathan in particular, thank you for your sacrifices and devotion throughout the completion of this work.

ABSTRACT

The integral moment method for treating interactions between a laminar boundary layer and an external supersonic flow is applied to the problem of the hypersonic laminar boundary layer near sharp and slightly rounded convex (expansion) corners. The general features of this type of interacting flow are established by an analytical solution of the integral equations using the method of matched asymptotic expansions for the case of small interaction parameter. Numerical solutions are obtained for flows for which the interaction parameter can no longer be considered small.

An experimental study is carried out in the GALCIT Mach 8 hypersonic wind tunnel in order to study the two-dimensional laminar boundary layer expansion. Major emphasis is placed on the acquisition of detailed data near the corner region. The basic measurements consist of the model surface pressure distribution and pitot pressure surveys of the boundary layer and inviscid flow field between the boundary layer and the leading edge shock wave both upstream and downstream of the corner region. The surface pressure measurements illustrate the striking departure of the flow field at hypersonic speeds from the classical Prandtl-Meyer description.

These data with appropriate assumptions made regarding the static pressure and temperature fields at points away from the model surface allow calculation of the distributions of profile functions defined in the integral moment method formulation. These distributions along with the surface pressure distribution are compared directly with solutions of the moment equations.

TABLE OF CONTENTS

TABLE OF CONTENTS (Continued)

LIST OF TABLES

LIST OF FIGURES

LIST OF FIGURES (Continued)

LIST OF SYMBOLS

a	velocity profile parameter; also speed of sound
a_1, a_2	integration constants
$A_1 - A_3$	functions defined in Eqs. (26) & (47)
$b_1 - b_3$	functions defined in Eqs. (47)
$B_1 - B_3$	functions defined in Eqs. (47)
c_v, c_p	specific heats at constant volume and constant pressure
C	$\left(\frac{\mu}{\mu_\infty}\right)\Big/\left(\frac{T}{T_\infty}\right)$, Chapman-Rubesin factor
C_B	$\delta_B J_B$
$C_1 - C_4$	integration constants
$d_1 - d_3$	functions defined in Eqs. (47)
$\tilde{D}$	determinant of system of equations, Eq. (28)
f	function defined in Eqs. (10); also quantity related to stream function in Falkner-Skan equation
F	$\mathcal{H} + \frac{1+m_e}{m_e}$
h_1	constant defined in Eqs. (19)
H	$\frac{1}{2}u^2 + c_p T$, total enthalpy
$\mathcal{H}$ or $\mathcal{H}$	$\frac{\theta_i}{\delta_i^*}$
$\mathcal{H}^*$ or $\mathcal{H}^*$	relaxation region variables
$\mathcal{H}_B$	constant defined in Eqs. (19)
$\mathcal{H}_p$	defined by $\frac{1}{\alpha} = \exp\left\{\int_{\mathcal{H}_B}^{\mathcal{H}_p} \frac{A_1(\mathcal{H})}{A_2(\mathcal{H})}\, d\mathcal{H}\right\}$
J	$\frac{\theta_i^*}{\delta_i^*}$
k	thermal conductivity

LIST OF SYMBOLS (Continued)

K_1-K_3	integration constants; also constants defined in Table II
L	distance from leading edge to corner
m	$\frac{\gamma-1}{2} M^2$
m_1	constant defined in Eqs. (19)
M	Mach number
$\tilde{M}$	$\frac{M_e}{M_\infty}$, inner region variable
M^*	$\epsilon M^* = 1-\alpha \tilde{M}$, relaxation region variable
N_2, N_3	functions defined by $N_n = \frac{A_n(\mathscr{K})}{A_1(\mathscr{K})} + \frac{B_n(\mathscr{K})}{B_1(\mathscr{K})}$
p	static pressure
p_∞ or $p_{-\infty}$	inviscid pressure upstream of corner
$p_{+\infty}$	inviscid pressure downstream of corner
p_{Ic}	weak interaction pressure at corner location based on flow conditions upstream of corner
$p_I(-)$	weak interaction pressure based on flow conditions upstream of corner
$p_I(+)$	weak interaction pressure based on flow conditions downstream of corner
p_p	pitot pressure
p_t	tunnel free stream total pressure
P	$\frac{\delta_i^*}{U_e}\left(\frac{\partial U}{\partial Y}\right)_{Y=0}$
P_N	$\frac{[p-p_I(+)]}{[p_I(-)-p_I(+)]}$
Pr	$\frac{\mu c_p}{k}$, Prandtl number

LIST OF SYMBOLS (Continued)

q	heat transfer
$\tilde{Q}_1$-$\tilde{Q}_3$	quadratures defined in Table II
Q_1^*, Q_2^*	quadratures defined in Table II
r	$\frac{1}{m_\infty}$
R	$\frac{2\delta_i^*}{U_e^2}\int_0^{\delta_i}\left(\frac{\partial U}{\partial Y}\right)^2 dY$
R_c	corner radius of curvature
Re	tunnel free stream unit Reynolds number (per inch)
Re_{L_∞}	Reynolds number based on approach plate length and flow conditions upstream of corner
s	distance along surface from corner
T	static temperature
T_t	tunnel free stream total temperature
u, v	velocity components parallel and normal to surface
U	Stewartson's transformed velocity component
x	distance along surface from leading edge
$\bar{x}$	$\frac{x}{L}$
$\tilde{x}$	$\frac{(\bar{x}-1)}{\epsilon}$, inner region variable
x^*	$\bar{x}-1$, relaxation region variable
X, Y	Stewartson's transformed coordinates
y	distance normal to surface
Z	$\frac{1}{\delta_i^*}\int_0^{\delta_i}\frac{U}{U_e}dY$

LIST OF SYMBOLS (Continued)

α	$1 - \frac{\gamma-1}{2} M_\infty \alpha_w$
α_w	inclination of local tangent to surface, measured positive for an expansion turn
β	Falkner-Skan pressure gradient parameter; also $\frac{a_e}{a_\infty} \frac{p_e}{p_\infty}$
γ	$\frac{c_p}{c_v}$, ratio of specific heats
δ	boundary layer thickness
δ_1	constant defined in Eqs. (19)
δ_B	constant defined in Eqs. (19)
δ_i	transformed boundary layer thickness
δ_p	$\frac{C_B \alpha^3}{J_p}$
$\tilde{\delta}$	$\frac{\delta_i^*}{L} \sqrt{\frac{Re_{L_\infty}}{C}}$, inner region variable
δ^*	$\int_0^\delta \left(1 - \frac{\rho u}{\rho_e u_e}\right) dy$, boundary layer displacement thickness; also relaxation region variable
δ_u	$\int_0^\delta \left(1 - \frac{u}{u_e}\right) dy$, velocity thickness
δ_i^*	$\int_0^{\delta_i} \left(1 - \frac{U}{U_e}\right) dY$, transformed displacement thickness
ϵ	$\left(\frac{\gamma-1}{2}\right)^2 \bar{\chi}_\infty$, perturbation parameter
η	Falkner-Skan variable
θ	$\int_0^\delta \frac{\rho u}{\rho_e u_e} \left(1 - \frac{u}{u_e}\right) dy$, boundary layer momentum thickness
θ_i	$\int_0^{\delta_i} \frac{U}{U_e} \left(1 - \frac{U}{U_e}\right) dY$, transformed momentum thickness

LIST OF SYMBOLS (Continued)

θ^*	$\int_0^{\delta_i} \frac{\rho u}{\rho_e u_e}\left(1 - \frac{u^2}{u_e^2}\right)dy$, mechanical energy thickness
θ_i^*	$\int_0^{\delta_i} \frac{U}{U_e}\left(1 - \frac{U^2}{U_e^2}\right)dY$, transformed mechanical energy thickness
Θ	$\tan^{-1}\frac{v_e}{u_e}$, local angle between external streamline at $y = \delta$ and the x-axis
λ	$\frac{4\gamma-2}{\gamma-1}$
μ	viscosity coefficient
ν	$\frac{\mu}{\rho}$, kinematic viscosity; also Prandtl-Meyer angle, Eq. (15)
ρ	gas density
$\overline{\chi}_\infty$	$\frac{M_\infty^3\sqrt{C}}{\sqrt{Re_{L_\infty}}}$, hypersonic viscous interaction parameter

Subscripts

$(\ )_B$	Blasius point
$(\ )_c$	critical
$(\ )_{comp.}$	composite
$(\ )_e$	local external
$(\ )_i$	transformed, incompressible
$(\ )_p$	evaluated at maximum value of χ_0
$(\ )_t$	tunnel free stream total
$(\ )_w$	wall, surface
$(\ )_0$	zeroth order perturbation quantity
$(\ )_1$	first order perturbation quantity

LIST OF SYMBOLS (Continued)

$( )_2$	second order perturbation quantity
$( )_\infty$	free stream conditions upstream of corner
$( )_{-\infty}$	free stream conditions upstream of corner
$( )_{+\infty}$	free stream conditions downstream of corner

Superscripts

$(\tilde{\ })$	indicates inner region variable
$( )^*$	indicates relaxation region variable

I. INTRODUCTION

This study is concerned with the laminar boundary layer in a fluid flowing at supersonic or hypersonic speeds over a sharp expansion corner. Interaction between the viscous boundary layer and the high speed inviscid outer flow and the subsequent requirement for a simultaneous solution of the coupled flow fields is always present to some extent. The degree to which it is present depends strongly on the Mach number and to a lesser extent on the Reynolds number of the developing flow. The presence of a local disturbance, in this case an expansion corner, can amplify the effect of the interaction by producing rapid flow changes in the vicinity of the corner. In the purely inviscid limit the flow is accelerated by an expansion fan centered at the corner and the flow properties downstream of the corner can be calculated with use of the classical Prandtl-Meyer function. At low supersonic Mach numbers and high Reynolds numbers, this idealization of the flow field is adequate. As the Mach number increases and/or the Reynolds number decreases the boundary layer can thicken significantly and the viscous-inviscid interaction becomes important even in the absence of a local disturbance. Furthermore, since a portion of the fluid in the boundary layer is flowing at subsonic speeds, the effect of the presence of an expansion corner is distributed over a region of finite extent upstream of the corner as well as downstream.

It has been observed experimentally that the extent of the corner interaction region is more limited upstream than downstream of the corner. The existence of a weakly interacting boundary layer

upstream of an expansion corner (and the resulting limited interaction region) does not guarantee weak interaction throughout the expansion. In fact, a strongly interacting boundary layer can be induced downstream of the corner simply by increasing the expansion angle with an attendant increase in Mach number and corresponding decrease in Reynolds number. Hence, the physical length scale for the relaxation of the boundary layer from the corner interaction can be expected to be larger than that for initiation of the interaction. Thus, the effects of viscous-inviscid interaction are amplified by introducing an expansion corner into the flow field and a detailed knowledge of the boundary layer-expansion wave interaction becomes important. Furthermore, the understanding of this problem can be related to other important problems such as the flow over a bluff based body.

Because of its complexity, various idealizations have been made in attacking the problem theoretically. These range from the early consideration of linearized equations to numerical integration of the (nearly) complete Navier-Stokes equations. The early work on a closely related problem, that of the interaction of a mixed (subsonic and supersonic) parallel shear flow and a weak disturbance has been carried out by Howarth,[1] Tsien and Finston,[2] Lighthill,[3, 4] and more recently by Sullivan et al.[5] The expansion of a rotational inviscid supersonic flow has been studied by Pai[6] and Weinbaum.[7, 8] Zakkay[9] uses the concept of an inviscid rotational layer bounded by an inviscid supersonic stream and a viscous sublayer downstream of the corner adjacent to the wall which originates at the corner. The

initial profile downstream of the corner is assumed to be given by an inviscid expansion of the upstream profile. Olsson and Messiter[10] use a similar concept in analyzing the boundary layer expansion upstream of a sharp corner. Integral methods of solution have been studied by Curle,[11, 12] Hunt and Sibulkin,[13] Oosthuizen[14] and Sullivan [15] with various approximations. Baum[16] and Tyson[17] have used finite difference schemes to obtain numerical solutions of the "generalized" boundary layer equations, which include a transverse momentum equation, for this and a related problem. Tyson, in addition, has examined, numerically, solutions of the moment equations of Lees and Reeves[18] for the corner expansion problem. Ko and Kubota[19, 20] have taken advantage of the singular behavior of the moment equations at a sharp expansion corner in the study of the finite plate effect for a compression corner. Klineberg[21] has examined, in detail, the various types of possible viscous-inviscid interactions for the expansion corner.

Experimentally, much less work has been done. Sternberg[22] at BRL and later Zakkay, Tani, Toba and Kuo[23, 24] at PIBAL carried out experiments in supersonic flow around a sharp convex corner using a cone-cylinder. Since they were interested primarily in surface temperatures and heat transfer only a very limited amount of fluid dynamical data was obtained. The viscous interaction was so small for these experiments that little detail of the surface pressure was observed. Murthy and Hammit[25] performed experiments downstream of the corner expansion of a turbulent boundary layer and carried out a characteristics calculation for the rotational supersonic

flow ignoring the subsonic portion of the boundary layer. The above experiments were conducted in the Mach number range 2-4 and hence at relatively low values of the viscous interaction parameter. At GALCIT, Puhl[26] studied the expansion of a laminar boundary layer around a sharp cone-cylinder juncture at Mach number 8. One of the more striking features of this work was a very detailed surface pressure distribution in the vicinity of the corner which well illustrated the strong departure of the distribution from an inviscid calculation.

The present study has a two-fold objective: (1) to gain a clearer understanding of the structure of the laminar flow field for the expansion corner as the viscous interaction parameter $\bar{\chi}_\infty \equiv M_\infty^3 (C/Re_{L_\infty})^{\frac{1}{2}}$ tends away from zero and to isolate the dominant driving mechanisms in the flow regions which result, and (2) to provide a two-dimensional experimental result to further illustrate the importance of the boundary layer-expansion wave interaction at hypersonic flow speeds and yield results which can be directly compared with theory.

The integral or moment equations of Lees and Reeves[18] and Klineberg[21] are chosen for the theoretical part of this study. The motivation for selecting the integral equations stems from the fact that, in spite of the misgivings that one may have regarding the lateral pressure gradients associated with an expanding boundary layer, a direct comparison of numerical solutions of (i) the moment equations[27] and (ii) a more complete representation of the Navier-Stokes equations[17] for a particular configuration indicate that the

lateral pressure gradients are important only in a region close to the corner. The results of this comparison are shown in Fig. 1. Qualitatively, a theory with zero lateral pressure gradients appears to describe the flow field correctly insofar as the pressure distribution is concerned. Furthermore, if the pressure distribution is not prescribed a priori but is obtained from the simultaneous solution of the viscous and inviscid flow fields, a mechanism for the upstream propagation of a disturbance to the boundary layer exists. Hence one may expect that the formulation of the problem of hypersonic corner expansion in a boundary layer framework may yield a representative description of the expansion phenomenon. With this in mind, one can formulate the following problem:

A laminar adiabatic boundary layer is assumed to be weakly interacting with an external hypersonic flow, i. e. the corner disturbance to the boundary layer is assumed to be located sufficiently far from the wall leading edge that the flow properties can be accurately represented by a weak interaction expansion of the integral boundary layer equations.[21,28] This expansion provides an outer solution for the flow entering the interaction region where $\bar{x}$ is the distance from the leading edge normalized with the distance from the leading edge to the corner location L. The problem then is to calculate the flow field which results from turning the boundary layer through an expansion turn defined by α_w.

In Section II, the expansion flow field is separated into regions dominated (i) by inviscid forces, i. e. the pressure gradient, and (ii) by viscous forces, i. e. the shear at the wall and the viscous

dissipation. Appropriate asymptotic solutions of the integral equations are developed for each region from which uniformly valid composite solutions can be constructed. These serve to illustrate the structure of the expansion flow field.

Section III contains the results of the experimental study. Quantities defined by the integral method are calculated from the measurements and the distributions are compared directly with numerical solutions of the integral equations since the range of parameters investigated exceeds the limits for the closed form solutions of Section II to be valid. The comparison between experiment and theory is presented in Section IV.

II. THEORETICAL INVESTIGATION

II. 1. Differential Equations

The geometry of the problem is that shown in Fig. 2; x is the distance from the leading edge and y the distance away from the surface normal to it. If the radius of curvature of the wall is large compared with the viscous layer thickness, the differential equations reduce to the usual boundary layer equations, in which the pressure gradient normal to the wall is neglected. In the neighborhood of a sharp expansion, however, the radius of curvature of a streamline is not large compared with the boundary layer thickness, and consequently the transverse pressure gradient may not be neglected. Nevertheless, the extent of this region is of the order of the boundary layer thickness, and outside this region we may use the boundary layer equations. Thus, for a steady, two-dimensional, compressible boundary layer expansion, the partial differential equations are:

Continuity

$$\frac{\partial(\rho u)}{\partial x} + \frac{\partial(\rho v)}{\partial y} = 0$$

Momentum

$$\rho u \frac{\partial u}{\partial x} + \rho v \frac{\partial u}{\partial y} = - \frac{dp}{dx} + \frac{\partial}{\partial y} \left(\mu \frac{\partial u}{\partial y} \right) \qquad (1)$$

Energy

$$\rho u \frac{\partial H}{\partial x} + \rho v \frac{\partial H}{\partial y} = \frac{\partial}{\partial y} \left(\frac{\mu}{Pr} \frac{\partial H}{\partial y} \right) + \frac{\partial}{\partial y} \left(\frac{Pr-1}{Pr} \mu u \frac{\partial u}{\partial y} \right)$$

$$H = \frac{1}{2} u^2 + c_p T$$

State

$$p = \rho R T \quad \text{(perfect gas)} .$$

The boundary conditions are:

$$u = v = 0, \quad k\frac{\partial T}{\partial y} = q_w \quad (\text{or } T = T_w) \quad \text{at } y = 0$$

and

$$u = u_e, \quad H = H_e \text{ at } y = \delta.$$

For the case of an adiabatic wall and Pr = 1,

$$H = H_e \text{ for } y \geq 0 \ .$$

For the sake of simplicity, the analysis will be limited to the adiabatic case.

In the ordinary boundary layer theory, the pressure distribution is assumed known. In the present analysis, however, the pressure is determined through the interaction of the boundary layer and the supersonic inviscid flow and has to be obtained simultaneously with the development of the boundary layer.

Integrating Equations (1) across the boundary layer to eliminate the y dependence gives:

$$\left.\begin{aligned} &\frac{d\delta^*}{dx} - (\delta-\delta^*)\frac{1}{\rho_e u_e}\frac{d}{dx}(\rho_e u_e) = \frac{v_e}{u_e} = \tan\Theta \\ &\frac{d}{dx}(\rho_e u_e^2\,\theta) + \delta^*\,\rho_e u_e\frac{du_e}{dx} = \left(\mu\frac{\partial u}{\partial y}\right)_{y=0} \\ &\frac{d}{dx}(\rho_e u_e^3\,\theta^*) + 2(\delta^*-\delta_u)\rho_e u_e^2\frac{du_e}{dx} = 2\int_0^\delta \mu\left(\frac{\partial u}{\partial y}\right)^2 dy \end{aligned}\right\} \qquad (2)$$

where

$$\left.\begin{aligned} \delta &= \int_0^\delta dy & \delta^* &= \int_0^\delta \left(1 - \frac{\rho u}{\rho_e u_e}\right) dy \\ \theta &= \int_0^\delta \frac{\rho u}{\rho_e u_e}\left(1 - \frac{u}{u_e}\right) dy & \theta^* &= \int_0^\delta \frac{\rho u}{\rho_e u_e}\left(1 - \frac{u^2}{u_e^2}\right) dy \\ \delta_u &= \int_0^\delta \left(1 - \frac{u}{u_e}\right) dy \quad . \end{aligned}\right\} \tag{3}$$

The third equation in (2) is obtained by multiplying the momentum equation by u and integrating across the boundary layer. The integral quantities, Equations (3), can be written in terms of corresponding incompressible quantities by using the Stewartson transformation[29]

$$dY = \frac{a_e}{a_\infty}\frac{\rho}{\rho_\infty}\, dy \tag{4}$$

and relating the longitudinal velocities by

$$U = \frac{a_\infty}{a_e}\, u \tag{5}$$

as:

$$\left.\begin{aligned} \delta^* &= \frac{a_\infty \rho_\infty}{a_e \rho_e}\, \delta_i^* \left[1 + m_e(1+\mathcal{K})\right] \\ \theta &= \frac{a_\infty \rho_\infty}{a_e \rho_e}\, \theta_i \\ \theta^* &= \frac{a_\infty \rho_\infty}{a_e \rho_e}\, \theta_i^* \\ \delta_u &= \frac{a_\infty \rho_\infty}{a_e \rho_e}\, \delta_i^* \left[1 + m_e(\mathcal{K}-J)\right] \end{aligned}\right\} \tag{6}$$

where

$$\left.\begin{aligned} \delta_i &= \int_0^{\delta_i} dY & \delta_i^* &= \int_0^{\delta_i} \left(1 - \frac{U}{U_e}\right) dY \\ \theta_i &= \int_0^{\delta_i} \frac{U}{U_e}\left(1 - \frac{U}{U_e}\right) dY & \theta_i^* &= \int_0^{\delta_i} \frac{U}{U_e}\left(1 - \frac{U^2}{U_e^2}\right) dY \\ \mathcal{H} &= \frac{\theta_i}{\delta_i^*} & J &= \frac{\theta_i^*}{\delta_i^*} \ . \end{aligned}\right\} \quad (7)$$

By applying the compressibility transformation, Equations (6), and using a viscosity law of the form:[30]

$$\frac{\mu}{\mu_\infty} = C \frac{T}{T_\infty} \ , \quad (8)$$

Equations (2) become

$$\left.\begin{aligned} F \frac{d\delta_i^*}{dx} + \delta_i^* \frac{d\mathcal{H}}{dx} + f \frac{\delta_i^*}{M_e} \frac{dM_e}{dx} &= \frac{\beta}{m_e} \frac{1+m_e}{1+m_\infty} \tan\Theta \\ \mathcal{H} \frac{d\delta_i^*}{dx} + \delta_i^* \frac{d\mathcal{H}}{dx} + (1+2\mathcal{H}) \frac{\delta_i^*}{M_e} \frac{dM_e}{dx} &= \beta C \frac{\nu_\infty}{a_\infty M_e} \frac{P}{\delta_i^*} \\ J \frac{d\delta_i^*}{dx} + \delta_i^* \frac{dJ}{dx} + 3J \frac{\delta_i^*}{M_e} \frac{dM_e}{dx} &= \beta C \frac{\nu_\infty}{a_\infty M_e} \frac{R}{\delta_i^*} \end{aligned}\right\} \quad (9)$$

where

$$\beta = \frac{a_e}{a_\infty}\frac{p_e}{p_\infty} \qquad m = \frac{\gamma-1}{2} M^2$$

$$F = \mathcal{K} + \frac{1+m_e}{m_e}$$

$$f = \left[2 + \frac{\gamma+1}{\gamma-1}\frac{m_e}{1+m_e}\right]\mathcal{K} + \frac{3\gamma-1}{\gamma-1} + \frac{M_e^2 - 1}{m_e(1+m_e)} Z \qquad (10)$$

$$P = \delta_i^* \left[\frac{\partial}{\partial Y}\left(\frac{U}{U_e}\right)\right]_{Y=0} \qquad R = 2\delta_i^* \int_0^{\delta_i} \left[\frac{\partial}{\partial Y}\left(\frac{U}{U_e}\right)\right]^2 dY$$

$$Z = \frac{1}{\delta_i^*}\int_0^{\delta_i}\left(\frac{U}{U_e}\right) dY \quad .$$

II. 1. 1. Profile Functions

The profile quantities in Equations (7) and (10) depend on the velocity distribution through the viscous layer. For the adiabatic problem at least one parameter is necessary for its definition. Since, in the integral method, only relations between the integral functions are required, it is necessary to obtain functional relations of the form $\mathcal{K} = \mathcal{K}(a)$, $J = J(a)$, etc. where a is a profile parameter. One method for generating these relationships is to assume similar-flow profiles and use the similarity solutions of Cohen and Reshotko to obtain this dependence. This procedure was followed by Klineberg and the details are given in his Ph. D. thesis.[21] The results from the numerical solutions of the Cohen and Reshotko equations were approximated by polynomials of a, where

$$a = \left[\frac{\partial(U/U_e)}{\partial(Y/\delta_i)}\right]_{Y=0} \quad .$$

The values of the coefficients are given in Table I. These functions have been adopted for this study, where applicable.

Alternatively, one can regard $\mathcal{N}$ as the parameter rather than a and write $J = J(\mathcal{N})$, $R = R(\mathcal{N})$, $P = P(\mathcal{N})$, etc. since a is an arbitrary parameter. The unknowns in Equations (9) are then δ_i^*, M_e and $\mathcal{N}$ since $\tan\Theta$ can be related to M_e.

II. 1. 2. Equations for Supersonic Flow

By defining the following dimensionless variables, all of which are O(1):

$$\frac{\delta_i^*}{L}\sqrt{\frac{u_\infty L}{\nu_\infty C}} \equiv \tilde{\delta} \; ; \; \frac{x}{L} \equiv \bar{x} \; ; \; \frac{M_e}{M_\infty} = \tilde{M} \tag{11}$$

where L is a characteristic length (here taken to be the plate approach length) and writing the viscous interaction parameter as

$$\left(\frac{\gamma-1}{2}\right)^2 M_\infty^{\,3} \Big/ \sqrt{\frac{u_\infty L}{\nu_\infty C}} \equiv \epsilon = \left(\frac{\gamma-1}{2}\right)^2 \bar{\chi}_\infty$$

Equations (9) become:

$$\left[F \frac{d\tilde{\delta}}{d\bar{x}} + \tilde{\delta} \frac{d\mathcal{N}}{d\bar{x}} + \tilde{\delta} \frac{f}{\tilde{M}} \frac{d\tilde{M}}{d\bar{x}}\right] \epsilon = \frac{\beta}{\tilde{M}^2} \frac{r+\tilde{M}^2}{r+1} \frac{\gamma-1}{2} M_\infty \tan\Theta$$

$$\mathcal{N} \frac{d\tilde{\delta}}{d\bar{x}} + \tilde{\delta} \frac{d\mathcal{N}}{d\bar{x}} + (2\mathcal{N}+1) \frac{\tilde{\delta}}{\tilde{M}} \frac{d\tilde{M}}{d\bar{x}} = \frac{\beta P}{\tilde{M}\tilde{\delta}} \tag{12}$$

$$J \frac{d\tilde{\delta}}{d\bar{x}} + \tilde{\delta} \frac{dJ}{d\bar{x}} + 3J \frac{\tilde{\delta}}{\tilde{M}} \frac{d\tilde{M}}{d\bar{x}} = \frac{\beta R}{\tilde{M}\tilde{\delta}}$$

where

$$
\begin{aligned}
F &= \mathcal{K} + \frac{r+\tilde{M}^2}{\tilde{M}^2} \\
f &= \left[2 + \frac{\gamma+1}{\gamma-1} \frac{\tilde{M}^2}{r+\tilde{M}^2} \right] \mathcal{K} + \frac{3\gamma-1}{\gamma-1} + r \frac{\frac{2}{\gamma-1}\tilde{M}^2 - r}{\tilde{M}^2 (r+\tilde{M}^2)} Z \\
r &= \frac{1}{m_\infty} \\
\beta &= \left[\frac{r+1}{r+\tilde{M}^2} \right]^{2\frac{3\gamma-1}{(\gamma-1)}} .
\end{aligned}
\tag{13}
$$

Equations (12) can be completed by specifying the relationship between M_e and $\tan \Theta$. In the manner of Lees and Reeves,[18] if the expansion is assumed to begin in a region of uniform flow, the streamline inclination can be related to the Mach number by using the Prandtl-Meyer relation:

$$
\Theta = \nu(M_\infty) - \nu(M_e) + \alpha_w(\bar{x}) \tag{14}
$$

where $\alpha_w(\bar{x})$ is the inclination of the local tangent to the surface and is positive for an expansion turn. The Prandtl-Meyer function ν is:

$$
\nu = \sqrt{\frac{\gamma+1}{\gamma-1}} \tan^{-1} \sqrt{\frac{\gamma-1}{\gamma+1}(M^2-1)} - \tan^{-1} \sqrt{M^2-1} . \tag{15}
$$

Equations (12)-(15) together with the definitions (7) and (10) form the basic differential equations in the three unknowns M_e, δ_i^* and $\mathcal{K}$.

II. 1. 3. Hypersonic Approximation

A convenient form of Equations (12) for analytical study is obtained by making the approximation $M_\infty \gg 1$ or $r \ll 1$. Expanding

the Prandtl-Meyer function for $M \gg 1$, one obtains

$$\nu(M_\infty) - \nu(M_e) = \frac{2}{\gamma-1}\frac{1}{M_e}\left[1 - \frac{M_e}{M_\infty}\right] + \cdots$$

and

$$\tan\Theta \simeq \Theta = \frac{2}{\gamma-1}\frac{1}{M_\infty}\frac{1}{\tilde{M}}\left\{1 - \tilde{M}\left[1 - \frac{\gamma-1}{2}M_\infty \alpha_w(\bar{x})\right]\right\} .$$

With the following definition

$$1 - \frac{\gamma-1}{2}M_\infty \alpha_w(\bar{x}) \equiv \alpha(\bar{x}) \quad , \tag{16}$$

Equations (12) and (13) become:

$$\left[(\mathscr{K}+1)\frac{d\tilde{\delta}}{d\bar{x}} + \tilde{\delta}\frac{d\mathscr{K}}{d\bar{x}} + \frac{3\gamma-1}{\gamma-1}(\mathscr{K}+1)\frac{\tilde{\delta}}{\tilde{M}}\frac{d\tilde{M}}{d\bar{x}}\right]\epsilon = \frac{1}{\tilde{M}^\lambda}\left[1 - \tilde{M}\alpha(\bar{x})\right] \tag{17a}$$

$$\mathscr{K}\frac{d\tilde{\delta}}{d\bar{x}} + \tilde{\delta}\frac{d\mathscr{K}}{d\bar{x}} + (2\mathscr{K}+1)\frac{\tilde{\delta}}{\tilde{M}}\frac{d\tilde{M}}{d\bar{x}} = \frac{P}{\tilde{M}^\lambda \tilde{\delta}} \tag{17b}$$

$$J\frac{d\tilde{\delta}}{d\bar{x}} + \tilde{\delta}\frac{dJ}{d\bar{x}} + 3J\frac{\tilde{\delta}}{\tilde{M}}\frac{d\tilde{M}}{d\bar{x}} = \frac{R}{\tilde{M}^\lambda \tilde{\delta}} \tag{17c}$$

where $\lambda \equiv \frac{4\lambda-2}{\lambda-1}$.

Clearly, the two parameters in Equations (17) are the viscous interaction parameter ϵ and the expansion angle $M_\infty \alpha_w$.

II. 2. Solution for Small Interaction Parameter

If the interaction parameter ϵ is small, we expand the solution in the region where the x-derivatives are of order unity in power series in ϵ:

$$\tilde{M}(\tilde{x};\epsilon) = \tilde{M}_0(\tilde{x}) + \epsilon\,\tilde{M}_1(\tilde{x}) + \cdots$$

$$\mathscr{K}(\tilde{x};\epsilon) = \mathscr{K}_0(\tilde{x}) + \epsilon\,\mathscr{K}_1(\tilde{x}) + \cdots$$

$$\tilde{\delta}(\tilde{x};\epsilon) = \tilde{\delta}_0(\tilde{x}) + \epsilon\,\tilde{\delta}_1(\tilde{x}) + \cdots \quad .$$

Then, from Equation (17a) we obtain

$$1 - \tilde{M}_0 \, \alpha(\bar{x}) = 0 \, .$$

Namely the Mach number and hence the pressure along the boundary layer edge are given by the inviscid flow without the boundary layer effect, and $\mathscr{V}_0$ and $\tilde{\delta}_0$ are obtained from Equations (17b, c). The correction $\tilde{M}_1$ is determined from Equation (17a) by substituting $\tilde{M}_0$, $\mathscr{V}_0$ and $\tilde{\delta}_0$ in the left-hand side, and the corresponding corrections $\mathscr{V}_1$ and $\tilde{\delta}_1$ are determined from (17b, c).

In particular, for a flat plate $\alpha_w(\bar{x}) = 0$, an expansion of the form:[21, 28]

$$\begin{aligned} \tilde{M} &= 1 + \epsilon \frac{m_1}{\sqrt{\bar{x}}} + \cdots \\ \mathscr{V} &= \mathscr{V}_B + \epsilon \frac{h_1}{\sqrt{\bar{x}}} + \cdots \\ \tilde{\delta} &= \delta_B \sqrt{\bar{x}} \left(1 + \epsilon \frac{\delta_1}{\sqrt{\bar{x}}} + \cdots\right) \end{aligned} \tag{18}$$

serves to describe the boundary layer in this region. Here the subscript B refers to Blasius conditions and the constants are given by:

$$\begin{aligned} \mathscr{V}_B &= .38414 \\ \delta_B &= \sqrt{\frac{2P_B}{\mathscr{V}_B}} = \sqrt{\frac{2R_B}{J_B}} = 1.72387 \\ m_1 &= -\frac{\delta_B}{2} \frac{(1+r)(1+\mathscr{V}_B+r)}{\sqrt{1 - \frac{\gamma-1}{2} r}} \\ h_1 &= \left[\left(\frac{1-\mathscr{V}_B}{\mathscr{V}_B}\right) m_1\right] \Big/ \left[\frac{d}{d\mathscr{V}} \ell n \frac{R}{P}\right]_{\mathscr{V}=\mathscr{V}_B} \\ \delta_1 &= \left[2 - \frac{3\gamma-1}{\gamma-1} \frac{1}{1+r}\right] m_1 + \left[\frac{d}{d\mathscr{V}} \ell n \, R\right]_{\mathscr{V}=\mathscr{V}_B} h_1 \, . \end{aligned} \tag{19}$$

With this expansion solution the effect of a sharp expansion corner does not appear in the region upstream of the corner. In the neighborhood of the corner we expect relatively rapid changes in the flow and hence the breakdown of the above series. In fact, if appreciable changes occur over a distance of order ϵ from the corner ($\bar{x} = 1$), the left-hand side and the right-hand side of Equation (17a) are of the same order. An asymptotic solution valid in this region is described in the following sections.

II. 2. 1. First Approximation

II. 2. 1. 1. Inner Solutions

In the vicinity of the corner the $\bar{x}$ coordinate is stretched as follows:

$$\frac{\bar{x} - 1}{\epsilon} = \tilde{x} \qquad \text{fixed as} \qquad \epsilon \to 0 \quad . \tag{20}$$

Then, Equations (17) become,

$$\begin{aligned}
&(\nu+1)\frac{d\tilde{\delta}}{d\tilde{x}} + \tilde{\delta}\frac{d\nu}{d\tilde{x}} + \frac{3\gamma-1}{\gamma-1}(\nu+1)\frac{\tilde{\delta}}{\tilde{M}}\frac{d\tilde{M}}{d\tilde{x}} = \frac{1}{\tilde{M}^{\lambda}}\left[1-\tilde{M}\alpha(x)\right] \\
&\nu\frac{d\tilde{\delta}}{d\tilde{x}} + \tilde{\delta}\frac{d\nu}{d\tilde{x}} + (2\nu+1)\frac{\tilde{\delta}}{\tilde{M}}\frac{d\tilde{M}}{d\tilde{x}} = \epsilon\frac{P}{\tilde{M}^{\lambda}\tilde{\delta}} \\
&J\frac{d\tilde{\delta}}{d\tilde{x}} + \tilde{\delta}\frac{dJ}{d\tilde{x}} + 3J\frac{\tilde{\delta}}{\tilde{M}}\frac{d\tilde{M}}{d\tilde{x}} = \epsilon\frac{R}{\tilde{M}^{\lambda}\tilde{\delta}} \quad .
\end{aligned} \tag{21}$$

Thus, on the scale $\tilde{x}$, the shear at the wall, P, and the viscous dissipation, R, enter the solution to first order in ϵ. It is implied in this region that $[1-\tilde{M}\alpha(\tilde{x})]$ is O(1).

In this region we expand the solution in the following form:

$$\begin{aligned}
\tilde{M}(\tilde{x};\epsilon) &= \tilde{M}_0(\tilde{x})\,[1+\epsilon\,\tilde{M}_1(\tilde{x}) + \cdots] \\
\mathscr{V}(\tilde{x};\epsilon) &= \mathscr{V}_0(\tilde{x}) + \epsilon\,\mathscr{V}_1(\tilde{x}) + \cdots \\
\tilde{\delta}(\tilde{x};\epsilon) &= \tilde{\delta}_0(\tilde{x})\,[1+\epsilon\,\tilde{\delta}_1(\tilde{x}) + \cdots] \quad .
\end{aligned} \tag{22}$$

Substituting the above expansion into Equations (21) and collecting coefficients of like powers in ϵ, we obtain

$$\begin{aligned}
(\mathscr{V}_0+1)\frac{d\tilde{\delta}_0}{d\tilde{x}} + \tilde{\delta}_0\frac{d\mathscr{V}_0}{d\tilde{x}} + \frac{3\gamma-1}{\gamma-1}(\mathscr{V}_0+1)\frac{\tilde{\delta}_0}{\tilde{M}_0}\frac{d\tilde{M}_0}{d\tilde{x}} &= \frac{1}{\tilde{M}_0^{\lambda}}\,[1-\tilde{M}_0\,\alpha(\tilde{x})] \\
\mathscr{V}_0\frac{d\tilde{\delta}_0}{d\tilde{x}} + \tilde{\delta}_0\frac{d\mathscr{V}_0}{d\tilde{x}} + (2\mathscr{V}_0+1)\frac{\tilde{\delta}_0}{\tilde{M}_0}\frac{d\tilde{M}_0}{d\tilde{x}} &= 0 \\
J_0\frac{d\tilde{\delta}_0}{d\tilde{x}} + \tilde{\delta}_0\frac{dJ_0}{d\tilde{x}} + 3J_0\frac{\tilde{\delta}_0}{\tilde{M}_0}\frac{d\tilde{M}_0}{d\tilde{x}} &= 0
\end{aligned} \tag{23}$$

$$\begin{aligned}
(\mathscr{V}_0+1)\frac{d\tilde{\delta}_1}{d\tilde{x}} + \frac{d\mathscr{V}_1}{d\tilde{x}} + \frac{3\gamma-1}{\gamma-1}(\mathscr{V}_0+1)\frac{d\tilde{M}_1}{d\tilde{x}} &= -\frac{[1-\tilde{M}_0\alpha(\tilde{x})]}{\tilde{M}_0^{\lambda}\,\tilde{\delta}_0}\,\tilde{\delta}_1 \\
&\quad -\left[\frac{1}{\tilde{\delta}_0}\frac{d\tilde{\delta}_0}{d\tilde{x}} + \frac{3\gamma-1}{\gamma-1}\frac{1}{\tilde{M}_0}\frac{d\tilde{M}_0}{d\tilde{x}}\right]\mathscr{V}_1 - \frac{1}{\tilde{M}_0^{\lambda}\tilde{\delta}_0}\{\tilde{M}_0\alpha(\tilde{x}) + \lambda[1-\tilde{M}_0\alpha(\tilde{x})]\}\tilde{M}_1 \\
\mathscr{V}_0\frac{d\tilde{\delta}_1}{d\tilde{x}} + \frac{d\mathscr{V}_1}{d\tilde{x}} + (2\mathscr{V}_0+1)\frac{d\tilde{M}_1}{d\tilde{x}} &= \frac{P_0}{\tilde{M}_0^{\lambda}\tilde{\delta}_0^2} - \left[\frac{1}{\tilde{\delta}_0}\frac{d\tilde{\delta}_0}{d\tilde{x}} + \frac{2}{\tilde{M}_0}\frac{d\tilde{M}_0}{d\tilde{x}}\right]\mathscr{V}_1 \\
J_0\frac{d\tilde{\delta}_1}{d\tilde{x}} + \left(\frac{dJ}{d\mathscr{V}}\right)_0\frac{d\mathscr{V}_1}{d\tilde{x}} + 3J_0\frac{d\tilde{M}_1}{d\tilde{x}} &= \frac{R_0}{\tilde{M}_0^{\lambda}\tilde{\delta}_0^2} - \left[\frac{1}{\tilde{\delta}_0}\frac{d\tilde{\delta}_0}{d\tilde{x}} + \frac{3}{\tilde{M}_0}\frac{d\tilde{M}_0}{d\tilde{x}}\right]\left(\frac{dJ}{d\mathscr{V}}\right)_0\mathscr{V}_1 \\
&\quad -\left(\frac{d^2J}{d\mathscr{V}^2}\right)_0\frac{d\mathscr{V}_0}{d\tilde{x}}\,\mathscr{V}_1 \quad .
\end{aligned} \tag{24}$$

The second and third of Equations (23) integrate immediately to give:

$$\begin{aligned}
\tilde{\delta}_0\,J_0\,\tilde{M}_0^{\,3} &= \text{const.} = C_1 \\
\tilde{M}_0 &= C_2\,\exp\left\{\int_{\mathscr{V}_B}^{\mathscr{V}_0}\frac{A_1(\mathscr{V})}{A_2(\mathscr{V})}\,d\mathscr{V}\right\}
\end{aligned} \tag{25}$$

where

$$A_1(\mathscr{K}) = \mathscr{K}\frac{dJ}{d\mathscr{K}} - J$$

$$A_2(\mathscr{K}) = (1-\mathscr{K})J \quad . \tag{26}$$

The constants C_1 and C_2 are determined by matching with the solution (18) as $\bar{x} \to 1$, which can be written as

$$\tilde{M} = 1 + \frac{m_1}{h_1}(\mathscr{K}-\mathscr{K}_B) + \cdots$$

$$\tilde{\delta} = \delta_B\left[1 + \frac{\delta_1}{h_1}(\mathscr{K}-\mathscr{K}_B) + \cdots\right] \quad .$$

Therefore

$$C_2 = 1, \quad C_1 = C_B \equiv \delta_B J_B \quad .$$

These solutions can be related to the physical plane by substitution into the first of Equations (21):

$$\frac{d\mathscr{K}_0}{d\tilde{x}} = -\frac{A_2(\mathscr{K}_0)\left[1-\tilde{M}_0\alpha(x)\right]}{\tilde{M}_0^{\lambda}\,\tilde{\delta}_0\,\tilde{D}(\mathscr{K}_0)} \tag{27}$$

where

$$D(\mathscr{K}) = \frac{A_2(\mathscr{K})}{\mathscr{K}} - A_1(\mathscr{K})(1+\mathscr{K})\left(\frac{\gamma+1}{\gamma-1} - \frac{1}{\mathscr{K}}\right) \quad . \tag{28}$$

The vanishing of the function $\tilde{D}(\mathscr{K}_0)$ gives a unique value of $\mathscr{K}_0 \equiv \mathscr{K}_c$ in the hypersonic limit. $\mathscr{K}_c$ is larger than $\mathscr{K}_B$ and corresponds to a boundary layer profile accelerated above its zero pressure gradient solution. Boundary layers for which $\mathscr{K}_0 > \mathscr{K}_c$ are termed supercritical. A subcritical boundary layer responds to a downstream disturbance with an exponential increase of the disturbance, whereas a supercritical boundary layer is one for which disturbances

are exponentially damped. The effect of an external disturbance, in this case an expansion corner, can be propagated upstream of the corner if the boundary layer upstream of the disturbance is subcritical. A complete discussion is given by Klineberg.[21]

For an expansion turn, then, if the wall angle, α_w, is sufficiently large, transition of the boundary layer from an initially subcritical state to a supercritical state will occur. Smooth transition from the subcritical state, $\mathscr{K}_0 < \mathscr{K}_c$, to the supercritical state, $\mathscr{K}_0 > \mathscr{K}_c$, requires the simultaneous vanishing of $[1-M_0\alpha(\tilde{x})]$ and $\tilde{D}(\mathscr{K}_0)$. The latter requirement defines a particular value of $\tilde{x} \equiv \tilde{x}_c$ and corresponding critical angle $\alpha_w(\tilde{x}_c) \equiv \alpha_{wc} > 0$. As defined, $\tilde{D}(\mathscr{K}_0) > 0$ for $\mathscr{K}_0 < \mathscr{K}_c$ and $\tilde{D}(\mathscr{K}_0) < 0$ for $\mathscr{K}_0 > \mathscr{K}_c$.

Since the location of $\tilde{x}_c$ is fixed by the requirement that $\alpha_w > \alpha_{wc}$ it is possible to examine the behavior of the solution in the vicinity of the critical point $(\mathscr{K}_c, \tilde{x}_c)$ by linearizing Equation (27) near this point. Defining $\hat{\mathscr{K}} = \mathscr{K}_0 - \mathscr{K}_c$ and $\hat{x} = \tilde{x} - \tilde{x}_c$ and, for simplicity, assuming a circular arc turn with radius of curvature R_c such that

$$\alpha(\tilde{x}) = 1 - \frac{\gamma-1}{2} M_\infty \frac{\bar{x}-1}{R_c/L} = 1 - \frac{\gamma-1}{2} \frac{M_\infty \epsilon}{R_c/L} \tilde{x} \tag{29}$$

we reduce Equation (27) to

$$\frac{d\hat{\mathscr{K}}}{d\hat{x}} = \beta \left[\frac{\hat{x}/\tilde{R} - \gamma\hat{\mathscr{K}}}{\hat{\mathscr{K}}} \right] \tag{30}$$

where

$$\beta = -\frac{A_2(\mathscr{V}_c)J_c}{\tilde{M}_c^2 \frac{\gamma-1}{2} C_1 (d\tilde{D}/d\mathscr{V})_{\mathscr{V}=\mathscr{V}_c}} > 0$$

$$\gamma = \frac{A_1(\mathscr{V}_c)}{A_2(\mathscr{V}_c)} \alpha_c$$

$$\tilde{R} = \frac{R_c/L}{\frac{\gamma-1}{2} M_\infty \epsilon} \quad .$$

Equation (30) can be integrated to give

$$[\hat{\mathscr{V}} - \lambda_1 \hat{x}/(\gamma\tilde{R})]^{\lambda_1} [\hat{\mathscr{V}} - \lambda_2 \hat{x}/(\gamma\tilde{R})]^{-\lambda_2} = C$$

where λ_1 and λ_2 are the roots of

$$\lambda^2 + \beta\gamma^2\tilde{R}\lambda - \beta\gamma^2\tilde{R} = 0 \quad .$$

Since $\lambda_1\lambda_2 = -\beta\gamma^2\tilde{R} < 0$, the origin ($\hat{x}=0$, $\hat{\mathscr{V}} = 0$) is a saddle point with two separatrices $\hat{\mathscr{V}} = \lambda_1\hat{x}/(\gamma\tilde{R})$ and $\hat{\mathscr{V}} = \lambda_2\hat{x}/(\gamma\tilde{R})$. Thus, the separatrix $\hat{\mathscr{V}} = \lambda_1 \hat{x}/(\gamma\tilde{R})$ ($\lambda_1 > 0$) is the solution for subcritical-supercritical passage.

If it is assumed that the linearized solution is valid on the entire curved portion of the wall, the total change in $\mathscr{V}_0$ between points ① and ② [see Fig. 3] as the radius of curvature tends to zero is:

$$\Delta\mathscr{V}_{①,②} \sim \frac{1}{\sqrt{\tilde{R}}}\Delta\tilde{x} \sim \frac{1}{\sqrt{\tilde{R}}}\tilde{R} = \sqrt{\tilde{R}}$$

$$\Delta\mathscr{V}_{①,②} \sim \sqrt{\tilde{R}} \to 0 \text{ as } \tilde{R} \to 0$$

$$\mathscr{V}_① = \mathscr{V}_② = \mathscr{V}_c \quad .$$

Therefore, in the limit of zero radius of curvature, this result suggests computing the flow upstream of the corner separately from the

flow downstream of the corner and matching the two flows at the corner. Continuity of $\mathscr{V}_0$ at the corner requires continuity of $\tilde{M}_0$ and hence continuity of $\tilde{\delta}_0$ from Equations (25). For the sharp corner, then,

$$\alpha_w(\tilde{x}) = \begin{cases} 0 & \text{for } \tilde{x} < 0 \\ \alpha_w, \text{ const.} & \text{for } \tilde{x} > 0 \end{cases} .$$

Rewriting Equations (25) and (27) for the two regions, noting that $\tilde{M}_0 - 1 \sim \frac{A_1(\mathscr{V}_B)}{A_2(\mathscr{V}_B)}(\mathscr{V}_0 - \mathscr{V}_B)$ near the Blasius point, we obtain

$$\left.\begin{aligned} \tilde{\delta}_0 J_0 \tilde{M}_0^3 &= C_B \\ \tilde{M}_0 &= \tilde{M}_c \exp\{\tilde{Q}_1(\mathscr{V}_0)\} \\ \tilde{x} &= C_B \tilde{Q}_2(\mathscr{V}_0) + C_B \frac{\tilde{D}(\mathscr{V}_B)}{A_1(\mathscr{V}_B) J_B} \ln\left(\frac{\mathscr{V}_0 - \mathscr{V}_B}{\mathscr{V}_c - \mathscr{V}_B}\right) \end{aligned}\right\} \tilde{x} < 0 \qquad (31)$$

$$\left.\begin{aligned} \tilde{\delta}_0 J_0 \tilde{M}_0^3 &= C_B \\ \tilde{M}_0 &= \tilde{M}_c \exp\{\tilde{Q}_1(\mathscr{V}_0)\} \\ \tilde{x} &= C_B \tilde{Q}_3(\mathscr{V}_0) + C_B \left(\frac{1}{\alpha}\right)^{\frac{\gamma+1}{\gamma-1}} \frac{\tilde{D}(\mathscr{V}_p)}{A_1(\mathscr{V}_p) J_p} \ln\left(\frac{\mathscr{V}_p - \mathscr{V}_0}{\mathscr{V}_p - \mathscr{V}_c}\right) \end{aligned}\right\} \tilde{x} > 0 \qquad (32)$$

where

$$\begin{aligned} \tilde{Q}_1 &= \int_{\mathscr{V}_c}^{\mathscr{V}_0} \frac{A_1(\mathscr{V})}{A_2(\mathscr{V})} \, d\mathscr{V} \\ \tilde{Q}_2 &= \int_{\mathscr{V}_c}^{\mathscr{V}_0} \left[\frac{\tilde{M}_0^{\frac{\gamma+1}{\gamma-1}} \tilde{D}(\mathscr{V})}{A_2(\mathscr{V}) J_0 (\tilde{M}_0 - 1)} - \frac{\tilde{D}(\mathscr{V}_B)}{A_1(\mathscr{V}_B) J_B} \frac{1}{\mathscr{V} - \mathscr{V}_B} \right] d\mathscr{V} \\ \tilde{Q}_3 &= \int_{\mathscr{V}_c}^{\mathscr{V}_0} \left[\frac{\tilde{M}_0^{\frac{\gamma+1}{\gamma-1}} \tilde{D}(\mathscr{V})}{A_2(\mathscr{V}) J_0 (\alpha \tilde{M}_0 - 1)} - \left(\frac{1}{\alpha}\right)^{\frac{\gamma+1}{\gamma-1}} \frac{\tilde{D}(\mathscr{V}_p)}{A_1(\mathscr{V}_p) J_p} \frac{1}{\mathscr{V} - \mathscr{V}_p} \right] d\mathscr{V} \\ \tilde{M}_c &= 1 / \exp\{\tilde{Q}_1(\mathscr{V}_B)\} \end{aligned} \qquad (33)$$

and $\mathscr{V}_p$ is given by

$$\frac{1}{\alpha} = \tilde{M}_c \exp\left\{\tilde{\Omega}_1(\mathscr{V}_p)\right\} \quad .$$

The solutions are defined in terms of quadratures which have $\mathscr{V}_0$ as independent variable. The parameter $M_\infty \alpha_w$ appears only in the downstream part of the solutions. Solutions can be readily tabulated in the form:

$$\left.\begin{aligned} \mathscr{V} &= \mathscr{V}_0(\tilde{x}) \\ \tilde{M} &= \tilde{M}_0(\tilde{x}) \\ \tilde{\delta} &= \tilde{\delta}_0(\tilde{x}) \end{aligned}\right\} -\infty < \tilde{x} < 0$$

$$\left.\begin{aligned} \mathscr{V} &= \mathscr{V}_0(\tilde{x};\, M_\infty \alpha_w) \\ \tilde{M} &= \tilde{M}_0(\tilde{x};\, M_\infty \alpha_w) \\ \tilde{\delta} &= \tilde{\delta}_0(\tilde{x};\, M_\infty a_w) \end{aligned}\right\} 0 < \tilde{x} < +\infty \quad .$$

However, the downstream solutions for $\mathscr{V}_0$ and $\tilde{\delta}_0$ are not uniformly valid and will be examined in Section II. 2. 1. 2.

II. 2. 1. 2. Relaxation Solution

In the upstream solution, as $\mathscr{V} \to \mathscr{V}_B$,

$$\tilde{x} \to C_B \tilde{\Omega}_2(\mathscr{V}_B) + \frac{1}{k_1^2} \ln\left(\frac{\mathscr{V}_0 - \mathscr{V}_B}{\mathscr{V}_c - \mathscr{V}_B}\right)$$

or

$$\mathscr{V}_0 - \mathscr{V}_B \sim \text{const.}\ e^{k_1^2 \tilde{x}} \quad .$$

Hence,

$$\left.\begin{aligned} &\mathscr{V}_0 \to \mathscr{V}_B \\ &\tilde{M}_0 \to 1 \\ &\tilde{\delta}_0 \to \delta_B \end{aligned}\right\} \quad \text{exponentially as } \tilde{x} \to -\infty \ .$$

The inner solutions for $\mathscr{V}_0(\tilde{x})$ and $\tilde{M}_0(\tilde{x})$ are uniformly valid. A uniformly valid solution for $\tilde{\delta}_{comp.} = \tilde{\delta}_{comp.}(\tilde{x};\epsilon)$ can be constructed from the inner and outer expansions:

$$\begin{aligned} \tilde{\delta}_{comp.} &= \tilde{\delta}_0(\tilde{x}) + \delta_B \left[\sqrt{\tilde{x}} - 1\right] \\ &= \tilde{\delta}_0(\tilde{x}) + \delta_B \left[\sqrt{1+\epsilon\tilde{x}} - 1\right] \quad . \end{aligned} \tag{34}$$

The downstream solution for $\tilde{M} = \tilde{M}_0(\tilde{x};M_\infty \alpha_w)$ is uniformly valid since $\tilde{M}_0 \to 1/\alpha = M_{+\infty}/M_{-\infty}$ for a particular value of $\mathscr{V}_0 \equiv \mathscr{V}_p$. However,

$$\mathscr{V}_p - \mathscr{V}_0 \sim \text{const.}\, e^{-k_2^2 \tilde{x}} \to 0$$

as $\tilde{x} \to +\infty$; i.e., $\mathscr{V}_0$ monotonically approaches a maximum value defined by α. Similarly $\tilde{\delta}_0 \to \delta_p$, a minimum value, as $\tilde{x} \to +\infty$. It is then necessary to return to the differential equations (17) and examine the solution for $1 - \alpha\tilde{M} = O(\epsilon)$, namely the solution for a region in which the boundary layer relaxes, interacting only weakly with the external flow, to the Blasius solution.

In this relaxation region the following variables are defined:

$$
\begin{aligned}
1 - \alpha\tilde{M} &= O(\epsilon) \equiv \epsilon\, M^*(x^*;\epsilon) \\
\bar{x} - 1 &= x^* \\
\tilde{\delta} &= \delta^* \\
\mathscr{V} &= \mathscr{V}^* \quad .
\end{aligned}
\tag{35}
$$

Equations (17) become:

$$
\begin{aligned}
(\mathscr{V}^*+1)\frac{d\delta^*}{dx^*} + \delta^*\frac{d\mathscr{V}^*}{dx^*} - \epsilon\frac{3\gamma-1}{\gamma-1}(\mathscr{V}^*+1)\frac{\delta^*}{1-\epsilon M^*}\frac{dM^*}{dx^*} &= \frac{M^*\alpha^\lambda}{(1-\epsilon M^*)^\lambda} \\
\mathscr{V}^*\frac{d\delta^*}{dx^*} + \delta^*\frac{d\mathscr{V}^*}{dx^*} - \epsilon(2\mathscr{V}^*+1)\frac{\delta^*}{1-\epsilon M^*}\frac{dM^*}{dx^*} &= \frac{P\,\alpha^\lambda}{(1-\epsilon M^*)^\lambda\delta^*} \\
J\frac{d\delta^*}{dx^*} + \delta^*\frac{dJ}{d\mathscr{V}^*}\frac{d\mathscr{V}^*}{dx^*} - \epsilon 3J\frac{\delta^*}{1-\epsilon M^*}\frac{dM^*}{dx^*} &= \frac{R\,\alpha^\lambda}{(1-\epsilon M^*)^\lambda\delta^*} \quad .
\end{aligned}
\tag{36}
$$

An outer expansion of the form

$$
\begin{aligned}
M^*(x^*;\epsilon) &= M_0^*(x^*)\,[1+\epsilon\, M_1^*(x^*) + \cdots] \\
\mathscr{V}^*(x^*;\epsilon) &= \mathscr{V}_0^*(x^*) + \epsilon\,\mathscr{V}_1(x^*) + \cdots \\
\delta^*(x^*;\epsilon) &= \delta_0^*(x^*)\,[1+\epsilon\,\delta_1^*(x^*) + \cdots]
\end{aligned}
$$

is assumed in this region. Substitution of this expansion into Equation (36) gives

$$
\begin{aligned}
(\mathscr{V}_0^*+1)\frac{1}{\delta_0^*}\frac{d\delta_0^*}{dx^*} + \frac{d\mathscr{V}_0^*}{dx^*} &= \frac{M_0^*\,\alpha^\lambda}{\delta_0^*} \\
\mathscr{V}_0^*\frac{1}{\delta_0^*}\frac{d\delta_0^*}{dx^*} + \frac{d\mathscr{V}_0^*}{dx^*} &= \frac{P_0\,\alpha^\lambda}{\delta_0^{*2}} \\
J_0\frac{1}{\delta_0^*}\frac{d\delta_0^*}{dx^*} + \left(\frac{dJ}{d\mathscr{V}^*}\right)_0\frac{d\mathscr{V}_0^*}{dx^*} &= \frac{R_0\,\alpha^\lambda}{\delta_0^{*2}}
\end{aligned}
\tag{37}
$$

$$(\mathscr{V}_0^*+1)\frac{d\delta_1^*}{dx^*}+\frac{d\mathscr{V}_1^*}{dx^*}=\frac{M_0^*\alpha^\lambda}{\delta_0^*}\left[(1+\lambda)M_1^*-\delta_1^*\right]-\frac{1}{\delta_0^*}\frac{d\delta_0^*}{dx^*}\mathscr{V}_1^*$$
$$+\frac{3\gamma-1}{\gamma-1}(\mathscr{V}_0^*+1)\frac{dM_0^*}{dx^*}$$

$$\mathscr{V}_0^*\frac{d\delta_1^*}{dx^*}+\frac{d\mathscr{V}_1^*}{dx^*}=\frac{\alpha^\lambda}{\delta_0^{*2}}\left[\left(\frac{dP}{d\mathscr{V}^*}\right)_0\mathscr{V}_1^*-2P_0\delta_1^*\right]-\frac{1}{\delta_0^*}\frac{d\delta_0^*}{dx^*}\mathscr{V}_1^*$$
$$+(2\mathscr{V}_0^*+1)\frac{dM_0^*}{dx^*} \qquad (38)$$

$$J_0\frac{d\delta_1^*}{dx^*}+\left(\frac{dJ}{d\mathscr{V}^*}\right)_0\frac{d\mathscr{V}_1^*}{dx^*}=\frac{\alpha^\lambda}{\delta_0^{*2}}\left[\left(\frac{dR}{d\mathscr{V}^*}\right)_0\mathscr{V}_1^*-2R_0\delta_1^*\right]+3J_0\frac{dM_0^*}{dx^*}$$
$$-\left[\left(\frac{dJ}{d\mathscr{V}^*}\right)_0\frac{1}{\delta_0^*}\frac{d\delta_0^*}{dx^*}+\left(\frac{d^2J}{d\mathscr{V}^{*2}}\right)_0\frac{d\mathscr{V}_0^*}{dx^*}\right]\mathscr{V}_1^* .$$

The second two of Equations (37) can be solved simply for the derivatives $d\mathscr{V}_0^*/dx^*$ and $d\delta_0^*/dx^*$:

$$\frac{1}{\delta_0^*}\frac{d\delta_0^*}{dx^*}=\frac{P_0\left(\frac{dJ}{d\mathscr{V}^*}\right)_0-R_0}{\mathscr{V}_0^*\left(\frac{dJ}{d\mathscr{V}^*}\right)_0-J_0}\cdot\frac{\alpha^\lambda}{\delta_0^{*2}}=\frac{P_0J_0'-R_0}{A_1(\mathscr{V}_0^*)}\frac{\alpha^\lambda}{\delta_0^{*2}}$$
$$\frac{d\mathscr{V}_0^*}{dx^*}=\frac{\mathscr{V}_0^*R_0-J_0P_0}{A_1(\mathscr{V}_0^*)}\frac{\alpha^\lambda}{\delta_0^{*2}} . \qquad (39)$$

As before, if the integration is performed in the phase plane, solutions are

$$\delta_0^*=K_1\exp\left\{\int_{\mathscr{V}_p}^{\mathscr{V}_0^*}\frac{P_0J_0'-R_0}{\mathscr{V}R_0-J_0P_0}\,d\mathscr{V}\right\}\equiv K_1\exp\{Q_1^*(\mathscr{V}_0^*)\}$$
$$x^*=\frac{1}{\alpha^\lambda}\int_{\mathscr{V}_p}^{\mathscr{V}_0^*}\frac{A_1(\mathscr{V})}{\mathscr{V}R_0-J_0P_0}\delta_0^{*2}(\mathscr{V})\,d\mathscr{V}+K_2\equiv Q_2^*(\mathscr{V}_0^*)+K_2. \qquad (40)$$

Substituting Equations (39) into the first of Equations (37) gives the solution for M_0^*:

$$M_0^* = -\frac{1}{\delta_0^*(\mathscr{V}_0^*)} \frac{B_1(\mathscr{V}_0^*)}{A_1(\mathscr{V}_0^*)} \qquad (41)$$

where $B_1(\mathscr{V}) = R - J'P - P A_1(\mathscr{V})$.

The solutions (40) exhibit no singular behavior for $\mathscr{V}_0^* = \mathscr{V}_c$ and no difficulty arises in evaluating the quadratures over the range $\mathscr{V}_p \geq \mathscr{V}_0^* > \mathscr{V}_B$. Near the Blasius point in the phase space, $\mathscr{V}_0^* R_0 \rightarrow J_0 P_0$ and

$$\delta_0^* \sim \text{const.} \; (\mathscr{V}_0^* - \mathscr{V}_B)^{-\beta_1}$$

$$M_0^* \sim (\mathscr{V}_0^* - \mathscr{V}_B)^{\beta_1} \rightarrow 0$$

where

$$\beta_1 = -\left\{ \frac{P_0 J_0' - R_0}{\left[\frac{d}{d\mathscr{V}_0^*} (\mathscr{V}_0^* R_0 - J_0 P_0) \right]} \right\}_{\mathscr{V}_0^* = \mathscr{V}_B} < 1 \quad .$$

The asymptotic forms of Equations (40), as $\mathscr{V}_0^* \rightarrow \mathscr{V}_p$ are given by

$$\delta_0^* = K_1 \left\{ 1 + f_1(\mathscr{V}_p)(\mathscr{V}_0^* - \mathscr{V}_p) + \cdots \right\}$$

$$x^* = \frac{1}{\alpha^\lambda} f_2(\mathscr{V}_p)(\mathscr{V}_0^* - \mathscr{V}_p) + \cdots + K_2$$

or

$$\mathscr{V}_0^* = \mathscr{V}_p + \frac{\alpha^\lambda}{f_2(\mathscr{V}_p)} (x^* - K_2) + \cdots$$

$$\delta_0^* = K_1 \left\{ 1 + \alpha^\lambda \frac{f_1(\mathscr{V}_p)}{f_2(\mathscr{V}_p)} (x^* - K_2) + \cdots \right\}$$

where

$$f_1(\mathscr{V}_p) = \left[\frac{P_0 J_0' - R_0}{\mathscr{V}_0^* R_0 - J_0 P_0}\right]_{\mathscr{V}_0^* = \mathscr{V}_p}$$

$$f_2(\mathscr{V}_p) = \left[\frac{A_1(\mathscr{V}_0^*)}{\mathscr{V}_0^* R_0 - J_0 P_0}\right]_{\mathscr{V}_0^* = \mathscr{V}_p} K_1^2 \quad .$$

If the outer solutions are expressed in terms of the inner variable $\tilde{x}$, solutions are, correct to order ε^0:

$$\mathscr{V}_0^*(\tilde{x}) = \mathscr{V}_p - \frac{\alpha^\lambda}{f_2(\mathscr{V}_p)} K_2 + \cdots$$

$$\delta_0^*(\tilde{x}) = K_1 \left\{1 - \alpha^\lambda \frac{f_1(\mathscr{V}_p)}{f_2(\mathscr{V}_p)} K_2 + \cdots\right\} \quad .$$

These must be matched to the inner solutions as $\tilde{x} \to \infty$,

$$\lim_{\tilde{x} \to \infty} \mathscr{V}_0(\tilde{x}) \to \mathscr{V}_p$$

$$\lim_{\tilde{x} \to \infty} \tilde{\delta}_0(\tilde{x}) \to \delta_p \quad .$$

Therefore,

$$K_1 = \delta_p, \qquad K_2 = 0 \quad .$$

A uniformly valid composite solution can now be constructed in the region downstream of the corner by subtracting out the common parts of the inner solution and outer solution:

$$\mathscr{V}_{comp.}(x^*;\varepsilon) = \mathscr{V}_0(\tilde{x}) + [\mathscr{V}_0^*(x^*) - \mathscr{V}_p]$$

$$\tilde{\delta}_{comp.}(x^*;\varepsilon) = \tilde{\delta}_0(\tilde{x}) + [\delta_0^*(x^*) - \delta_p]$$

$$\tilde{M}_{comp.}(\tilde{x}) = \tilde{M}_0(\tilde{x}) \quad .$$

Summary

Summarizing the results of the first approximation gives:

Upstream of the corner, $\tilde{x} < 0$:

INNER SOLUTION:

$$\tilde{M}_0(\mathscr{V}_0) = \tilde{M}_c \exp\{\tilde{Q}_1(\mathscr{V}_0)\}$$

$$\tilde{\delta}_0(\mathscr{V}_0) = \frac{C_B}{J_0 \tilde{M}_0^3}$$

$$\tilde{x}(\mathscr{V}_0) = C_B \left\{\tilde{Q}_2(\mathscr{V}_0) + \frac{\tilde{D}(\mathscr{V}_B)}{A_1(\mathscr{V}_B) J_B} \ell n \left(\frac{\mathscr{V}_0 - \mathscr{V}_B}{\mathscr{V}_c - \mathscr{V}_B}\right)\right\} .$$

OUTER SOLUTION:

$$\tilde{M}_0(x^*) = 1$$

$$\tilde{\delta}_0(x^*) = \delta_B \sqrt{1+x^*}$$

$$\mathscr{V}_0(x^*) = \mathscr{V}_B .$$

COMPOSITE SOLUTION:

$$\tilde{M}(x^*;\epsilon) = \tilde{M}_0(\tilde{x})$$

$$\tilde{\delta}(x^*;\epsilon) = \tilde{\delta}_0(\tilde{x}) + \delta_B \{\sqrt{1+x^*} - 1\}$$

$$\mathscr{V}(x^*;\epsilon) = \mathscr{V}_0(\tilde{x}) .$$

Downstream of the corner, $\tilde{x} > 0$:

INNER SOLUTION:

$$\tilde{M}_0(\mathscr{V}_0) = \tilde{M}_c \exp\{\tilde{Q}_1(\mathscr{V}_0)\}$$

$$\tilde{\delta}_0(\mathscr{V}_0) = \frac{C_B}{J_0 \tilde{M}_0^3}$$

$$\tilde{x}(\mathscr{V}_0) = C_B \left\{\tilde{Q}_3(\mathscr{V}_0) + \left(\frac{1}{\alpha}\right)^{\frac{\gamma+1}{\gamma-1}} \frac{\tilde{D}(\mathscr{V}_p)}{A_1(\mathscr{V}_p) J_p} \ell n \left(\frac{\mathscr{V}_p - \mathscr{V}_0}{\mathscr{V}_p - \mathscr{V}_c}\right)\right\} .$$

OUTER SOLUTION:

$$\tilde{M}_0(\mathscr{V}_0^*) = \frac{1}{\alpha}$$

$$\delta_0^*(\mathscr{V}_0^*) = \delta_p \exp\left\{ \int_{\mathscr{V}_p}^{\mathscr{V}_0^*} \frac{P_0 J_0' - R_0}{\mathscr{V} R_0 - J_0 P_0} d\mathscr{V} \right\} \equiv \delta_p \exp\{\Omega_1^*(\mathscr{V}_0^*)\}$$

$$x^*(\mathscr{V}_0^*) = \frac{1}{\alpha^\lambda} \int_{\mathscr{V}_p}^{\mathscr{V}_0^*} \frac{A_1(\mathscr{V})}{\mathscr{V} R_0 - J_0 P_0} \delta_0^{*2}(\mathscr{V}) d\mathscr{V} \equiv \Omega_2^*(\mathscr{V}_0^*) \quad .$$

COMPOSITE SOLUTION:

$$\tilde{M}(x^*;\epsilon) = \tilde{M}_0(\tilde{x})$$

$$\delta^*(x^*;\epsilon) = \tilde{\delta}_0(\tilde{x}) + \{\delta_0^*(x^*) - \delta_p\}$$

$$\mathscr{V}^*(x^*;\epsilon) = \mathscr{V}_0(\tilde{x}) + \{\mathscr{V}_0^*(x^*) - \mathscr{V}_p\} \quad .$$

These solutions are sketched in Fig. 4. The solutions of the differential equations in this limit show that the pressure drops to within $O(\epsilon)$ of its final downstream value on the scale $(\bar{x}-1)/\epsilon$ while the relaxation of the profile shape back to a Blasius condition takes place on the physical scale $(\bar{x} - 1)$. Furthermore, the upstream solution is independent of the expansion angle provided the angle exceeds the critical angle for supercritical flow downstream of the corner. To the order of this approximation, the critical angle is given by

$$M_\infty \alpha_{wc} = \frac{2}{\gamma-1}\left[1 - \exp\left\{\Omega_1(\mathscr{V}_B)\right\}\right] \quad . \tag{42}$$

Evaluating the quantity $\exp\left\{\tilde{\Omega}_1(\mathscr{V}_B)\right\}$ gives

$$\exp\left\{\Omega_1(\mathscr{V}_B)\right\} = 0.9804 \quad . \tag{43}$$

Hence $M_\infty \alpha_{wc} = 0.0980$ for $\gamma = 1.4$ and for $M_\infty \gtrsim 5.6$, $\alpha_{wc} \lesssim 1^\circ$. The critical angle is plotted versus M_∞ in Fig. 5. It is of interest to

compute the pressure at the corner which is:

$$\frac{p_c}{p_\infty} = \left[\exp\left\{\tilde{Q}_1(\mathcal{V}_B)\right\}\right]^{\frac{2\gamma}{\gamma-1}} = 0.8707 \quad . \tag{44}$$

This value agrees with the value given by Olsson and Messiter[10] to three decimal places. Solutions for the pressure distribution can be written in the form:

$$\begin{aligned} \frac{p}{p_\infty} &= G_1(\tilde{x}) && \tilde{x} < 0 \\ &= G_2(\tilde{x}; M_\infty \alpha_w) && \tilde{x} > 0 \end{aligned} \tag{45}$$

where the functions G_1 and G_2 can be computed once and for all. It must be emphasized that this result is valid for flows which have very small values of the interaction parameter.

Up to this point, little has been said about the maximum value of $\mathcal{V}_0 = \mathcal{V}_p$. $\mathcal{V}_p$ is defined by

$$\frac{1}{\alpha} = \exp\left\{\int_{\mathcal{V}_B}^{\mathcal{V}_p} \frac{A_1(\mathcal{V})}{A_2(\mathcal{V})}\, d\mathcal{V}\right\} \quad .$$

In general, the value of $\mathcal{V}_p$ can be expected to exceed the limiting value of $\mathcal{V}$ computed from the similar equations written for adiabatic flow. This limit corresponds to the pressure gradient parameter, β, tending to infinity. Previous investigators of problems involving expansion turns[21, 31] have assumed that $\mathcal{V}$ and hence all other profile quantities remain fixed at values corresponding to this maximum until $\mathcal{V}$ begins to decrease after the expansion is completed. Solutions of the similar equations which admit a small amount of heat transfer have been found which allow extension of all of the profile quantities

beyond this limit. These solutions are the subject of the Appendix.

The subject of Section II. 2. 1 has been concerned with flows for which the interaction parameter tends to zero. It is worthwhile to obtain the next approximation for ϵ considered small but finite to see if it is possible to construct solutions which are of practical interest. This is the subject of Section II. 2. 2.

II. 2. 2. Second Approximation

II. 2. 2. 1. Inner Solutions

For convenience, Equations (24) are written as follows:

$$\frac{d\tilde{M}_1}{d\tilde{x}} = -\frac{1}{\tilde{M}_0}\frac{d\tilde{M}_0}{d\tilde{x}}\left\{\frac{d_1'(\mathscr{V}_0)}{d_1(\mathscr{V}_0)}\mathscr{V}_1 + \tilde{\delta}_1 + \left[\frac{\alpha\tilde{M}_0}{1-\alpha\tilde{M}_0} + \lambda\right]\tilde{M}_1 - \frac{b_1(\mathscr{V}_0)}{\tilde{\delta}_0(1-\alpha\tilde{M}_0}\right\}$$

$$\frac{d\mathscr{V}_1}{d\tilde{x}} = -\frac{d\mathscr{V}_0}{d\tilde{x}}\left\{\frac{d_2'(\mathscr{V}_0)}{d_2(\mathscr{V}_0)}\mathscr{V}_1 + \tilde{\delta}_1 + \left[\frac{\alpha\tilde{M}_0}{1-\alpha\tilde{M}_0} + \lambda\right]\tilde{M}_1 + \frac{b_2(\mathscr{V}_0)}{\tilde{\delta}_0(1-\alpha\tilde{M}_0)}\right\} \qquad (46)$$

$$\frac{d\tilde{\delta}_1}{d\tilde{x}} = -\frac{1}{\tilde{\delta}_0}\frac{d\tilde{\delta}_0}{d\tilde{x}}\left\{\frac{d_3'(\mathscr{V}_0)}{d_3(\mathscr{V}_0)}\mathscr{V}_1 + \tilde{\delta}_1 + \left[\frac{\alpha\tilde{M}_0}{1-\alpha\tilde{M}_0} + \lambda\right]\tilde{M}_1 + \frac{b_3(\mathscr{V}_0)}{\tilde{\delta}_0(1-\alpha\tilde{M}_0)}\right\}$$

where

$$d_i(\mathscr{V}) = \frac{\tilde{D}(\mathscr{V})}{A_i(\mathscr{V})} \quad ; \quad b_i(\mathscr{V}) = \frac{B_i(\mathscr{V})}{A_i(\mathscr{V})}$$

$$\lambda = \frac{4\gamma-2}{\gamma-1}$$

$$A_1(\mathscr{V}) = \mathscr{V}\frac{dJ}{d\mathscr{V}} - J$$

$$A_2(\mathscr{V}) = (1-\mathscr{V})J \qquad (47)$$

$$A_3(\mathscr{V}) = -3A_1(\mathscr{V}) - (1-\mathscr{V})\frac{dJ}{d\mathscr{V}}$$

$$B_1(\mathscr{V}) = R - P\frac{dJ}{d\mathscr{V}} - PA_1(\mathscr{V})$$

$$B_2(\mathscr{V}) = (1+\mathscr{V})\left[(1-\mathscr{V})R - \frac{2}{\gamma-1}(\mathscr{V}R-JP)\right]$$

$$B_3(\mathscr{V}) = \frac{3\gamma-1}{\gamma-1}(1+\mathscr{V})\left(R-P\frac{dJ}{d\mathscr{V}}\right) + 3JP - (1+2\mathscr{V})R \quad .$$

As before, these equations can be integrated in the phase plane by choosing $\mathscr{V}_0$ as the independent variable. The differential form is

$$\left.\begin{aligned}
\frac{d}{d\mathscr{V}_0}\left[\tilde{M}_1 - \frac{A_1(\mathscr{V}_0)}{A_2(\mathscr{V}_0)}\mathscr{V}_1\right] &= \frac{A_1(\mathscr{V}_0}{A_2(\mathscr{V}_0)}\,\frac{b_1(\mathscr{V}_0)+b_2(\mathscr{V}_0)}{\tilde{\delta}_0(1-\alpha\tilde{M}_0)} \\
\frac{d}{d\mathscr{V}_0}\left[\tilde{\delta}_1 - \frac{A_3(\mathscr{V}_0)}{A_2(\mathscr{V}_0)}\mathscr{V}_1\right] &= \frac{A_3(\mathscr{V}_0)}{A_2(\mathscr{V}_0)}\,\frac{b_2(\mathscr{V}_0)-b_3(\mathscr{V}_0)}{\tilde{\delta}_0(1-\alpha\tilde{M}_0)}
\end{aligned}\right\} \tag{48}$$

$$\begin{aligned}
\frac{d}{d\mathscr{V}_0}\left[\mathscr{V}_1\,\frac{d_2(\mathscr{V}_0)\tilde{\delta}_0\tilde{M}_0^{\lambda}}{(1-\alpha\tilde{M}_0)}\right] = -\frac{d_2(\mathscr{V}_0)\tilde{\delta}_0\tilde{M}_0^{\lambda}}{1-\alpha\tilde{M}_0}\Bigg\{&\left[\tilde{\delta}_1 - \frac{A_3(\mathscr{V}_0)}{A_2(\mathscr{V}_0)}\mathscr{V}_1\right] \\
&+\left[\frac{\alpha\tilde{M}_0}{1-\alpha\tilde{M}_0}+\lambda\right]\left[\tilde{M}_1 - \frac{A_1(\mathscr{V}_0)}{A_2(\mathscr{V}_0)}\mathscr{V}_1\right] \\
&+\frac{b_2(\mathscr{V}_0)}{\tilde{\delta}_0(1-\alpha\tilde{M}_0)}\Bigg\}
\end{aligned} \tag{49}$$

$$\frac{d\tilde{x}}{d\mathscr{V}_0} = -\frac{d_2(\mathscr{V}_0)\tilde{\delta}_0\tilde{M}_0^{\lambda}}{(1-\alpha\tilde{M}_0)} \quad . \tag{50}$$

One restriction that must be placed on solutions of Equations (48) and (49) is that $\mathscr{V}_1 \equiv 0$ at $\mathscr{V}_0 = \mathscr{V}_c$. This is a consequence of Section II. 2. 1. 1, i. e., $\tilde{D}(\mathscr{V}) = 0$ defines $\mathscr{V}_c$ which is a pure number, hence all higher order terms in the expansion for $\mathscr{V}$ must be zero at the critical point. Near $\mathscr{V}_0 = \mathscr{V}_c$, $d_i(\mathscr{V}_0) \sim (\mathscr{V}_0 - \mathscr{V}_c)$, hence Equation (49) has the solution:

$$\mathscr{V}_1 \sim \frac{\text{const.}}{\mathscr{V}_0 - \mathscr{V}_c} + \Phi(\mathscr{V}_c)(\mathscr{V}_0 - \mathscr{V}_c) + \cdots \quad .$$

Thus, the constant of integration for Equation (49) must be chosen to be zero. All of the perturbation functions $\tilde{M}_1$, $\tilde{\delta}_1$ and $\mathscr{V}_1$ are then regular at the critical point. Analytically matching of the downstream solution to the upstream solution presents no problems.

Attention will first be focused on the solution for $\tilde{x} < 0$. In this region $\alpha \equiv 1$. Turning to the right hand sides of Equations (48) one finds that the functions can be written:

$$\frac{A_1(\mathscr{X})}{A_2(\mathscr{X})}\,\frac{[b_1(\mathscr{X})+b_2(\mathscr{X})]}{\tilde{\delta}_0} = \frac{\mathscr{X}R-JP}{[A_2(\mathscr{X})]^2}\,\frac{\tilde{D}(\mathscr{X})}{\tilde{\delta}_0} \equiv E(\mathscr{X})$$

$$\frac{A_3(\mathscr{X})}{A_2(\mathscr{X})}\,\frac{[b_2(\mathscr{X})-b_3(\mathscr{X})]}{\tilde{\delta}_0} = -3E(\mathscr{X}) - \frac{R}{JA_2(\mathscr{X})}\,\frac{\tilde{D}(\mathscr{X})}{\tilde{\delta}_0}$$

$$= -3E(\mathscr{X}) - G(\mathscr{X})$$

where $G(\mathscr{X}) \equiv \frac{R}{JA_2(\mathscr{X})}\,\frac{\tilde{D}(\mathscr{X})}{\tilde{\delta}_0}$. The function $\frac{E(\mathscr{X}_0)}{1-\tilde{M}_0}$ is non-singular as $\tilde{M}_0 \to 1$ ($\mathscr{X}_0 \to \mathscr{X}_B$) since $\mathscr{X}_0 R_0 = J_0 P_0$ defines $\mathscr{X}_0 = \mathscr{X}_B$. Splitting the function $G(\mathscr{X}_0)$ into a non-singular and a singular part and noting that, near $\mathscr{X}_0 = \mathscr{X}_B$, $\tilde{M}_0 - 1 \sim \frac{A_1(\mathscr{X}_B)}{A_2(\mathscr{X}_B)}(\mathscr{X}_0 - \mathscr{X}_B)$, we can write solutions of Equations (48) as

$$\begin{aligned} \tilde{M}_1 - \frac{A_1(\mathscr{X}_0)}{A_2(\mathscr{X}_0)}\,\mathscr{X}_1 &= \tilde{V}_1(\mathscr{X}_0) + C_1 \\ \tilde{\delta}_1 - \frac{A_3(\mathscr{X}_0)}{A_2(\mathscr{X}_0)}\,\mathscr{X}_1 &= \tilde{V}_2(\mathscr{X}_0) + K_1 \ln\left(\frac{\mathscr{X}_0-\mathscr{X}_B}{\mathscr{X}_c-\mathscr{X}_B}\right) + C_2 \end{aligned} \tag{51}$$

where $\tilde{V}_1(\mathscr{X}_0)$, $\tilde{V}_2(\mathscr{X}_0)$ and K_1 are defined in Table II. The functions $\tilde{V}_1$ and $\tilde{V}_2$ are regular functions at $\mathscr{X}_0 = \mathscr{X}_B$. Substituting Equations (51) into Equation (49) yields:

$$\frac{d}{d\mathscr{X}_0}\left[\mathscr{X}_1\,\frac{T(\mathscr{X}_0)}{\tilde{M}_0-1}\right] = -\frac{T(\mathscr{X}_0)}{\tilde{M}_0-1}\left\{\tilde{V}_2(\mathscr{X}_0)+K_1 \ln\frac{\mathscr{X}_0-\mathscr{X}_B}{\mathscr{X}_c-\mathscr{X}_B} + C_2 + \left[\lambda - \frac{\tilde{M}_0}{\tilde{M}_0-1}\right][\tilde{V}_1(\mathscr{X}_0)+C_1] - \frac{b_2(\mathscr{X}_0)}{\tilde{\delta}_0(\tilde{M}_0-1)}\right\} \tag{52}$$

where $T(\mathscr{M}_0)$ is defined in Table II. Equation (52) can be written as

$$\frac{d}{d\mathscr{M}_0}\left[\mathscr{M}_1 \frac{T(\mathscr{M}_0)}{\tilde{M}_0-1}\right] = \frac{I_1(\mathscr{M}_0)}{\tilde{M}_0-1} - K_1 \frac{T(\mathscr{M}_0)}{\tilde{M}_0-1} \ell n\left(\frac{\mathscr{M}_0-\mathscr{M}_B}{\mathscr{M}_c-\mathscr{M}_B}\right) - \left\{\frac{I_2(\mathscr{M}_0)}{(\tilde{M}_0-1)^2} - \frac{I_2(\mathscr{M}_B)}{(\mathscr{M}_0-\mathscr{M}_B)^2}\left[\frac{A_2(\mathscr{M}_B)}{A_1(\mathscr{M}_B}\right]^2\right\} - I_2(\mathscr{M}_B)\left[\frac{A_2(\mathscr{M}_B)}{A_1(\mathscr{M}_B)}\right]^2 \frac{1}{(\mathscr{M}_0-\mathscr{M}_B)^2} \tag{53}$$

where $I_1(\mathscr{M}_0)$ and $I_2(\mathscr{M}_0)$ are defined in Table II. The most singular part of the right hand side of Equation (53), as $\mathscr{M}_0 \to \mathscr{M}_B$, is the last term which is $\sim 1/(\mathscr{M}_0-\mathscr{M}_B)^2$. When integrated and multiplied by $\tilde{M}_0-1 \sim (\mathscr{M}_0-\mathscr{M}_B)$, a constant remains. All other terms vanish with $\tilde{M}_0-1$. Hence the solution of Equation (53) is most conveniently written as:

$$\mathscr{M}_1 = \frac{\tilde{M}_0-1}{T(\mathscr{M}_0)}\left\{\tilde{S}_1(\mathscr{M}_0) + K_2 \frac{\mathscr{M}_c-\mathscr{M}_0}{\mathscr{M}_0-\mathscr{M}_B}\right\} \tag{54}$$

where $\tilde{S}_1(\mathscr{M}_0)$ and K_2 are defined in Table II and the constant of integration has been set to zero in accordance with the previous discussion.

Finally, the solution of Equation (50) is:

$$\tilde{x} = C_B\left\{\tilde{\Omega}_2(\mathscr{M}_0) + K_3 \ell n \frac{\mathscr{M}_0-\mathscr{M}_B}{\mathscr{M}_c-\mathscr{M}_B}\right\} \tag{55}$$

where $\tilde{\Omega}_2(\mathscr{M}_0)$ and K_3 are defined in Table II.

This completes the derivation of the first order solution for $\tilde{x} < 0$ except that the constants C_1 and C_2 are still unknown. The solution for $\tilde{x} > 0$ can be found in a similar manner. In this region $\alpha \equiv 1 - \frac{\gamma-1}{2} M_\infty \alpha_w$. The function $\frac{E(\mathscr{K}_0)}{1-\alpha\tilde{M}_0}$ must be split into a singular and non-singular part in this region since $E(\mathscr{K}_0)$ does not tend to zero as $\mathscr{K}_0 \to \mathscr{K}_p$. Otherwise the forms of the solution are the same as for the upstream solution:

$$\begin{aligned} \tilde{M}_1 - \frac{A_1(\mathscr{K}_0)}{A_2(\mathscr{K}_0)}\mathscr{K}_1 &= \tilde{W}_1(\mathscr{K}_0) - L_1 \ln\left(\frac{\mathscr{K}_p-\mathscr{K}_0}{\mathscr{K}_p-\mathscr{K}_c}\right) + C_3 \\ \tilde{\delta}_1 - \frac{A_3(\mathscr{K}_0)}{A_2(\mathscr{K}_0)}\mathscr{K}_1 &= \tilde{W}_2(\mathscr{K}_0) - L_2 \ln\left(\frac{\mathscr{K}_p-\mathscr{K}_0}{\mathscr{K}_p-\mathscr{K}_c}\right) + C_4 \end{aligned} \qquad (56)$$

where $\tilde{W}_1(\mathscr{K}_0)$, $\tilde{W}_2(\mathscr{K}_0)$, L_1 and L_2 are defined in Table II. Matching these solutions at the corner gives:

$$C_3 = C_1 \quad ; \quad C_4 = C_2 \quad .$$

In a manner similar to that used to derive the upstream solution for $\mathscr{K}_1$, the downstream solution is:

$$\mathscr{K}_1 = \frac{1-\alpha\tilde{M}_0}{T(\mathscr{K}_0)}\left\{\tilde{S}_2(\mathscr{K}_0) + L_4 \frac{\mathscr{K}_0-\mathscr{K}_c}{\mathscr{K}_p-\mathscr{K}_0} + \frac{L_5}{\mathscr{K}_p-\mathscr{K}_0}\ln\left(\frac{\mathscr{K}_p-\mathscr{K}_0}{\mathscr{K}_p-\mathscr{K}_c}\right)\right\} \qquad (57)$$

where $\tilde{S}_2(\mathscr{K}_0)$, L_4 and L_5 are defined in Table II. Again, the singular integral $\tilde{S}_2(\mathscr{K}_0)$ tends to infinity more slowly than $\mathscr{K}_p - \mathscr{K}_0$ tends to zero; $(1-\alpha\tilde{M}_0)\tilde{S}_2(\mathscr{K}_0) \to 0$ as $\mathscr{K}_0 \to \mathscr{K}_p$.

Finally, the physical plane solution is:

$$\tilde{x} = C_B\left\{\tilde{Q}_3(\mathscr{K}_0) + L_6 \ln\left(\frac{\mathscr{K}_p-\mathscr{K}_0}{\mathscr{K}_p-\mathscr{K}_c}\right)\right\} \qquad (58)$$

where $\tilde{Q}_3(\mathscr{V}_0)$ and L_6 are defined in Table II.

The results for this section can be summarized as follows:

$$\begin{aligned}
\tilde{M}_1(\mathscr{V}_0) - \frac{A_1(\mathscr{V}_0)}{A_2(\mathscr{V}_0)}\mathscr{V}_1(\mathscr{V}_0) &= \tilde{V}_1(\mathscr{V}_0) + C_1 \\
\tilde{\delta}_1(\mathscr{V}_0) - \frac{A_3(\mathscr{V}_0)}{A_2(\mathscr{V}_0)}\mathscr{V}_1(\mathscr{V}_0) &= \tilde{V}_2(\mathscr{V}_0) + K_1 \ln\left(\frac{\mathscr{V}_0-\mathscr{V}_B}{\mathscr{V}_c-\mathscr{V}_B}\right) + C_2 \qquad (59) \\
\mathscr{V}_1(\mathscr{V}_0) &= \frac{\tilde{M}_0-1}{T(\mathscr{V}_0)}\left\{\tilde{S}_1(\mathscr{V}_0) + K_2\frac{\mathscr{V}_c-\mathscr{V}_0}{\mathscr{V}_0-\mathscr{V}_B}\right\}
\end{aligned}$$

are the phase plane solutions valid for $\mathscr{V}_B < \mathscr{V}_0 \le \mathscr{V}_c$. The above phase plane solutions are related to the physical plane by:

$$\tilde{x} = C_B\left\{\tilde{Q}_2(\mathscr{V}_0) + K_3 \ln\left(\frac{\mathscr{V}_0-\mathscr{V}_B}{\mathscr{V}_c-\mathscr{V}_B}\right)\right\} \quad . \qquad (60)$$

The constants of integration C_1 and C_2 remain in the solutions for $\mathscr{V}_B < \mathscr{V}_0 \le \mathscr{V}_c$. These can be obtained by matching the solutions with the outer solutions (weak interaction expansions).

$$\begin{aligned}
\tilde{M}_1(\mathscr{V}_0) - \frac{A_1(\mathscr{V}_0)}{A_2(\mathscr{V}_0)}\mathscr{V}_1(\mathscr{V}_0) &= \tilde{W}_1(\mathscr{V}_0 - L_1 \ln\left(\frac{\mathscr{V}_p-\mathscr{V}_0}{\mathscr{V}_p-\mathscr{V}_c}\right) + C_1 \\
\tilde{\delta}_1(\mathscr{V}_0) - \frac{A_3(\mathscr{V}_0)}{A_2(\mathscr{V}_0)}\mathscr{V}_1(\mathscr{V}_0) &= \tilde{W}_2(\mathscr{V}_0) - L_2 \ln\left(\frac{\mathscr{V}_p-\mathscr{V}_0}{\mathscr{V}_p-\mathscr{V}_c}\right) + C_2 \qquad (61) \\
\mathscr{V}_1(\mathscr{V}_0) &= \frac{1-\alpha\tilde{M}_0}{T(\mathscr{V}_0)}\left\{\tilde{S}_2(\mathscr{V}_0) + L_4\frac{\mathscr{V}_0-\mathscr{V}_c}{\mathscr{V}_p-\mathscr{V}_0} + \frac{L_5}{\mathscr{V}_p-\mathscr{V}_0}\ln\left(\frac{\mathscr{V}_p-\mathscr{V}_0}{\mathscr{V}_p-\mathscr{V}_c}\right)\right\}
\end{aligned}$$

are the phase plane solutions valid for $\mathscr{V}_c \le \mathscr{V}_0 < \mathscr{V}_p$. The phase plane solutions for $\mathscr{V}_c \le \mathscr{V}_0 < \mathscr{V}_p$ are related to the physical plane by

$$\tilde{x} = C_B\left\{\tilde{Q}_3(\mathscr{V}_0) + L_6 \ln\left(\frac{\mathscr{V}_p-\mathscr{V}_0}{\mathscr{V}_p-\mathscr{V}_c}\right)\right\} \quad . \qquad (62)$$

Evaluation of the constants C_1 and C_2 completes the derivation of the inner solution. Recalling that the outer solution, upstream of the corner, is given by:

$$\tilde{M} = 1 + \frac{\epsilon\, m_1}{\sqrt{\bar{x}}} + \cdots$$

$$\tilde{\delta} = \delta_B \sqrt{\bar{x}} \left\{1 + \epsilon \frac{\delta_1}{\sqrt{\bar{x}}} + \cdots\right\}$$

$$\mathscr{K} = \mathscr{K}_B + \epsilon \frac{h_1}{\sqrt{\bar{x}}} + \cdots$$

one can write, in terms of the inner variable, $\bar{x}-1 = \epsilon\, \tilde{x}$:

$$\tilde{M} = 1 + \epsilon\, m_1 + \cdots$$

$$\tilde{\delta} = \delta_B \left\{1 + \epsilon \left[\delta_1 + \frac{\tilde{x}}{2}\right] + \cdots\right\}$$

$$\mathscr{K} = \mathscr{K}_B + \epsilon\, h_1 + \cdots$$

correct to order ϵ. The asymptotic forms of the inner solution, as $\tilde{x} \to -\infty$, are:

$$\frac{\mathscr{K}_0 - \mathscr{K}_B}{\mathscr{K}_c - \mathscr{K}_B} \sim \exp\left\{\frac{1}{K_3 C_B}\left[\tilde{x} - C_B \tilde{Q}_2(\mathscr{K}_B)\right]\right\}$$

$$\tilde{M}_1 - \frac{A_1(\mathscr{K}_B)}{A_2(\mathscr{K}_B)}\mathscr{K}_1 \sim \tilde{V}_1(\mathscr{K}_B) + C_1$$

$$\tilde{\delta}_1 - \frac{A_3(\mathscr{K}_B)}{A_2(\mathscr{K}_B)}\mathscr{K}_1 \sim \tilde{V}_2(\mathscr{K}_B) + \frac{K_1}{K_3 C_B}\left[\tilde{x} - C_B \tilde{Q}_2(\mathscr{K}_B)\right] + C_2$$

$$\mathscr{K}_1 \sim \frac{A_1(\mathscr{K}_B)}{A_2(\mathscr{K}_B)} \frac{K_2}{T(\mathscr{K}_B)} \cdot (\mathscr{K}_c - \mathscr{K}_B) = -\frac{A_2(\mathscr{K}_B)}{A_1(\mathscr{K}_B)}\left[\tilde{V}_1(\mathscr{K}_B) + C_1 + \frac{b_2(\mathscr{K}_B)}{\delta_B}\right]$$

therefore,

$$\tilde{M}_1 \sim -\frac{b_2(\mathscr{K}_B)}{\delta_B} = \frac{b_1(\mathscr{K}_B)}{\delta_B} = -\frac{R_B}{J_B}\frac{(1+\mathscr{K}_B)}{\delta_B} \equiv m_1$$

$$\tilde{\delta}_1 \sim \tilde{V}_2(\mathscr{K}_B) + \frac{1}{2}\left[\tilde{x} - C_B\tilde{Q}_2(\mathscr{K}_B)\right] - \frac{A_3(\mathscr{K}_B)}{A_1(\mathscr{K}_B)}\left[\tilde{V}_1(\mathscr{K}_B)+C_1-m_1\right]+C_2 .$$

The matching requirements are then:

$$\begin{aligned} C_1 &= m_1 - \frac{A_1(\mathscr{K}_B)}{A_2(\mathscr{K}_B)}h_1 - \tilde{V}_1(\mathscr{K}_B) \\ C_2 &= \delta_1 - \frac{A_3(\mathscr{K}_B)}{A_2(\mathscr{K}_B)}h_1 - \tilde{V}_2(\mathscr{K}_B) + \frac{C_B}{2}\tilde{Q}_2(\mathscr{K}_B) \quad . \end{aligned} \tag{63}$$

Determination of the constants C_1 and C_2 completes the inner solution; the downstream solution is uniquely determined. The asymptotic forms of the downstream solution can now be determined. These forms can be used to determine the constants of the outer solution ($x^* > 0$) and a uniformly valid composite solution can then be constructed.

II. 2. 2. 2. Relaxation Solution

The asymptotic forms of the inner solution can now be determined as $\tilde{x} \to +\infty$ ($\mathscr{K}_0 \to \mathscr{K}_p$). They are:

$$\mathscr{K}_p - \mathscr{K}_0 \sim (\mathscr{K}_p - \mathscr{K}_c)\exp\left\{\frac{\alpha^\lambda}{d_1(\mathscr{K}_p)\delta_p}\left[\tilde{x} - C_B\tilde{Q}_3(\mathscr{K}_p)\right]\right\}$$

which tends to zero exponentially since $d_1(\mathscr{K}_p) < 0$.

$$\tilde{M}_0 \sim \frac{1}{\alpha}\left\{1 - \frac{A_1(\mathscr{K}_p)}{A_2(\mathscr{K}_p)}(\mathscr{K}_p - \mathscr{K}_0)\right\} = \frac{1}{\alpha}\left\{1 - \text{const. } e^{-\gamma_1^2\tilde{x}}\right\}$$

$$\tilde{\delta}_0 \sim \delta_p\left\{1 + \text{const. } e^{-\gamma_2^2\tilde{x}}\right\}$$

where $\delta_p = C_B\,\alpha^3/J_p$.

$$\mathscr{K}_1 \sim \mathscr{K}_{1p} + S_1 \left[\tilde{x} - C_B \tilde{Q}_3(\mathscr{K}_p) \right]$$

$$\tilde{M}_1 \sim \frac{b_1(\mathscr{K}_p)}{\delta_p}$$

$$\tilde{\delta}_1 \sim \delta_{1p} + S_2 \left[\tilde{x} - C_B \tilde{Q}_3(\mathscr{K}_p) \right]$$

where

$$\mathscr{K}_{1p} = \frac{A_2(\mathscr{K}_p)}{A_1(\mathscr{K}_p)} \left\{ \frac{b_1(\mathscr{K}_p)}{\delta_p} - \left[\tilde{W}_1(\mathscr{K}_p) + C_1 \right] \right\}$$

$$\delta_{1p} = \frac{A_3(\mathscr{K}_p)}{A_2(\mathscr{K}_p)} \mathscr{K}_{1p} + \tilde{W}_2(\mathscr{K}_p) + C_2$$

$$S_1 = \frac{A_2(\mathscr{K}_p)}{A_1(\mathscr{K}_p)} \left[b_1(\mathscr{K}_p) + b_2(\mathscr{K}_p) \right] \frac{\alpha^\lambda}{d_1(\mathscr{K}_p)\delta_p^2}$$

$$S_2 = \frac{A_3(\mathscr{K}_p)}{A_1(\mathscr{K}_p)} \left[b_1(\mathscr{K}_p) + b_3(\mathscr{K}_p) \right] \frac{\alpha^\lambda}{d_1(\mathscr{K}_p)\delta_p^2} \quad .$$

Thus the expansion, in the inner region is:

$$\tilde{M}(\tilde{x};\epsilon) \sim \frac{1}{\alpha} \left[1 + \epsilon \frac{b_1(\mathscr{K}_p)}{\delta_p} + \cdots \right]$$

$$\tilde{\delta}(\tilde{x};\epsilon) \sim \delta_p \left[1 + \epsilon \left\{ \delta_{1p} + S_2 \left[\tilde{x} - C_B \tilde{Q}_3(\mathscr{K}_p) \right] \right\} + \cdots \right] \qquad (64)$$

$$\mathscr{K}(\tilde{x};\epsilon) \sim \mathscr{K}_p + \epsilon \left\{ \mathscr{K}_{1p} + S_1 \left[\tilde{x} - C_B \tilde{Q}_3(\mathscr{K}_p) \right] \right\} + \cdots \quad .$$

Equations (64) provide the constants to complete the downstream solution. With this, attention is turned to the outer solution.

Equations (38) are rewritten in the form:

$$M_1^* + \delta_1^* = \frac{b_1'(\mathscr{K}_0^*)}{b_1(\mathscr{K}_0^*)}\mathscr{K}_1^* - \frac{d_1(\mathscr{K}_0^*)}{b_1(\mathscr{K}_0^*)}\,\frac{\delta_0^{*2}}{\alpha^\lambda}\,\frac{dM_0^*}{dx^*}$$

$$\frac{d\mathscr{K}_1^*}{dx^*} = \frac{d\mathscr{K}_0^*}{dx^*}\left\{\lambda M_0^* - 2\delta_1^* + (M_1^*+\delta_1^*)\,\frac{b_1(\mathscr{K}_0^*)}{b_1(\mathscr{K}_0^*)+b_2(\mathscr{K}_0^*)}\right.$$

$$\left. + \left[\frac{b_2(\mathscr{K}_0^*)}{b_1(\mathscr{K}_0^*)+b_2(\mathscr{K}_0^*)}\cdot\frac{b_2'(\mathscr{K}_0^*)}{b_2(\mathscr{K}_0^*)} - \frac{d_2'(\mathscr{K}_0^*)}{d_2(\mathscr{K}_0^*)}\right]\mathscr{K}_1^*\right\} \qquad (65)$$

$$\frac{d\delta_1^*}{dx^*} = \frac{1}{\delta_0^*}\,\frac{d\delta_0^*}{dx^*}\left\{\lambda M_0^* - 2\delta_1^* + (M_1^*+\delta_1^*)\,\frac{b_1(\mathscr{K}_0^*)}{b_1(\mathscr{K}_0^*)+b_3(\mathscr{K}_0^*)}\right.$$

$$\left. + \left[\frac{b_3(\mathscr{K}_0^*)}{b_1(\mathscr{K}_0^*)+b_3(\mathscr{K}_0^*)}\,\frac{b_3'(\mathscr{K}_0^*)}{b_3(\mathscr{K}_0^*)} - \frac{d_3'(\mathscr{K}_0^*)}{d_3(\mathscr{K}_0^*)}\right]\mathscr{K}_1^*\right\} .$$

The term involving dM_0^*/dx^* in the first of Equations (65) can be written with use of Equation (41) as follows:

$$\frac{d_1(\mathscr{K}_0^*)}{b_1(\mathscr{K}_0^*)}\,\frac{\delta_0^{*2}}{\alpha^\lambda}\,\frac{dM_0^*}{dx^*} = N_2(\mathscr{K}_0^*)\left[\frac{b_1'(\mathscr{K}_0^*)}{b_1(\mathscr{K}_0^*)} - \frac{N_3(\mathscr{K}_0^*)}{N_2(\mathscr{K}_0^*)}\right]M_0^* \qquad (66)$$

where

$$N_i(\mathscr{K}) \equiv \frac{A_i(\mathscr{K})}{A_1(\mathscr{K})} + \frac{B_i(\mathscr{K})}{B_1(\mathscr{K})} .$$

M_1^* can now be eliminated from the second and third of Equations (65) to give:

$$\frac{d}{d\mathscr{K}_0^*}\left[\delta_1^* - \frac{N_3(\mathscr{K}_0^*)}{N_2(\mathscr{K}_0^*)}\,\mathscr{K}_1^*\right] = Z_1(\mathscr{K}_0^*)$$

$$\frac{d}{d\mathscr{K}_0^*}\left[\mathscr{K}_1^*\,T^*(\mathscr{K}_0^*)\right] = T^*(\mathscr{K}_0^*)\left\{Z_2(\mathscr{K}_0^*) - 2\left[\delta_1^* - \frac{N_3(\mathscr{K}_0^*)}{N_2(\mathscr{K}_0^*)}\,\mathscr{K}_1^*\right]\right\} \qquad (67)$$

where $Z_1(\mathscr{K}_0^*)$, $Z_2(\mathscr{K}_0^*)$ and $T^*(\mathscr{K}_0^*)$ are defined in Table II. The functions

$N_3(\mathscr{V}_0^*)/N_2(\mathscr{V}_0^*)$, $Z_1(\mathscr{V}_0^*)$, $Z_2(\mathscr{V}_0^*)$ and $T^*(\mathscr{V}_0^*)$ are all regular at $\mathscr{V}_0^*=\mathscr{V}_c$. Hence the quantities M_0^*, δ_0^*, x^*, M_1^*, δ_1^* and $\mathscr{V}_1^*$ can be computed in the range $\mathscr{V}_B < \mathscr{V}_0^* \leq \mathscr{V}_p$ with no difficulty. Requirements that must be placed on the solutions are:

$$\left.\begin{aligned} M_0^* &\to 0 \\ M_1^* &\to \text{const.} \\ \mathscr{V}_1^* &\to 0 \end{aligned}\right\} \text{ as } \mathscr{V}_0^* \to \mathscr{V}_B.$$

It has been shown previously that $M_0^* \sim (\mathscr{V}_0 - \mathscr{V}_B)^{\beta_1}$ as $\mathscr{V}_0^* \to \mathscr{V}_B$. As $\mathscr{V}_0^* \to \mathscr{V}_B$, $N_2(\mathscr{V}_0^*) \to 0$, therefore

$$\frac{d}{d\mathscr{V}_0^*}\left[\delta_1^* - \frac{N_3(\mathscr{V}_0^*)}{N_2(\mathscr{V}_0^*)}\mathscr{V}_1^*\right] \sim \Phi_1^*(\mathscr{V}_B)(\mathscr{V}_0^*-\mathscr{V}_B)^{\beta_1-2}$$

$$\delta_1^* - \frac{N_3(\mathscr{V}_0^*)}{N_2(\mathscr{V}_0^*)}\mathscr{V}_1^* \sim \frac{\Phi_1^*(\mathscr{V}_B)}{\beta_1-1}(\mathscr{V}_0^*-\mathscr{V}_B)^{\beta_1-1} + \text{const.}$$

$$\frac{d}{d\mathscr{V}_0^*}[\mathscr{V}_1^* T(\mathscr{V}_0^*)] \sim \Phi_2^*(\mathscr{V}_B)(\mathscr{V}_0^*-\mathscr{V}_B)^{-(\beta_1+2)}$$

$$\mathscr{V}_1^* \sim \Phi_3^*(\mathscr{V}_B)(\mathscr{V}_0^*-\mathscr{V}_B)^{\beta_1} \to 0 \quad .$$

The function $\Phi_1^*(\mathscr{V}_B)/(\beta_1-1) = -\Phi_3^*(\mathscr{V}_B)N_3(\mathscr{V}_B)/[N_2'(\mathscr{V}_0^*)]_{\mathscr{V}_0^*=\mathscr{V}_B}$,

therefore

$$\delta_1^* \sim \text{const.}$$

and

$$M_1^* \sim \text{const.}$$

as required. These limiting values guarantee that

$$\left.\begin{aligned} \tilde{M} &= \frac{1}{\alpha}\{1-\epsilon M_0^*(1+\epsilon M_1^*+\cdots)\} \to \frac{1}{\alpha} \\ \mathscr{V} &= \mathscr{V}_0^* + \epsilon\mathscr{V}_1 \to \mathscr{V}_B \end{aligned}\right\} \text{ as } x^* \to +\infty \quad .$$

Solutions of Equations (67) are thus:

$$\begin{aligned} \delta_1^* - \frac{N_3(\mathscr{M}_0^*)}{N_2(\mathscr{M}_0^*)}\,\mathscr{M}_1^* &= U_1^*(\mathscr{M}_0^*) + a_1 \\ \mathscr{M}_1^* &= \frac{1}{T^*(\mathscr{M}_0^*)}\,\{U_2^*(\mathscr{M}_0^*) + a_2\} \end{aligned} \tag{68}$$

where $U_1^*(\mathscr{M}_0^*)$ and $U_2^*(\mathscr{M}_0^*)$ are defined in Table II. The constants a_1 and a_2 can be obtained by matching with the inner solution.

As $\mathscr{M}_0^* \to \mathscr{M}_p$, the asymptotic forms of Equations (40) are given by

$$\begin{aligned} \mathscr{M}_0^* &= \mathscr{M}_p + \frac{\alpha^\lambda}{f_2(\mathscr{M}_p)}\,x^* + \cdots \\ \delta_0^* &= \delta_p\left\{1 + \alpha^\lambda \frac{f_1(\mathscr{M}_p)}{f_2(\mathscr{M}_p)} x^* + \cdots\right\} \end{aligned}$$

where

$$\begin{aligned} f_1(\mathscr{M}_p) &= \frac{N_3(\mathscr{M}_p)}{N_2(\mathscr{M}_p)} \\ f_2(\mathscr{M}_p) &= \frac{d_1(\mathscr{M}_p)}{b_1(\mathscr{M}_p)}\,\frac{\delta_p^2}{N_2(\mathscr{M}_p)} \end{aligned} .$$

Therefore, correct to order ϵ, the outer solution is, written in terms of the inner variable,

$$\begin{aligned} \tilde{M}(\tilde{x};\epsilon) &\sim \frac{1}{\alpha}\left[1 + \epsilon\,\frac{b_1(\mathscr{M}_p)}{\delta_p} + \cdots\right] \\ \delta^*(\tilde{x};\epsilon) &\sim \delta_p\left[1+\epsilon\left\{\alpha^\lambda \frac{f_1(\mathscr{M}_p)}{f_2(\mathscr{M}_p)}\,\tilde{x} + \frac{N_3(\mathscr{M}_p)}{N_2(\mathscr{M}_p)}\,\frac{a_2}{T^*(\mathscr{M}_p)} + a_1\right\} + \cdots\right] \\ \mathscr{M}^*(\tilde{x};\epsilon) &\sim \mathscr{M}_p + \epsilon\left\{\frac{\alpha^\lambda}{f_2(\mathscr{M}_p)}\,\tilde{x} + \frac{a_2}{T^*(\mathscr{M}_p)}\right\} + \cdots \end{aligned} .$$

These forms must be matched to Equations (64); this requires:

$$a_1 = \delta_{1p} - \frac{N_3(\mathscr{K}_p)}{N_2(\mathscr{K}_p)} \mathscr{K}_{1p} - \left[S_2 - \frac{N_3(\mathscr{K}_p)}{N_2(\mathscr{K}_p)} S_1\right] C_B \tilde{Q}_3(\mathscr{K}_p)$$

$$a_2 = T^*(\mathscr{K}_p)\left[\mathscr{K}_{1p} - S_1 C_B \tilde{Q}_3(\mathscr{K}_p)\right] \quad . \tag{69}$$

With a_1 and a_2 determined, a uniformly valid composite solution can now be constructed in the region downstream of the corner as in Section II. 2. 1:

$$\mathscr{K}_{comp.}(x^*;\epsilon) = \mathscr{K}(\tilde{x};\epsilon) + \mathscr{K}^*(x^*;\epsilon) - \mathscr{K}^*(\tilde{x};\epsilon)$$

$$\tilde{\delta}_{comp.}(x^*;\epsilon) = \tilde{\delta}(\tilde{x};\epsilon) + \delta^*(x^*;\epsilon) - \delta^*(\tilde{x};\epsilon) \tag{70}$$

$$\tilde{M}_{comp.}(x^*;\epsilon) = \tilde{M}(\tilde{x};\epsilon) - \epsilon \frac{1}{\alpha}\{M^*(x^*;\epsilon) - M^*(\tilde{x};\epsilon)\}$$

$$\tilde{x} \equiv x^*/\epsilon \quad .$$

II. 3. Summary

The results of Sections II. 2. 1 and II. 2. 2 are summarized in this Section. The quadratures [defined in Table II] are universal functions of the independent variables noted and can be tabulated once and for all. The results, in composite form, are written as follows:

$\tilde{x} \equiv \dfrac{\bar{x} - 1}{\epsilon} \equiv \dfrac{x^*}{\epsilon} < 0$:

$$\tilde{M}(x^*;\epsilon) = \tilde{M}_0(\mathscr{M}_0)\left\{1+\epsilon\,\tilde{M}_1(\mathscr{M}_0)\right\} + \epsilon\, m_1\left\{\frac{1}{\sqrt{1+x^*}} - 1\right\}$$

$$\tilde{\delta}(x^*;\epsilon) = \tilde{\delta}_0(\mathscr{M}_0)\left\{1+\epsilon\,\tilde{\delta}_1(\mathscr{M}_0)\right\} + \delta_B\left\{\sqrt{1+x^*} - \left[1 + \frac{x^*}{2}\right]\right\} \tag{71}$$

$$\mathscr{M}(x^*;\epsilon) = \mathscr{M}_0(\tilde{x}) + \epsilon\left\{\mathscr{M}_1(\mathscr{M}_0)+h_1\left[\frac{1}{\sqrt{1+x^*}} - 1\right]\right\}$$

$$\frac{x^*}{\epsilon} \equiv \tilde{x}(\mathscr{M}_0) = C_B\left[\tilde{Q}_2(\mathscr{M}_0) + K_3\,\ell n\left(\frac{\mathscr{M}_0-\mathscr{M}_B}{\mathscr{M}_c-\mathscr{M}_B}\right)\right]$$

$\tilde{x} > 0$:

$$\tilde{M}(x^*;\epsilon) = \tilde{M}_0(\mathscr{M}_0)\{1+\epsilon\,\tilde{M}_1(\mathscr{M}_0)\} - \epsilon\,\frac{1}{\alpha}\left[M_0^*(\mathscr{M}_0^*)+\frac{b_1(\mathscr{M}_p)}{\delta_p}\right]$$

$$\tilde{\delta}(x^*;\epsilon) = \tilde{\delta}_0(\mathscr{M}_0)\{1+\epsilon\,\tilde{\delta}_1(\mathscr{M}_0)\} + \delta_0^*(\mathscr{M}_0^*)\{1+\epsilon\,\delta_1^*(\mathscr{M}_0^*)\}$$

$$- \delta_p\left\{1+S_2 x^* + \epsilon\left[\frac{N_3(\mathscr{M}_p)}{N_2(\mathscr{M}_p)}\,\frac{a_2}{T^*(\mathscr{M}_p)} + a_1\right]\right\} \tag{72}$$

$$\mathscr{M}(x^*;\epsilon) = \mathscr{M}_0(\tilde{x}) + \epsilon\mathscr{M}_1(\mathscr{M}_0) + \mathscr{M}_0^*(x^*) + \epsilon\mathscr{M}_1(\mathscr{M}_0^*)$$

$$- \left\{\mathscr{M}_p + S_1 x^* + \epsilon\,\frac{a_2}{T^*(\mathscr{M}_p)}\right\}$$

$$\tilde{x}(\mathscr{M}_0) = C_B\left[\tilde{Q}_3(\mathscr{M}_0) + L_6\,\ell n\left(\frac{\mathscr{M}_p-\mathscr{M}_0}{\mathscr{M}_p-\mathscr{M}_c}\right)\right];\ x^*(\mathscr{M}_0^*) = Q_2^*(\mathscr{M}_0^*)$$

The functions $\tilde{M}_1$, $\tilde{\delta}_1$ and $\tilde{\mathscr{M}}_1$ have different definitions upstream and downstream of the corner. They are:

$$\tilde{M}_1(\mathscr{X}_0) = \begin{cases} \dfrac{A_1(\mathscr{X}_0)}{A_2(\mathscr{X}_0)}\,\mathscr{X}_1 + \tilde{V}_1(\mathscr{X}_0) + C_1 & \mathscr{X}_B < \mathscr{X}_0 \le \mathscr{X}_c \\ \dfrac{A_1(\mathscr{X}_0)}{A_2(\mathscr{X}_0)}\,\mathscr{X}_1 + \tilde{W}_1(\mathscr{X}_0) - L_1 \ell n\left(\dfrac{\mathscr{X}_p - \mathscr{X}_0}{\mathscr{X}_p - \mathscr{X}_c}\right) + C_1 & \mathscr{X}_c \le \mathscr{X}_0 < \mathscr{X}_p \end{cases}$$

$$\tilde{\delta}_1(\mathscr{X}_0) = \begin{cases} \dfrac{A_3(\mathscr{X}_0)}{A_2(\mathscr{X}_0)}\,\mathscr{X}_1 + \tilde{V}_2(\mathscr{X}_0) + K_1 \ell n\left(\dfrac{\mathscr{X}_0 - \mathscr{X}_B}{\mathscr{X}_c - \mathscr{X}_B}\right) + C_2 & \mathscr{X}_B < \mathscr{X}_0 \le \mathscr{X}_c \\ \dfrac{A_3(\mathscr{X}_0)}{A_2(\mathscr{X}_0)}\,\mathscr{X}_1 + \tilde{W}_2(\mathscr{X}_0) - L_2 \ell n\left(\dfrac{\mathscr{X}_p - \mathscr{X}_0}{\mathscr{X}_p - \mathscr{X}_c}\right) + C_2 & \mathscr{X}_c \le \mathscr{X}_0 < \mathscr{X}_p \end{cases} \tag{73}$$

$$\mathscr{X}_1(\mathscr{X}_0) = \begin{cases} \dfrac{\tilde{M}_0 - 1}{T(\mathscr{X}_0)}\left[\tilde{S}_1(\mathscr{X}_0) + K_2 \dfrac{\mathscr{X}_c - \mathscr{X}_0}{\mathscr{X}_0 - \mathscr{X}_B}\right] & \mathscr{X}_B < \mathscr{X}_0 \le \mathscr{X}_c \\ \dfrac{1 - \alpha \tilde{M}_0}{T(\mathscr{X}_0)}\left[\tilde{S}_2(\mathscr{X}_0) + L_4 \dfrac{\mathscr{X}_0 - \mathscr{X}_c}{\mathscr{X}_p - \mathscr{X}_0} + \dfrac{L_5}{\mathscr{X}_p - \mathscr{X}_0} \ell n\left(\dfrac{\mathscr{X}_p - \mathscr{X}_0}{\mathscr{X}_p - \mathscr{X}_c}\right)\right] & \mathscr{X}_c \le \mathscr{X}_0 < \mathscr{X}_p \end{cases}$$

Composites of these solutions are sketched in Fig. 6. The feature of major interest which arises in these solutions is the relaxation region which appears near $\tilde{M} = 1/\alpha$ in the solution for edge Mach number. The Mach number increases to within $\epsilon M_0^*(\mathscr{X}_p)/\alpha$ of its final downstream value $1/\alpha$ on the scale $\tilde{x} = x^*/\epsilon$ while the final increase to $1/\alpha$ takes place on the scale x^*. The requirement that the ratio of the magnitude of this relaxation region to the total inviscid Mach number rise $(1/\alpha - 1)$ be small is representative of the conditions which must exist for the small parameter solutions to be valid. Stating this more precisely, asymptotic solutions of the moment equations can be found which are (i) pressure gradient dominated and (ii) shear and dissipation dominated provided the ratio $\epsilon M_0^*(\mathscr{X}_p)/(1-\alpha) \ll 1$. This ratio is, alternatively,

$$\frac{\epsilon\, M_0^*(\mathcal{K}_p)}{1-\alpha} = \frac{\gamma-1}{2}\frac{\bar{\chi}_\infty}{M_\infty \alpha_w} M_0^*(\mathcal{K}_p) \quad . \tag{74}$$

The function $M_0^*(\mathcal{K}_p)$ can be written as

$$M_0^*(\mathcal{K}_p) \propto \frac{[P]_{\mathcal{K}_p}}{\alpha^3} \propto \frac{[R]_{\mathcal{K}_p}}{\alpha^3}$$

since P and R differ by a constant for $\mathcal{K} \geq \mathcal{K}_{AL}$ (see Appendix). $\mathcal{K}_p$ itself is a unique function of α defined by

$$\mathcal{K}_p = \frac{1 + 0.270\,\alpha^{6.21}}{1 + 1.946\,\alpha^{6.21}} \quad .$$

This expression can be easily derived with the results in the Appendix and is plotted in Fig. 7. Since the wall shear P (or the viscous dissipation R) is proportional to $1/(1-\mathcal{K}_p)$ and $\mathcal{K}_p \to 1$ for $\alpha \to 0$, increasing $M_\infty \alpha_w$ (or decreasing α) forces the ratio given by Equation (74) to increase. If arbitrary values are given this ratio, a limiting curve can be plotted as $\bar{\chi}_\infty$ vs. $M_\infty \alpha_w$ [see Fig. 8] and a convenient measure of flow regime can be obtained. For points above a given curve the ratio of the magnitude of the relaxation region Mach number rise to the total inviscid Mach number rise is larger than the value for that curve (and smaller for points below that curve). A practical limit for which the closed form solutions may be expected to be valid is taken to be

$$\frac{\gamma-1}{2}\frac{\bar{\chi}_\infty}{M_\infty \alpha_w} M_0^*(\mathcal{K}_p) = 0.3 \tag{75}$$

and a check of the solutions was made for a point on this curve.

For points above the line described by Equation (75), one must resort to numerical solutions of Equations (12). Solutions of

this section were obtained for a point on this curve,

$$\left.\begin{aligned} M_\infty &= 5.80 \\ \alpha_w &= 7.4^\circ \end{aligned}\right\} \quad M_\infty \alpha_w = 0.75 \ (\alpha = 0.85 \text{ for } \gamma = 1.4)$$

$$\left.\begin{aligned} \bar{\chi}_\infty &= 0.1 \end{aligned}\right\} \quad \epsilon = 0.004,$$

and compared with a numerical integration of Equations (12).* The composites of the asymptotic solutions are shown in Figs. 9-11. The comparisons with the numerical solutions are shown in Figs. 12-14. For the numerical integration, a finite radius of curvature was used (R_c = .095 inch; R_c/L = .0475, $R_c/\delta^* \sim 5.6$) and this may account for some of the deviation immediately downstream of the critical point (for subcritical-supercritical transition) since the slopes of solutions increase near the critical point as $R_c \to 0$. A composite of the pressure ratio p/p_∞ was constructed from the Mach number solutions since this was the quantity of interest. The composite solutions are:

$$x^* < 0: \quad \frac{p_{comp.}}{p_\infty} = \left[\frac{1}{\tilde{M}_0(\tilde{x})}\right]^{\frac{2\gamma}{\gamma-1}} \left[1 - \frac{2\gamma}{\gamma-1}\,\epsilon \tilde{M}_1(\tilde{x})\right] - \frac{2\gamma}{\gamma-1}\,\epsilon\, m_1\left[\frac{1}{\sqrt{1+x^*}} - 1\right]$$

$$x^* > 0: \quad \frac{p_{comp.}}{p_\infty} = \left[\frac{1}{\tilde{M}_0(\tilde{x})}\right]^{\frac{2\gamma}{\gamma-1}} \left[1 - \frac{2\gamma}{\gamma-1}\,\epsilon \tilde{M}_1(x)\right] + \frac{2\gamma}{\gamma-1}\,\epsilon\alpha^{\frac{2\gamma}{\gamma-1}} \left[M_0^*(x^*) - M_0^*(x_p)\right]$$

The zeroth order and first order functions which were computed are plotted in Figs. 15-18.

The ratio in Equation (74) is a measure of the viscous-inviscid interaction downstream of a sharp corner. A function quite similar

---

* A computer program for numerical solutions was developed by D. Ko at GALCIT. The pertinent details are given in his Ph. D. thesis.(20)

to this can be derived in an intuitive manner. Downstream of an expansion corner the ratio of the induced flow angle, Θ, to the wall angle, α_w, is a measure of the viscous-inviscid interaction (see Fig. 2). Since, for hypersonic flow $\Theta \simeq d\delta^*/dx$ and when properly non-dimensionalized, $d\delta^*/dx = O(\bar{\chi}_\infty/M_\infty)$, the parameter $\bar{\chi}_\infty/(M_\infty \alpha_w)$ is a convenient measure of the flow regime in the expansion problem. If, however, $\bar{\chi}$ is based on flow conditions at downstream infinity, i.e. $\bar{\chi}_2 = (M_2/M_\infty)^3 (Re_{L_\infty}/Re_{L_2})^{\frac{1}{2}} \bar{\chi}_\infty$, where $M_2/M_\infty = 1/\alpha$, it is easily shown that

$$\bar{\chi}_2 \simeq (1/\alpha)^{\frac{2\gamma-1}{\gamma-1}} \bar{\chi}_\infty .$$

Hence, the requirement for small viscous-inviscid interaction downstream of the corner is

$$\left(\frac{1}{\alpha}\right)^{\frac{2\gamma-1}{\gamma-1}} \frac{\bar{\chi}_\infty}{M_\infty \alpha_w} \ll 1 \quad .$$

The downstream interaction parameter $\bar{\chi}_2$ is amplified by a factor $(1/\alpha)^{4.5}$ (for $\gamma = 1.4$) for the expansion corner and the ratio $(1/\alpha)^{4.5} \bar{\chi}_\infty/(M_\infty \alpha_w)$ first decreases as α_w is increased, then rapidly increases (as $\alpha \to 0$). Even for small but finite $\bar{\chi}_\infty$, a strongly interacting boundary layer can be induced by simply increasing the expansion angle.

III. EXPERIMENTAL STUDY

III. 1. Scope

The experimental studies of supersonic flows expanded by a corner which have been reported in the literature have been concerned with relatively low Mach numbers ($\sim$ 2 to 4) and as a consequence relatively low values of the viscous interaction parameters $\overline{\chi}_\infty$. As a result, detailed measurements of flow quantities in the vicinity of the corner have not been obtained. The experiments of Puhl[26] carried out for a 10^o cone-cylinder expansion have given a beautifully detailed picture of the pressure distribution near the juncture (cone Mach number $\sim$ 6), however an axisymmetric experimental result is not subject to a simple analytical treatment.

The objective of this part of the study was to provide a two-dimensional experimental study with attention given to measurement of flow properties in the vicinity of the corner. No exhaustive variation of parameters was attempted; specifically, the Reynolds number was varied, to a limited extent, for a fixed expansion angle and the effect of radius of curvature was briefly examined.

Surface pressure data were obtained for four different Reynolds numbers and pitot pressure surveys of the boundary layer were made at seven locations in the vicinity of the corner for two of these Reynolds numbers. These data serve to describe the profile quantities of interest with appropriate assumptions made regarding the static pressure and temperature fields at points away from the surface.

III. 2. Wind Tunnel, Models and Measurements

The experiments described herein were conducted in "leg 2" of the GALCIT hypersonic wind tunnel facility. Leg 2 is a continuously operating, closed circuit tunnel with a nichrome-wire heater, a symmetrical, flexible-plate nozzle, a variable second throat and an after cooler. Details of the facility can be found in Reference (32).

The nozzle plates were adjusted for a nominal Mach number of 8. With this configuration the test section is approximately $7\frac{1}{4}$ inches square. To avoid air liquification, the air in the supply section was heated to 900°F; all tests were conducted at this temperature.

The tests were carried out at four supply pressures ranging from 264.3 p.s.i.a. to 66.2 p.s.i.a. . More completely, the test conditions were:

	①	②	③	④
M	7.93	7.88	7.85	7.78
p_t (p.s.i.a.)	264.3	198.2	132.3	66.2
T_t ($^{\circ}$F)	900	900	900	900
Re (per inch)	1.022×10^5	$.780 \times 10^5$	$.525 \times 10^5$	$.268 \times 10^5$

The supply pressure and temperature were controlled within ± 0.05 p.s.i. and ± 3° F, respectively.

The tests were conducted under steady state conditions. Adequate time was available to establish thermal and dynamic equilibrium in all cases so that the data reported herein are considered for an adiabatic model. No cooling of the model was considered.

Two models were used in the experiments. The dimensions of the first, Model S-1, are shown in Fig. 19. This was a symmetrical

wedge model with a half angle, α_w, of 5^o. The ramp length L was long enough to assure a weakly interacting boundary layer before the corner expansion. The ramp flow, shocked to a pressure well above tunnel free stream pressure, was expanded back to free stream conditions by a 5^o sharp turn to a flat plate. The model did not span the tunnel but rather was sting mounted. Side plates were mounted on the model to prevent outflow; the angle of the plates, α_s, was large enough to completely enclose the leading edge shock wave. The model and side plates were made of stainless steel.

In order that accurate inviscid conditions could be calculated on the approach ramp (these conditions were used as a reference), two precautions were necessary:

(1) The leading edge had to be sharp. The maximum Reynolds number based on tunnel free stream conditions and the measured model wedge tip diameter was 250.

(2) The model had to be aligned at zero incidence with the tunnel free stream. Static pressure orifices were located on the upper and lower wedge surfaces well ahead of the corner interaction region at equal distances from the leading edge. The angle of incidence of the model was varied until the pressures at these two orifices were equal.

With the measured tunnel free stream conditions and wedge half-angle, the inviscid wedge conditions could then be accurately calculated using the oblique shock relations.

The model was instrumented with static pressure orifices distributed along the model centerline. In the corner region the orifices were staggered slightly off centerline to obtain a detailed static pressure distribution very close to the corner. A typical orifice diameter was 0.02 inch, approximately 1/5 of the minimum boundary layer thickness at the corner location. The surface pressures were measured with a multiple-tube silicone oil manometer board. The pressures were recorded for almost every run and the total spread in these data is shown in Fig. 20.

Pitot pressure surveys were made at several stations in the vicinity of the corner from the model surface to the leading edge shock wave. The pitot measurements were made with a flattened (0.04" x 0.004" outer dimensions; 0.0286 x 0.002" inner dimensions) tip probe. The pitot pressure was measured with a Statham 5-psia pressure transducer which was calibrated before and after the test program. The transducer excitation voltage was maintained constant during each run. The pitot measurements were recorded on the Y-scale of a Moseley autograph. The position of the probe relative to the model surface was measured by a helipot connected to the tunnel drive mechanism and recorded on the X-scale. The attitude of the probe was maintained parallel to the model surface upstream and downstream of the corner. All surveys were made normal to the downstream surface. The zero position (surface of the model) was located by electrical contact between the probe tip and the model. The probe position was accurate to ± 0.002 in.

Model S-2 was similar in all respects to Model S-1 except for the following:

(1) The model and side plates were made of brass. The number of measurements for Model S-2 was not expected to be the same as for Model S-1, hence a softer metal was acceptable.

(2) The expansion corner had a finite radius of curvature. This radius was made equal to the approach ramp length (L = 4.100 inches).

III. 3. Evaluation of the Data

III. 3. 1. Experimental Correlations

According to the solutions of Section II. 2., the physical scale for the major portion of the pressure drop is $\tilde{x} \equiv s/(L\epsilon)$. With the approach ramp inviscid pressure as a reference, the static pressures for Model S-1 are plotted as a function of $\tilde{x}$ in Fig. 21. Also shown are the data of Puhl[26] for a 10° axisymmetric configuration. The interaction parameter for an axisymmetric configuration is reduced by a factor $1/\sqrt{3}$ due to the extra dimensional effect, hence the definition $\bar{\chi}_{\infty\,\text{Axisym.}} \equiv \frac{1}{\sqrt{3}}\ \bar{\chi}_{\infty\,2\text{-D}}$ has been used in reducing these data.

According to the first approximation solution of Section II. 2. 1., $p_e/p_\infty \to 1$ as $\tilde{x} \to -\infty$, the pressure ratio is a universal function of $\tilde{x}$ for a given $M_\infty \alpha_w$. Furthermore, the pressure ratio at the corner location is 0.871 and the upstream distribution is a universal curve independent of the expansion angle if the angle is sufficiently large to induce subcritical-supercritical transition (1°-2°). The parameter $M_\infty \alpha_w$ centers only the downstream solution. If the pressures of

Fig. 21 are divided by p_{Ic}/p_{∞} where p_{Ic} is the weak interaction pressure computed at x = L, the corner location, the upstream interaction is effectively scaled out of the distribution and a reasonable correlation is obtained, Fig. 22. In an attempt to scale out the effect of expansion angle, the nondimensional pressure $P_N = [p-p_I(-)] / [p_I(-) - p_I(+)]+1$ was defined and plotted vs. $\tilde{x}$ for the four Reynolds numbers of these experiments and the two Reynolds numbers of the experiments of Puhl.[26] $p_I(-)$ and $p_I(+)$ are the weak interaction pressure distributions corresponding to the upstream and downstream flow conditions, respectively, for the same distance x measured from the leading edge. The results are shown in Fig. 23. The last four points for each of the two-dimensional experimental distributions are systematically low. Otherwise the correlation is good. The reduction in pressure for the last four orifices may be due in part to experimental error since the lowest pressures in the distributions occur at these orifice locations. Another effect may be that of finite plate length.

III. 3. 2. Effect of Radius of Curvature

Static pressure distributions were obtained with Model S-2 which had a corner radius of curvature equal to the ramp length for the same range of Reynolds number as for Model S-1. The ratio of radius of curvature to the boundary layer thickness at the corner varied from about 24 to 33. The difference in the distributions when compared with those for Model S-1 was within the experimental deviation for any one distribution, hence only the data for Model S-1 are presented.

III. 3. 3. Boundary Layer Surveys

The distributions of pitot pressure from the model surface to the leading edge shock wave for the stations surveyed are presented in Figures 24 to 30. These data were reduced to Mach number profiles with the assumption that the static pressure was constant across the boundary layer. The static temperature distribution was approximated by

$$\frac{T}{T_e} = \frac{1 + \sqrt{Pr}\,\frac{\gamma-1}{2} M_e^2}{1 + \sqrt{Pr}\,\frac{\gamma-1}{2} M^2} \quad , \quad Pr = 0.725$$

in computing the density variation through the boundary layer.

In any experiment in which the interaction of boundary layer and leading edge shock wave is significant, measurements at a location well downstream of the leading edge are influenced by non-isentropic effects. The curvature of the leading edge shock wave introduces an entropy gradient across streamlines entering the boundary layer downstream of the leading edge. For the present experiments the total pressure ratio at the edge of the boundary layer p_{t_e}/p_{t_i} was found to be 0.634 at the first surveyed station upstream of the corner interaction region. Here, p_{t_i} is the ideal total pressure computed for the configuration in the absence of a boundary layer. In order to examine the effect of the edge total pressure reduction on the boundary layer profiles, two theoretical calculations were made for a zero pressure gradient boundary layer using the Sutherland viscosity law and assuming Pr = 0.725. For the first of these $p_{t_e}/p_{t_i} = 1$; for the second $p_{t_e}/p_{t_i} = 0.634$. The deviation of the non-ideal Mach number profile from the ideal case is shown in Fig. 31. The

experimental deviation, although qualitatively correct, is larger. The comparison, in fact, is qualitative since the experimental boundary layer was subject to a finite pressure gradient along the entire approach ramp. Figs. 32 and 33 show the deviation in the quantities $\frac{\rho u}{\rho_e u_e}(1 - \frac{u}{u_e})$ and $\frac{\rho}{\rho_e}(1 - \frac{u}{u_e})$ which were used to calculate the form parameter $\mathcal{H}$. Again, the experimental deviation is qualitatively correct but larger for the quantity $\frac{\rho u}{\rho_e u_e}(1 - \frac{u}{u_e})$ and smaller for the quantity $\frac{\rho}{\rho_e}(1 - \frac{u}{u_e})$. Since

$$\mathcal{H} = \frac{\Theta_i}{\delta_i^*} = \frac{\int_0^{\delta_i} \frac{U}{U_e}(1 - \frac{U}{U_e})dY}{\int_0^{\delta_i}(1 - \frac{U}{U_e})dY} = \frac{\int_0^{\delta} \frac{\rho u}{\rho_e u_e}(1 - \frac{u}{u_e})dy}{\int_0^{\delta} \frac{\rho}{\rho_e}(1 - \frac{u}{u_e})dy}$$

the larger percentage increase in the integrand of the numerator compared with integrand of the numerator leads to a value of $\mathcal{H}$ on the approach ramp which is high when compared with the theoretical value. Fig. 34 shows the deviation in the boundary layer mass flux $(1 - \frac{\rho u}{\rho_e u_e})$.

IV. COMPARISON OF THEORY WITH EXPERIMENTAL RESULTS

IV. 1. Numerical Solutions

The experimental results for Model S-1 have been compared with a numerical solution of Equations (12). The lowest experimental value for the interaction parameter $\bar{\chi}_\infty$ is too large for the series solutions of Section II to be valid over the entire range of s. For $s < 0$, however, excellent agreement with numerical solutions was obtained for $\bar{\chi}_\infty$ as large as 0.56. The analytical solutions were used to locate a suitable value for an initial point x_0 from which the numerical integration was started. The details of numerical solutions of Equations (12) are given by Ko[20] and Klineberg.[21] A brief outline for obtaining solutions for the expansion problem is as follows:

The quantities M_e, χ and δ_i^* are "kicked off" from a weak interaction solution at a suitable x_0 which must be found by trial and error (solution Ⓐ below). A good first approximation to x_0 can be obtained using the solutions of Section II. The magnitude of the kick is fixed and x_0 is varied until a solution close to the one which passes smoothly through the critical point (subcritical-supercritical transition) is found. The first critical point is located on the curved portion of the turn (expansion angles of approximately 1°-2° are required to produce a supercritical boundary layer downstream of the corner). Then x_0 is fixed and the magnitude of the kick is varied until the solution is found which passes smoothly through the critical point. Location of the first critical point (M_{e_c}, χ_c, $\delta_{i_c}^*$, x_c) determines the complete solution. The integration from x_c to x_1 (solution Ⓑ below) is a straightforward procedure. To complete the integral solution

(solution Ⓒ below), the quantities M_e, δ_i^* and $\mathcal{H}$ are "kicked off" from a weak interaction solution at a suitable x_2 which, again, must be found by trial and error. The procedure is similar to that for solution Ⓐ. The iteration is continued until M_e, $\mathcal{H}$ and δ_i^* are matched at x_1.

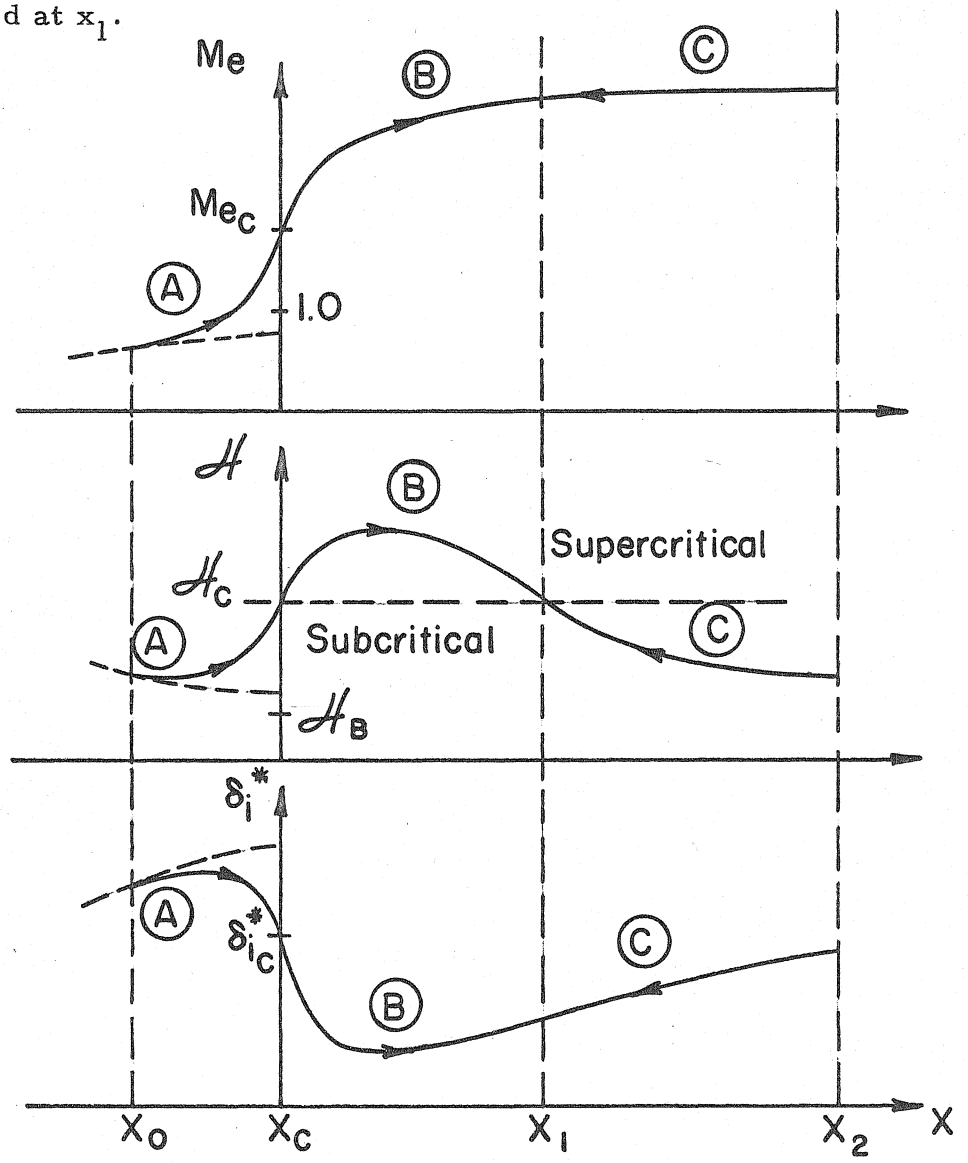

The flow quantities of interest can be computed from these solutions.

IV. 2. Surface Pressure and Profile Quantities

The surface pressure distribution [on the physical scale

$\tilde{x} = s/(L\epsilon)$] is compared with the theoretical result in Fig. 35. The radius of curvature used in the theoretical calculation was $R_c = 0.05$ inch. The integral functions $\mathcal{N}$, R, J, P, etc. were allowed to exceed their adiabatic maximums with use of the extended integral functions for the theoretical calculation. The agreement is fairly good over the complete range of data.

Fig. 36 shows a comparison of the compressible displacement thickness [on the physical scale $x^* = s/L$] with the theoretical result. The displacement thickness was normalized with the theoretical, zero pressure gradient displacement thickness computed at the corner location x = L,

$$\delta_c^* = 1.7239\, L\, \sqrt{C}\, /\sqrt{Re_{L_\infty}}\, [1 + m_\infty\, (1.3841)].$$

The theoretical curve was calculated from the moment method solution as follows:

$$\delta^* = \left(\frac{1+m_e}{1+m_\infty}\right)^{\frac{\gamma+1}{2(\gamma-1)}} \delta_i^*\, [1+m_e(1+\mathcal{N})] .$$

The experimental points are consistently low, however the slopes of the distributions upstream and downstream of the corner are in good agreement. The theoretical curve for the incompressible displacement thickness $\delta_i^* \sqrt{Re_{L_\infty}}\, /(L\sqrt{C}\,) \equiv \tilde{\delta}$ is shown in Fig. 37.

The distribution of $\mathcal{N}$ is compared with the theoretical prediction in Fig. 38. The agreement is fairly good except for the points upstream of the corner. This is due in part to the effect discussed in Section III. 3. 3. ($p_{t_e}/p_{t_i} = 1$ for the theoretical calculation). The experimental results for δ^* and $\mathcal{N}$ are, in addition, subject to the inaccuracy of measurements close to the model surface.

V. CONCLUSIONS

The moment method equations have been used to study the corner expansion of a hypersonic boundary layer. Asymptotic solutions of these equations can be constructed as the viscous interaction parameter $\bar{\chi}_\infty$ tends to zero. These solutions illustrate two distinct physical length scales for the expansion problem. The pressure gradient dominates the interaction on the scale $\tilde{x} \equiv s/(L\varepsilon)$ and the wall shear and dissipation do not influence the solutions to a first approximation. The first approximation solution for the pressure distribution is uniformly valid on this scale. Relaxation solutions for the incompressible displacement thickness $\tilde{\delta}$ and form parameter $\mathcal{H}$ can be obtained on the scale $x^* = s/L$ which allow construction of uniformly valid composite solutions for the entire interaction region. The pressure gradient is absent to a first approximation on the scale x^* and the wall shear and dissipation dominate the interaction in this region.

Higher order solutions in each region show that the pressure drops to within $O(\varepsilon)$ on the physical scale $\tilde{x}$ and gradually decays to the final downstream value on the scale x^*. The second term of the expansion for Mach number in the relaxation region increases rapidly with increasing expansion angle in the matching region ($x^* \to 0$), indicating an amplification of the interaction effect even for small values of $\bar{\chi}_\infty$. This amplification is consistent with a simple examination of the relationship between the viscous interaction parameters based on inviscid conditions upstream and downstream of the corner. The amplification is proportional to $(1/\alpha)^e$ where the exponent, e, is 4.5

for $\gamma = 1.4$. Since α decreases for increasing α_w, the effect of expanding the flow is to induce a strongly interacting boundary layer downstream of the corner. The range of parameters for which the asymptotic solutions may be used has been well defined.

Two-dimensional experimental results have been obtained for a range of parameters which illustrate the nature of the corner interaction both upstream and downstream of the corner for a hypersonic flow. The distributions of displacement thickness δ^* and form parameter $\mathcal{H}$ have been calculated from the data and compared with numerical solutions of the integral equations. The experimental results are in reasonably good agreement with the theoretical predictions. The measured surface pressure distribution has been compared with the moment method solution and the results show good agreement over the entire interaction region.

The integral theory has been modified to allow the profile functions to exceed their limiting values predicted for large pressure gradients and adiabatic flow. Solutions of the Cohen-Reshotko similar flow equations which admit small but finite wall heat transfer have been found which allow this extension.

The effect of transverse pressure gradient near the sharp corner has not been included in the present theoretical study and awaits future investigation. Also, in the course of present study it became apparent that the effect of the entropy jump caused by strong interaction between the boundary layer and the shock wave near the leading edge is important even in the weak interaction region, which merits a further investigation.

TABLE I: PROFILE FUNCTIONS FOR ATTACHED FLOW-ADIABATIC WALL						
SYM	C_0	C_1	C_2	C_3	C_4	C_5
$\mathscr{V}$	0.24711	0.110560	-0.0212235	0.00434545	-0.00097238	0.000099207
J	0.37372	0.169689	-0.023356	0.0057239	-0.00174700	0.000191236
R	1.25782	-0.55550	0.319639	-0.0907667	0.0139831	-0.000934818
P	----	0.487447	-0.0992735	0.0096044	-0.00311057	----
Z	1.03539	0.48373	-0.0150246	0.02609535	-0.00369675	----
$d\mathscr{V}/da$	0.11056	-0.042447	0.01303636	-0.00388951	0.000496034	----
$dJ/d\mathscr{V}$	1.50031	0.28105	-0.042867	0.0026238	----	----

$$SYM = C_0 + C_1 a + C_2 a^2 + \cdots$$

TABLE II

QUADRATURES, FUNCTIONS AND CONSTANTS FOR SECTION II. 2.2.

$$\tilde{V}_1(\mathscr{X}_0) = \int_{\mathscr{X}_c}^{\mathscr{X}_0} \frac{E(\mathscr{X})}{1-\tilde{M}_0}\, d\mathscr{X}$$

$$\tilde{V}_2(\mathscr{X}_0) = -3\, V_1(\mathscr{X}_0) - \int_{\mathscr{X}_c}^{\mathscr{X}_0} \left[\frac{G(\mathscr{X})}{1-\tilde{M}_0} + \frac{G(\mathscr{X}_B)}{(\mathscr{X}-\mathscr{X}_B)} \cdot \frac{A_2(\mathscr{X}_B)}{A_1(\mathscr{X}_B)}\right] d\mathscr{X}$$

$$\tilde{S}_1(\mathscr{X}_0) = \int_{\mathscr{X}_c}^{\mathscr{X}_0} \frac{I_1(\mathscr{X})}{(\tilde{M}_0-1)}\, d\mathscr{X} - K_1 \int_{\mathscr{X}_c}^{\mathscr{X}_0} \frac{T(\mathscr{X})}{\tilde{M}_0-1}\, \ell n \left(\frac{\mathscr{X}-\mathscr{X}_B}{\mathscr{X}_c-\mathscr{X}_B}\right) d\mathscr{X}$$

$$- \int_{\mathscr{X}_c}^{\mathscr{X}_0} \left\{\frac{I_2(\mathscr{X})}{(\tilde{M}_0-1)^2} - \frac{I_2(\mathscr{X}_B)}{(\mathscr{X}-\mathscr{X}_B)^2}\left[\frac{A_2(\mathscr{X}_B)}{A_1(\mathscr{X}_B)}\right]^2\right\} d\mathscr{X}$$

$$K_1 = G(\mathscr{X}_B) \cdot \frac{A_2(\mathscr{X}_B)}{A_1(\mathscr{X}_B)}$$

$$K_2 = I_2(\mathscr{X}_B)\left[\frac{A_2(\mathscr{X}_B)}{A_1(\mathscr{X}_B)}\right]^2 \frac{1}{\mathscr{X}_c-\mathscr{X}_B}$$

$$K_3 = \frac{d_1(\mathscr{X}_B)}{J_B}$$

$$E(\mathscr{X}_0) = \frac{\mathscr{X}_0 R_0 - J_0 P_0}{[A_2(\mathscr{X}_0)]^2} \frac{\tilde{D}(\mathscr{X}_0)}{\tilde{\delta}_0}$$

$$G(\mathscr{X}_0) = \frac{R_0}{J_0 A_2(\mathscr{X}_0)} \frac{\tilde{D}(\mathscr{X}_0)}{\tilde{\delta}_0}$$

$$I_1(\mathscr{X}_0) = -T(\mathscr{X}_0)\{\tilde{V}_2(\mathscr{X}_0) + C_2 + \lambda[\tilde{V}_1(\mathscr{X}_0) + C_1]\}$$

$$I_2(\mathscr{X}_0) = -T(\mathscr{X}_0)\left\{\tilde{M}_0[\tilde{V}_1(\mathscr{X}_0)+C_1] + \frac{b_2(\mathscr{X}_0)}{\tilde{\delta}_0}\right\}$$

$$T(\mathscr{X}_0) = \frac{d_2(\mathscr{X}_0)\tilde{M}_0^{\frac{\gamma+1}{\gamma-1}}}{J_0}$$

TABLE II (Continued)

$$\tilde{Q}_2(\mathscr{N}_0) = \int_{\mathscr{N}_c}^{\mathscr{N}_0}\left[\frac{d_2(\mathscr{N})\tilde{M}_0^{\frac{\gamma+1}{\gamma-1}}}{J_0(\tilde{M}_0-1)} - \frac{d_1(\mathscr{N}_B)}{J_B}\ \frac{1}{\mathscr{N}-\mathscr{N}_B}\right]d\mathscr{N}$$

$$\tilde{W}_1(\mathscr{N}_0) = \int_{\mathscr{N}_c}^{\mathscr{N}_0}\left[\frac{E(\mathscr{N})}{1-\alpha\tilde{M}_0} - \frac{E(\mathscr{N}_p)}{\mathscr{N}_p-\mathscr{N}}\cdot\frac{A_2(\mathscr{N}_p)}{A_1(\mathscr{N}_p)}\right]d\mathscr{N}$$

$$\tilde{W}_2(\mathscr{N}_0) = -3\,\tilde{W}_1(\mathscr{N}_0) - \int_{\mathscr{N}_c}^{\mathscr{N}_0}\left[\frac{G(\mathscr{N})}{1-\alpha\tilde{M}_0} - \frac{G(\mathscr{N}_p)}{\mathscr{N}_p-\mathscr{N}}\frac{A_2(\mathscr{N}_p)}{A_1(\mathscr{N}_p)}\right]d\mathscr{N}$$

$$\tilde{S}_2(\mathscr{N}_0) = \int_{\mathscr{N}_c}^{\mathscr{N}_0}\frac{I_3(\mathscr{N})}{1-\alpha\tilde{M}_0}\,d\mathscr{N} + L_3\int_{\mathscr{N}_c}^{\mathscr{N}_0}\frac{T(\mathscr{N})}{1-\alpha\tilde{M}_0}\ln\left(\frac{\mathscr{N}_p-\mathscr{N}}{\mathscr{N}_p-\mathscr{N}_c}\right)d\mathscr{N}$$

$$+\int_{\mathscr{N}_c}^{\mathscr{N}_0}\left\{\frac{I_4(\mathscr{N})}{(1-\alpha\tilde{M}_0)^2} - \frac{I_4(\mathscr{N}_p)}{(\mathscr{N}_p-\mathscr{N})^2}\left[\frac{A_2(\mathscr{N}_p)}{A_1(\mathscr{N}_p)}\right]^2\right\}d\mathscr{N}$$

$$+L_1\int_{\mathscr{N}_c}^{\mathscr{N}_0}\left\{\frac{\alpha\tilde{M}_0\,T(\mathscr{N})}{(1-\alpha\tilde{M}_0)^2} - \frac{T(\mathscr{N}_p)}{(\mathscr{N}_p-\mathscr{N})^2}\left[\frac{A_2(\mathscr{N}_p)}{A_1(\mathscr{N}_p)}\right]^2\right\}\ln\left(\frac{\mathscr{N}_p-\mathscr{N}}{\mathscr{N}_p-\mathscr{N}_c}\right)d\mathscr{N}$$

$$L_1 = E(\mathscr{N}_p)\cdot\frac{A_2(\mathscr{N}_p)}{A_1(\mathscr{N}_p)}$$

$$L_2 = F(\mathscr{N}_p)\cdot\frac{A_2(\mathscr{N}_p)}{A_1(\mathscr{N}_p)}$$

$$L_3 = [F(\mathscr{N}_p) + \lambda E(\mathscr{N}_p)]\frac{A_2(\mathscr{N}_p)}{A_1(\mathscr{N}_p)}$$

$$L_4 = [I_4(\mathscr{N}_p) + L_1\,T(\mathscr{N}_p)]\cdot\left[\frac{A_2(\mathscr{N}_p)}{A_1(\mathscr{N}_p)}\right]^2\frac{1}{\mathscr{N}_p-\mathscr{N}_c}$$

$$L_5 = L_1\,T(\mathscr{N}_p)\left[\frac{A_2(\mathscr{N}_p)}{A_1(\mathscr{N}_p)}\right]^2$$

$$L_6 = \left(\frac{1}{\alpha}\right)^{\frac{\gamma+1}{\gamma-1}}\frac{d_1(\mathscr{N}_p)}{J_p}$$

TABLE II (Continued)

$$F(\mathscr{V}_0) = -[3E(\mathscr{V}_0) + G(\mathscr{V}_0)]$$

$$I_3(\mathscr{V}_0) = -T(\mathscr{V}_0)\{\tilde{W}_2(\mathscr{V}_0) + C_2 + \lambda[\tilde{W}_1(\mathscr{V}_0) + C_1]\}$$

$$I_4(\mathscr{V}_0) = -T(\mathscr{V}_0)\left\{\alpha\tilde{M}_0[\tilde{W}_1(\mathscr{V}_0) + C_1] + \frac{b_2(\mathscr{V}_0)}{\tilde{\delta}_0}\right\}$$

$$\tilde{Q}_3(\mathscr{V}_0) = \int_{\mathscr{V}_c}^{\mathscr{V}_0}\left[\frac{d_2(\mathscr{V})\tilde{M}_0^{\frac{\gamma+1}{\gamma-1}}}{J_0(\alpha\tilde{M}_0 - 1)} + \left(\frac{1}{\alpha}\right)^{\frac{\gamma+1}{\gamma-1}}\frac{d_1(\mathscr{V}_p)}{J_p}\frac{1}{\mathscr{V}_p - \mathscr{V}}\right]d\mathscr{V}$$

$$Z_1(\mathscr{V}_0^*) \equiv \frac{A_2(\mathscr{V}_0^*)}{A_1(\mathscr{V}_0^*)}\left[\frac{b_1'(\mathscr{V}_0^*)}{b_1(\mathscr{V}_0^*)} - \frac{N_3(\mathscr{V}_0^*)}{N_2(\mathscr{V}_0^*)}\right]\left[\frac{N_3(\mathscr{V}_0^*)}{N_2(\mathscr{V}_0^*)} - \frac{A_3(\mathscr{V}_0^*)}{A_2(\mathscr{V}_0^*)}\right]M_0^*$$

$$Z_2(\mathscr{V}_0^*) = \left\{\lambda - \frac{A_2(\mathscr{V}_0^*)}{A_1(\mathscr{V}_0^*)}\left[\frac{b_1'(\mathscr{V}_0^*)}{b_1(\mathscr{V}_0^*)} - \frac{N_3(\mathscr{V}_0^*)}{N_2(\mathscr{V}_0^*)}\right]\right\}M_0^*$$

$$T^*(\mathscr{V}_0^*) = \frac{d_1(\mathscr{V}_0^*)\,\delta_0^{*2}}{b_1(\mathscr{V}_0^*)\,N_2(\mathscr{V}_0^*)}$$

$$U_1^*(\mathscr{V}_0^*) = \int_{\mathscr{V}_p}^{\mathscr{V}_0^*} Z_1(\mathscr{V})d\mathscr{V}$$

$$U_2^*(\mathscr{V}_0^*) = \int_{\mathscr{V}_p}^{\mathscr{V}_0^*} T^*(\mathscr{V})\{Z_2(\mathscr{V}) - 2[U_1(\mathscr{V}) + a_1]\}d\mathscr{V}$$

$$Q_1^*(\mathscr{V}_0^*) = \int_{\mathscr{V}_p}^{\mathscr{V}_0^*}\frac{P_0J_0' - R_0}{\mathscr{V}R_0 - J_0P_0}d\mathscr{V}$$

$$Q_2^*(\mathscr{V}_0^*) = \frac{1}{\alpha\lambda}\int_{\mathscr{V}_p}^{\mathscr{V}_0^*}\frac{A_1(\mathscr{V})}{\mathscr{V}R_0 - J_0P_0}\delta_0^{*2}(\mathscr{V})d\mathscr{V}$$

REFERENCES

1. Howarth, L.: "The Propagation of Steady Disturbances in a Supersonic Stream Bounded on One Side by a Parallel Subsonic Stream," Proc. Camb. Phil. Soc., Vol. 44, Part 3, 380 (1947).

2. Tsien, H. S. and Finston, M.: "Interaction Between Parallel Streams of Subsonic and Supersonic Velocities," J. Aeronaut. Sci., 16:9, 515-528 (1949).

3. Lighthill, M. J.: "Reflection at a Laminar Boundary Layer of a Weak Steady Disturbance to a Supersonic Stream Neglecting Viscosity and Heat Conduction," Quart. J. Mech. Appl. Math., Vol. III, Part 3, 303-325 (1950).

4. Lighthill, M. J.: "On Boundary Layers and Upstream Influence: II. Supersonic Flows Without Separation," Proc. Roy. Soc. (A), Vol. 217, 478 (1953).

5. Sullivan, R. D., Donaldson, C. du P. and Hayes, W. D.: "Linearized Pressure Distributions with Strong Supersonic Entropy Layers," J. Fl. Mech., Vol. 16, 481 (1963).

6. Pai, S. I.: "Two-Dimensional Supersonic Shear Flow Around a Corner," ASME Proc. Sec. U. S. Nat'l Congress of Appl. Mech., 637 (1954).

7. Weinbaum, S.: "The Rapid Expansion of a Supersonic Shear Flow," Avco-Everett Research Report 204, Jan., 1965.

8. Weinbaum, S.: "Rapid Expansion of a Supersonic Boundary Layer and its Application to the Near Wake," AIAA J., 4:2, 217 (1966).

9. Zakkay, V.: "Heat Transfer at a Corner," J. Aerospace Sci., 27:2, 157-158 (1960).

10. Olsson, G. R. and Messiter, A. F.: "The Hypersonic Laminar Boundary Layer Approaching the Base of a Slender Body," Preprint No. 68-67, AIAA 6th Aerospace Sciences Meeting, New York, N. Y., Jan. 22-24, 1968.

11. Curle, N.: "Shock-Induced Separation of a Laminar Boundary Layer in Supersonic Flow Past a Convex Corner," Aero. Quart., Vol. 16, 33-41 (Feb., 1965).

12. Curle, N.: "The Effects of Heat Transfer on Laminar Boundary Layer Separation in Supersonic Flow," Aero. Quart., Vol. XII (Nov., 1961).

REFERENCES (Continued)

13. Hunt, B. L. and Sibulkin, M.: "An Estimate of Compressible Boundary Layer Development Around a Convex Corner in Supersonic Flow," Report of Div. of Eng., Brown University, Nov., 1964.

14. Oosthuizen, P. H.: "An Analysis of the Interaction of a Boundary Layer and the Corner-Expansion Wave in Supersonic Flow," University of Toronto Institute for Aerospace Studies, Technical Note No. 117, August, 1967.

15. Sullivan, P. A.: "On the Interaction of a Laminar Hypersonic Boundary Layer and a Corner Expansion Wave," University of Toronto Institute for Aerospace Studies, Technical Note No. 129, August, 1968.

16. Baum, E.: "An Interaction Model of a Supersonic Laminar Boundary Layer Near a Sharp Backward Facing Step," TRW Systems, BSD TR 67-81 (1966).

17. Tyson, T. J.: "Laminar Boundary Layers in the Neighborhood of Abrupt Spatial Disturbances," Calif. Inst. of Technology, Pasadena, Calif., Ph. D. Thesis (1967).

18. Lees, L. and Reeves, B. L.: "Supersonic Separated and Reattaching Laminar Flows: I. General Theory and Application to Adiabatic Boundary-Layer/Shock-Wave Interactions," AIAA J., 2:11, 1907-1920 (1964).

19. Ko, D. R. S. and Kubota, T.: "Supersonic Laminar Boundary Layer Along a Two-Dimensional Adiabatic Curved Ramp," Preprint No. 68-109, AIAA 6th Aerospace Sciences Meeting, New York, N. Y., Jan. 22-24, 1968.

20. Ko, D. R. S.: "I. Supersonic Laminar Boundary Layer Along a Two-Dimensional Adiabatic Curved Ramp. II. Non-Linear Stability Theory for a Laminar, Incompressible Wake," Calif. Inst. of Technology, Pasadena, Calif. Inst. of Technology, Pasadena, Calif., Ph. D. Thesis (1969).

21. Klineberg, J. M.: "Theory of Laminar Viscous-Inviscid Interactions in Supersonic Flow," Calif. Inst. of Technology, Pasadena, Calif., Ph. D. Thesis (1968).

22. Sternberg, J.: "The Transition From a Turbulent to a Laminar Boundary Layer," Ballistic Research Laboratories, Aberdeen Proving Ground, Report No. 906, May, 1954.

REFERENCES (Continued)

23. Zakkay, V. and Tani, T.: "Theoretical and Experimental Investigation of the Laminar Heat Transfer Downstream of a Sharp Corner," Polytechnic Inst. of Brooklyn, Dept. of Aerospace Engrg. and Appl. Mech., PIBAL Rept. No. 708, Oct., 1961.

24. Zakkay, V., Toba, K. and Kuo, T. J.: "Laminar, Transitional, and Turbulent Heat Transfer after a Sharp Convex Corner," AIAA J., 2:8, 1389-1395 (1964).

25. Murthy, K. R. A.: "Investigation of the Interaction of a Turbulent Boundary Layer with Prandtl-Meyer Expansion Fans at M = 1.88," Princeton Univ., Dept. of Aero. Engrg., Report 403, Nov., 1957.

26. Puhl, A.: "Hypersonic Boundary Layer Flow Around a Sharp Corner," Calif. Inst. of Technology, Pasadena, Calif., Ae. E. Thesis (1966).

27. Ko, D. R. S.: Private Communication (1968).

28. Kubota, T. and Ko, D. R. S.: "A Second-Order Weak Interaction Expansion for Moderately Hypersonic Flow Past a Flat Plate," AIAA J. 5, 1915-1917 (1967).

29. Stewartson, K.: "Correlated Incompressible and Compressible Boundary Layers," Proc. Roy. Soc. (London), Ser. A, Vol. 200, No. A1060, 84-100 (1949).

30. Chapman, D. R. and Rubesin, M. W.: "Temperature and Velocity Profiles in the Compressible Laminar Boundary Layer with Arbitrary Distribution of Surface Temperature," J. Aeronaut. Sci., 16:9, 547-565 (1949).

31. Grange, J. M., Klineberg, J. M. and Lees, L.: "Laminar Boundary-Layer Separation and Near-Wake Flow for a Smooth Blunt Body at Supersonic and Hypersonic Speeds," AIAA J., 5:6, 1089-1096 (1967).

32. Baloga, P. E. and Nagamatsu, H. T.: "Instrumentation of GALCIT Hypersonic Wind Tunnels," GALCIT Hypersonic Research Project, Memorandum No. 29, July 31, 1955.

33. Falkner, V. M. and Skan, S. N.: "Some Approximate Solutions of the Boundary Layer Equations," R & M. No. 1314, British A. R. C. (1930).

REFERENCES (Continued)

34. Cohen, C. B. and Reshotko, E.: "Similar Solutions for the Compressible Laminar Boundary Layer with Heat Transfer and Pressure Gradient," NACA Rept. 1293 (1956).

35. Coles, D.: "The Laminar Boundary Layer Near a Sonic Throat," 1957 Heat Transfer and Fluid Mechanics Institute, Preprints of Papers, Stanford University Press, Stanford, Calif., 119-137.

APPENDIX

EXTENSION OF THE PROFILE FUNCTIONS BEYOND THE ADIABATIC LIMIT

The self-similar flows of compressible boundary layers for Prandtl number Pr = 1 and constant wall enthalpy are given by the system of ordinary equations:[21, 33, 34]

$$\frac{d^3f}{d\eta^3} + f\frac{d^2f}{d\eta^2} + \beta\left[1 - S - \left(\frac{df}{d\eta}\right)^2\right] = 0$$

$$\frac{d^2S}{d\eta^2} + f\frac{dS}{d\eta} = 0 \qquad \text{(A. 1)}$$

subject to the boundary conditions

$$f(0) = \frac{df}{d\eta}(0) = 0$$

$$\frac{df}{d\eta}(\infty) = 1$$

$$S(0) = S_w \qquad \text{(A. 2)}$$

$$S(\infty) = 0 \quad .$$

The quantities in Equations (A. 1) and (A. 2) are:

$$\frac{df}{d\eta} = \frac{U}{U_e}$$

$$S = 1 - \frac{H}{H_e}$$

$$\eta = Y\left[\frac{1+m}{2}\,\frac{U_e}{\nu_\infty X}\right]^{\frac{1}{2}}$$

$$U_e \sim X^m$$

$$dX = C\frac{a_e}{a_\infty}\frac{p_e}{p_\infty}\,dx \; ; \; dY = \frac{a_e}{a_\infty}\frac{\rho}{\rho_\infty}\,dy$$

and β is the pressure gradient parameter defined by

$$\beta = \frac{2m}{m+1} \quad .$$

As $\beta \to \infty$, a limiting solution of the adiabatic form ($S_w \equiv 0$) of Equations (A. 1) and (A. 2) can be found analytically.[21, 35] This solution allows definition of a limiting maximum for the integral quantity $\mathcal{K}$; the result is:

$$\mathcal{K} = \mathcal{K}_{AL} = 0.4785 \quad .$$

Correspondingly, maximum values of J, R, P and $dJ/d\mathcal{K}$ are:

$$J(\mathcal{K}_{AL}) = 0.7891$$

$$R(\mathcal{K}_{AL}) = 0.9609$$

$$P(\mathcal{K}_{AL}) = 0.8908$$

$$\frac{dJ}{d\mathcal{K}}(\mathcal{K}_{AL}) = 2.0556$$

The quantity $\mathcal{K}_p$ is defined by

$$\frac{1}{\alpha} = \exp\left\{\int_{\mathcal{K}_B}^{\mathcal{K}_p} \frac{A_1(\mathcal{K})}{A_2(\mathcal{K})}\, d\mathcal{K}\right\}$$

and if $\mathcal{K}_p$ is taken to be $\mathcal{K}_{AL}$, $\alpha_{AL} = 0.962$. Hence, for $\alpha < 0.962$, $\mathcal{K}$ will exceed its adiabatic limit. The integral functions $\mathcal{K}$, J, R, P, etc. can be extended beyond their respective limits, however, by allowing a non-zero value of S_w and considering the limit:

$$\beta \to \infty\ ,\ S_w \to 0;\ S_w \sqrt{\beta} = \tilde{S}_w \text{ fixed.}$$

Solutions of Equations (A. 1) and (A. 2) subject to this limit are derived in the following two sections. The third section deals with higher order solutions of the adiabatic equations.

A. 1. Limiting Solutions for $S_w \neq 0$.

A. 1. 1. Outer Solutions

Series of the form:

$$f(\eta;\beta) = \eta + \frac{1}{\sqrt{\beta}} f_1(\eta) + \frac{1}{\beta} f_2(\eta) + \cdots$$
$$S(\eta;\beta) = \frac{1}{\sqrt{\beta}} S_1(\eta) + \frac{1}{\beta} S_2(\eta) + \cdots \qquad \text{(A. 3)}$$

are assumed to be valid in the region $\eta = O(1)$. Substituting Equations (A. 3) into (A. 1) and collecting coefficients of like powers of $1/\beta$ gives, to order $1/\sqrt{\beta}$:

$$2\frac{df_1}{d\eta} + S_1 = 0$$
$$\frac{d^2S_1}{d\eta^2} + \eta\frac{dS_1}{d\eta} = 0 \quad . \qquad \text{(A. 4)}$$

The boundary conditions, Equations (A. 2), which must be satisfied by the outer solutions are:

$$\frac{df_1}{d\eta}(\infty) = 0$$
$$S_1(0) = \tilde{S}_w \qquad \text{(A. 5)}$$
$$S_1(\infty) = 0 \quad .$$

Solutions of Equations (A. 4) and (A. 5) can be readily obtained and are:

$$S_1(\eta) = \tilde{S}_w \operatorname{erfc}\left(\frac{\eta}{\sqrt{2}}\right)$$
$$f_1(\eta) = \frac{\tilde{S}_w}{2}\int_\eta^\infty \operatorname{erfc}\left(\frac{\xi}{\sqrt{2}}\right) d\xi \qquad \text{(A. 6)}$$
$$u_1(\eta) = \frac{df_1}{d\eta} = -\frac{\tilde{S}_w}{2} \operatorname{erfc}\left(\frac{\eta}{\sqrt{2}}\right)$$
$$u_{outer} = 1 + \frac{u_1(\eta)}{\sqrt{\beta}} + \cdots$$

A. 1. 2. Inner Solutions

The solutions obtained in Section A. 1. 1. do not satisfy the boundary conditions $f(0) = \frac{df}{d\eta}(0) = 0$, hence, in the inner region, the variables f and η are expanded by $\sqrt{\beta}$:

$$\zeta = \sqrt{\beta}\,\eta$$

$$F(\zeta) = \sqrt{\beta}\, f(\eta) \quad .$$

The corresponding differential equations (A. 1) and boundary conditions (A. 2) are:

$$\frac{d^3F}{d\zeta^3} + \frac{1}{\beta} F \frac{d^2F}{d\zeta^2} + \left[1 - S - \left(\frac{dF}{d\zeta}\right)^2\right] = 0$$

$$\frac{d^2S}{d\zeta^2} + \frac{1}{\beta} F \frac{dS}{d\zeta} = 0$$

$$F(0) = \frac{dF}{d\zeta}(0) = 0 \qquad \text{(A. 7)}$$

$$\frac{dF}{d\zeta}(\infty) = 1 + \frac{u_1(0)}{\sqrt{\beta}} + \cdots$$

$$S(0) = S(\infty) = S_w \quad .$$

The functions F and S can now be expanded in the form:

$$F(\zeta;\beta) = F_0(\zeta) + \frac{1}{\sqrt{\beta}} F_1(\zeta) + \cdots$$

$$S(\zeta;\beta) = \frac{1}{\sqrt{\beta}} \Theta_0(\zeta) + \frac{1}{\beta} \Theta_1(\zeta) + \cdots \quad . \qquad \text{(A. 8)}$$

Substituting the series, Equations (A. 8) into Equations (A. 7) and collecting coefficients of like powers of $1/\beta$ gives, to order

$$\frac{1}{\sqrt{\beta}} : \frac{d^3F_0}{d\zeta^3} + 1 - \left(\frac{dF_0}{d\zeta}\right)^2 = 0$$

$$\frac{d^2\Theta_0}{d\zeta^2} = 0$$

$$F_0(0) = \frac{dF_0}{d\zeta}(0) = 0 \qquad \text{(A. 9)}$$

$$\frac{dF_0}{d\zeta}(\infty) = 1$$

$$\Theta_0(0) = \Theta_0(\infty) = \tilde{S}_w$$

$$\frac{1}{\beta} : \frac{d^3F_1}{d\zeta^3} - 2\frac{dF_0}{d\zeta}\frac{dF_1}{d\zeta} = \Theta_0$$

$$\frac{d^2\Theta_1}{d\zeta^2} = 0$$

$$F_1(0) = \frac{dF_1}{d\zeta}(0) = 0 \qquad \text{(A. 10)}$$

$$\frac{dF_1}{d\zeta}(\infty) = u_1(0)$$

$$\Theta_1(0) = \Theta_1(\infty) = 0 \quad .$$

The solutions for $\Theta_0(\zeta)$ and $\Theta_1(\zeta)$ can be written immediately as $\Theta_0 = \tilde{S}_w$, $\Theta_1 = 0$. If one multiplies the equation for F_0 by $d^2F_0/d\zeta^2$, its integral is easily obtained and the solution for $U_0 = dF_0/d\zeta$ is

$$U_0(\zeta) = 3\tanh^2\left(\frac{\zeta}{\sqrt{2}} + \tanh^{-1}\sqrt{\frac{2}{3}}\right) - 2 \quad . \qquad \text{(A. 11)}$$

The solution for $U_1(\zeta) = dF_1/d\zeta$ can now be obtained from

$$\frac{d^2U_1}{d\zeta^2} - 2U_0U_1 = \tilde{S}_w$$

$$U_1(0) = 0 \qquad \text{(A. 12)}$$

$$U_1(\infty) = u_1(0) \quad .$$

Differentiating the equation for $U_0(\zeta)$ once more gives

$$\frac{d^2}{d\zeta^2}\left(\frac{dU_0}{d\zeta}\right) - 2\,U_0\left(\frac{dU_0}{d\zeta}\right) = 0$$

and hence by putting $U_1 = \tau(\zeta)\ dU_0/d\zeta$ Equations (A. 12) become

$$\frac{d}{d\zeta}\left[\frac{d\tau}{d\zeta}\left(\frac{dU_0}{d\zeta}\right)^2\right] = \mathfrak{S}_w \frac{dU_0}{d\zeta}$$

$$\tau(0) = 0 \qquad \text{(A. 13)}$$

$$\lim_{\zeta \to \infty} \tau(\zeta)\ \frac{dU_0}{d\zeta} = u_1(0) = -\frac{\mathfrak{S}_w}{2} \quad .$$

From the solution of Equations (A. 13), we obtain

$$U_1(\zeta) = -\frac{\mathfrak{S}_w}{2}\left\{U_0 + \frac{\sqrt{2+U_0}}{\sqrt{3}}(1-U_0)\,\ell n\left[\frac{\sqrt{3}+\sqrt{2+U_0}}{(\sqrt{3}+\sqrt{2})\sqrt{1-U_0}}\right]\right\} \quad . \qquad \text{(A. 14)}$$

Finally, one can write the velocity in the inner region, using Equations (A. 11) and (A. 14), as:

$$u_{inner} = U_0(\zeta) + \frac{1}{\sqrt{\beta}}\,U_1(\zeta) + \cdots \quad . \qquad \text{(A. 15)}$$

A uniformly valid composite velocity ratio can be written by subtracting out the common parts of Equation (A. 15) and the last of Equations (A. 6) and is:

$$u_{composite} = \left[1 + \frac{1}{\sqrt{\beta}}\,u_1(\eta) + \cdots\right] + \left[U_0(\zeta) + \frac{1}{\sqrt{\beta}}\,U_1(\zeta) + \cdots\right]$$

$$- \left[1 + \frac{1}{\sqrt{\beta}}\,u_1(0) + \cdots\right]$$

or

$$u_{composite} = U_0(\zeta) + \frac{1}{\sqrt{\beta}}\,u_1(\eta) + \frac{1}{\sqrt{\beta}}\,[U_1(\zeta) - u_1(0)] + \cdots \quad . \qquad \text{(A. 16)}$$

A. 2. Profile Functions

The solutions of interest are the profile quantities $\mathcal{H}$, J, R, P, etc. which are defined by

$$\mathcal{H} = \frac{\Theta}{\Delta^*}$$

$$J = \frac{\Theta^*}{\Delta^*}$$

$$R = 2\Delta^* \int_0^\infty \left(\frac{\partial u_c}{\partial \eta} \right)^2 d\eta \qquad \text{(A. 17)}$$

$$P = \Delta^* \left(\frac{\partial u_c}{\partial \eta} \right)_{\eta=0}$$

where

$$\Delta^* = \int_0^\infty (1 - u_c) d\eta$$

$$\Theta = \int_0^\infty u_c (1 - u_c) d\eta$$

$$\Theta^* = \int_0^\infty u_c (1 - u_c^2) d\eta \qquad \text{(A. 18)}$$

$$u_c = u_{composite} = U/U_e$$

$$\eta = Y \left[\frac{1+m}{2} \frac{U_e}{\nu_\infty X} \right]^{\frac{1}{2}}$$

Substitution of Equation (A. 16) into Equations (A. 18) gives:

$$\Delta^* = \frac{1}{\sqrt{\beta}} \left[(I_1 + \tilde{S}_w V) + O\left(\frac{1}{\sqrt{\beta}}\right) \right]$$

$$\Theta = \frac{1}{\sqrt{\beta}} \left[(I_2 + \tilde{S}_w V) + O\left(\frac{1}{\sqrt{\beta}}\right) \right]$$

$$\Theta^* = \frac{1}{\sqrt{\beta}} \left[(I_3 + \tilde{S}_w V) + O\left(\frac{1}{\sqrt{\beta}}\right) \right] \qquad \text{(A. 19)}$$

$$\int_0^\infty \left(\frac{\partial u_c}{\partial \eta} \right)^2 d\eta = \sqrt{\beta} \left[I_4 + O\left(\frac{1}{\sqrt{\beta}}\right) \right]$$

$$\left(\frac{\partial u_c}{\partial \eta} \right)_{\eta=0} = \sqrt{\beta} \left[\frac{2}{\sqrt{3}} + O\left(\frac{1}{\sqrt{\beta}}\right) \right]$$

where

$$I_1 = \int_0^\infty [1-U_0(\zeta)]\,d\zeta = \sqrt{\frac{3}{2}} \int_0^1 \frac{dU_0}{\sqrt{2+U_0}}$$

$$I_2 = \int_0^\infty U_0(\zeta)\,[1-U_0)]d\zeta = \sqrt{\frac{3}{2}} \int_0^1 \frac{U_0 dU_0}{\sqrt{2+U_0}}$$

$$I_3 = \int_0^\infty U_0(\zeta)\,[1-U_0^2(\zeta)]d\zeta = \sqrt{\frac{3}{2}} \int_0^1 \frac{U_0(1+U_0)dU_0}{\sqrt{2+U_0}} \qquad \text{(A. 20)}$$

$$I_4 = \int_0^\infty \left(\frac{dU_0}{d\zeta}\right)^2 d\zeta = \sqrt{\frac{2}{3}} \int_0^1 (1-U_0)\sqrt{2+U_0}\; dU_0$$

$$V = \frac{1}{\sqrt{2}} \int_0^\infty \text{erfc } t\; dt = \frac{1}{\sqrt{2\pi}} \quad .$$

The latter forms for I_1-I_4 can be obtained using Equation (A. 11).

The values of I_1-I_4 are:

$$I_1 = \sqrt{6}\;(\sqrt{3} - \sqrt{2}\;)$$

$$I_2 = I_1\left(\frac{2}{\sqrt{3}\,I_1} - 1\right)$$

$$I_3 = I_4 = \frac{4}{5} I_1$$

and the expressions for $\mathcal{K} = \mathcal{K}(\tilde{S}_w)$, etc., can be written as

$$\mathcal{K} = \frac{(Q-1)+\hat{S}_w}{1+\hat{S}_w}$$

$$J = \frac{4/5 + 2\,\hat{S}_w}{1+\hat{S}_w}$$

$$R = \frac{8}{5} I_1^2\,(1 + \hat{S}_w) \qquad \text{(A. 21)}$$

$$P = \frac{2}{\sqrt{3}}\, I_1 (1 + \hat{S}_w)$$

$$\frac{dJ}{d\mathcal{K}} = \frac{dJ}{d\hat{S}_w}\,\frac{d\hat{S}_w}{d\mathcal{K}} = \frac{6/5}{2-Q}$$

where

$$Q = \frac{2}{\sqrt{3}\, I_1} \qquad \text{and} \qquad \hat{S}_w = \frac{\tilde{S}_w V}{I_1} \quad .$$

Thus a family of similarity solutions exists described by the parameter $\tilde{S}_w = S_w \sqrt{\beta}$ which allows an extension of the integral functions beyond their adiabatic limits. The parameter $\tilde{S}_w$ (or $\hat{S}_w$) can be eliminated by writing $\hat{S}_w = \hat{S}_w(\mathcal{N})$, say, and this family can be written simply as a function of $\mathcal{N}$. This form is most convenient and is written as:

$$\begin{aligned}
J &= \frac{4/5 + 2(1-Q)}{2-Q} + \frac{6/5}{2-Q}\,\mathcal{N} \\
R &= \frac{8}{5}\, I_1^2 \left(\frac{2-Q}{1-\mathcal{N}}\right) \\
P &= \frac{2}{\sqrt{3}}\, I_1 \left(\frac{2-Q}{1-\mathcal{N}}\right) \\
\frac{dJ}{d\mathcal{N}} &= \frac{6/5}{2-Q} \\
\frac{dR}{d\mathcal{N}} &= \frac{R}{1-\mathcal{N}} \\
\frac{dP}{d\mathcal{N}} &= \frac{P}{1-\mathcal{N}} \\
\mathcal{N} &= \frac{(Q-1) + \hat{S}_w}{1 + \hat{S}_w} \quad .
\end{aligned} \tag{A. 22}$$

These solutions are plotted in Figs. (A. 1) and (A. 2) along with the curve fits of the numerical solutions for $\mathcal{N}_B \le \mathcal{N} \le \mathcal{N}_{AL}$.

One difficulty encountered with use of the extended functions is that $dJ/d\mathcal{N}$ is discontinuous at $\mathcal{N}_{AL}$. This means that the functions $\tilde{D}(\mathcal{N})$, $A_1(\mathcal{N})$, $A_3(\mathcal{N})$, $B_1(\mathcal{N})$ and $B_3(\mathcal{N})$ defined in the text are also discontinuous at $\mathcal{N}_{AL}$. As $\beta \to \infty$ with $S_w \equiv 0$, solutions are of the form,

[see Section (A. 3)],

$$\mathcal{K} = \frac{I_2 + \frac{1}{\beta}(Q_1 - 2Q_2)}{I_1 - \frac{1}{\beta} Q_1}$$

$$J = \frac{I_3 + \frac{1}{\beta}(Q_1 - 3Q_3)}{I_1 - \frac{1}{\beta} Q_1} \quad .$$

If the restriction on S_w is relaxed such that $\beta \to \infty$, $S_w \to 0$ with $S_w\sqrt{\beta}$ fixed, solutions are of the form

$$\mathcal{K} = \frac{(I_2 + \tilde{S}_w V) + O(\frac{1}{\sqrt{\beta}})}{(I_1 + \tilde{S}_w V) + O(\frac{1}{\sqrt{\beta}})}$$

$$J = \frac{(I_3 + \tilde{S}_w V) + O(\frac{1}{\sqrt{\beta}})}{(I_1 + S_w V) + O(\frac{1}{\sqrt{\beta}})} \quad .$$

Hence,

$$\left.\frac{dJ}{d\mathcal{K}}\right|_{\substack{\beta\to\infty \\ S_w \equiv 0}} = \left.\frac{dJ/d\beta}{d\mathcal{K}/d\beta}\right|_{\substack{\beta\to\infty \\ S_w \equiv 0}} = \frac{(I_3/I_1 + 1) - 3(Q_3/Q_1)}{(I_2/I_1 + 1) - 2(Q_2/Q_1)} = 2.0556$$

$$\left.\frac{dJ}{d\mathcal{K}}\right|_{\substack{\beta\to\infty \\ \tilde{S}_w \to 0}} = \left.\frac{dJ/d\tilde{S}_w}{d\mathcal{K}/d\tilde{S}_w}\right|_{\substack{\beta\to\infty \\ \tilde{S}_w \to 0}} = \frac{(I_3/I_1) - 1}{(I_2/I_1) - 1} = 2.3218$$

and the two limits are not equivalent.

A. 3. Higher Order Solutions for $S_w \equiv 0$

This section deals with higher order solutions of the equations of Section A. 1. 2. Equations (A. 7) are repeated below with the restriction that $S_w \equiv 0$:

$$\frac{d^3F}{d\zeta^3} + \frac{1}{\beta} F \frac{d^2F}{d\zeta^2} + \left[1 - \left(\frac{dF}{d\zeta}\right)^2\right] = 0$$

$$F(0) = \frac{dF}{d\zeta}(0) = 0 \qquad \text{(A. 23)}$$

$$\frac{dF}{d\zeta}(\infty) = 1 \quad .$$

Since solutions for $\beta \to \infty$ are of interest, F is assumed to be

$$F(\zeta;\beta) = F_0(\zeta) + \frac{1}{\sqrt{\beta}} F_1(\zeta) + \frac{1}{\beta} F_2(\zeta) + \cdots \quad . \qquad \text{(A. 24)}$$

Substitution of the series, Equation (A. 24), into Equations (A. 23) and collection of coefficients of like powers of $1/\beta$ gives, to order

$$\frac{1}{\beta^0}: \quad \frac{d^3F_0}{d\zeta^3} + 1 - \left(\frac{dF_0}{d\zeta}\right)^2 = 0$$

$$F_0(0) = \frac{dF_0}{d\zeta}(0) = 0 \qquad \text{(A. 25)}$$

$$\frac{dF_0}{d\zeta}(\infty) = 1$$

$$\frac{1}{\sqrt{\beta}}: \quad \frac{d^3F_1}{d\zeta^3} - 2\frac{dF_0}{d\zeta}\frac{dF_1}{d\zeta} = 0$$

$$F_1(0) = \frac{dF_1}{d\zeta}(0) = \frac{dF_1}{d\zeta}(\infty) = 0 \qquad \text{(A. 26)}$$

$$\frac{1}{\beta}: \quad \frac{d^3F_2}{d\zeta^3} - 2\frac{dF_0}{d\zeta}\frac{dF_2}{d\zeta} = \left(\frac{dF_1}{d\zeta}\right)^2 - F_0\frac{d^2F_0}{d\zeta^2}$$

$$F_2(0) = \frac{dF_2}{d\zeta}(0) = \frac{dF_2}{d\zeta}(\infty) = 0 \qquad \text{(A. 27)}$$

etc. Equations (A. 25) have the solution found in Section A. 1. 2, Equation (A. 11):

$$U_0 = \frac{dF_0}{d\zeta} = 3 \tanh^2 \left(\frac{\zeta}{\sqrt{2}} + \tanh^{-1} \sqrt{\frac{2}{3}} \right) - 2 \quad .$$

With $U_1 = dF_1/d\zeta$, Equations (A. 26) become

$$\frac{d^2 U_1}{d\zeta^2} - 2 U_0 U_1 = 0$$

$$U_1(0) = U_1(\infty) = 0 \quad . \tag{A. 28}$$

Hence U_1 = const. $dU_0/d\zeta$ is a solution of the differential equation which satisfies the boundary condition $U_1(\infty) = 0$. However, $U_1(0)$ = const., therefore $U_1 = 0$ is a solution of Equation (A. 28). The form $U_1 = \lambda(\zeta)\ dU_0/d\zeta$ is assumed to see if there exists a non-trivial solution of Equations (A. 28) with

$$\frac{d}{d\zeta}\left[\frac{d\lambda}{d\zeta} \left(\frac{dU_0}{d\zeta} \right)^2 \right] = 0$$

$$\lambda(0) = 0 \tag{A. 29}$$

$$\lim_{\zeta \to \infty} (1 - U_0)\, \lambda(\zeta) = 0 \quad .$$

Now, $dU_0/d\zeta = \sqrt{2/3}\ (1 - U_0)\ \sqrt{2 + U_0}$, therefore

$$\frac{d\lambda}{dU_0} = \frac{C_1'}{(dU_0/d\zeta)^3}$$

where C_1' is a constant. Near $U_0 \to 1$ $(\zeta \to \infty)$

$$\lambda \sim \frac{C_1}{(1 - U_0)^2} + C_2$$

and $(1 - U_0)\lambda \sim C_1/(1 - U_0)$ unless $C_1 \equiv 0$. C_2 must be zero to satisfy $\lambda(0) = 0$; therefore

$$U_1 \equiv 0 \tag{A. 30}$$

is the only possible solution of Equations (A. 28).

With $U_1 = 0$, Equations (A. 27) simplify to:

$$\frac{d^2U_2}{d\zeta^2} - 2\,U_0U_2 = -F_0\,\frac{dU_0}{d\zeta}$$

$$U_2(0) = U_2(\infty) = 0 \quad . \tag{A. 31}$$

After letting $U_2 = \lambda(U_0)\ dU_0/d\zeta$,

$$\frac{d}{dU_0}\left[\frac{d\lambda}{dU_0}\left(\frac{dU_0}{d\zeta}\right)^3\right] = -F_0\,\frac{dU_0}{d\zeta}$$

$$\lambda(0) = 0 \tag{A. 32}$$

$$\lim_{U_0 \to 1} (1-U_0)\lambda(U_0) = 0 \quad .$$

To obtain a solution of Equations (A. 32) for $\lambda(U_0)$ is a formidable task since the right hand side of the first equation must be integrated twice. However, a complete solution is not required; in fact, only $d\lambda/dU_0$ is required to define the profile quantities and the task is reduced to a relatively simple one. Since the velocity is

$$u = U/U_e = U_0(\zeta) + \frac{1}{\beta}\,U_2(\zeta) + \cdots$$

the functions Δ^*, Θ, and Θ^* can be written:

$$\Delta^*\sqrt{\beta} = I_1 - \frac{1}{\beta}\,Q_1 + \cdots$$

$$\Theta\sqrt{\beta} = I_2 + \frac{1}{\beta}\,(Q_1 - 2Q_2) + \cdots \tag{A. 33}$$

$$\Theta^*\sqrt{\beta} = I_3 + \frac{1}{\beta}\,(Q_1 - 3Q_3) + \cdots$$

where

$$Q_1 = \int_0^\infty U_2(\zeta)\, d\zeta$$

$$Q_2 = \int_0^\infty U_2(\zeta) U_0(\zeta) d\zeta$$

$$Q_3 = \int_0^\infty U_2(\zeta) U_0^2(\zeta) d\zeta \quad .$$

With use of the differential equations, Equations (A. 27) and (A. 31), the integral Q_1 can be written as a function of Q_3 and Q_2 can be evaluated directly. The results are

$$\frac{Q_1}{I_1} = \frac{2}{5} - \frac{Q_3}{I_1}$$

$$\frac{Q_2}{I_1} = \frac{1}{2}\left[(Q-1)-D\right] \qquad \text{(A. 34)}$$

where $D = 4/(3I_1)\,(d\lambda/dU_0)_{U_0=0}$, and Q_3 is

$$\frac{Q_3}{I_1} = \frac{1}{5} + \frac{1}{2I_1}\left[\frac{1}{3}\int_0^1 (1-U_0)^3 \frac{d\lambda}{dU_0}\, dU_0 - \int_0^1 (1-U_0)^2 \frac{d\lambda}{dU_0}\, dU_0\right]. \qquad \text{(A. 35)}$$

Thus only one integral of Equations (A. 32) is required and is

$$\frac{d\lambda}{dU_0} = \frac{3}{\sqrt{2}} \frac{1}{(1-U_0)^3 (2+U_0)^{3/2}} \left\{F(t_1) + F(t_2) + \sqrt{3}\, U_0\left[2 - \frac{U_0}{2} - \frac{U_0^2}{3}\right]\right.$$

$$\left. + k_3\left[(2+U_0)^{3/2}(3-U_0) - 6\sqrt{2}\right] - (k_1+k_2) + C_1\right\} \qquad \text{(A. 36)}$$

where

$$F(t) = \frac{t^5}{5}\left[\ell n t - \frac{1}{5}\right] - \sqrt{3}\, t^4\left[\ell n t - \frac{1}{4}\right] + 5t^3\left[\ell n t - \frac{1}{3}\right] - 3\sqrt{3}\, t^2\left[\ell n t - \frac{1}{2}\right]$$

$$t_1 = \sqrt{3} - \sqrt{2+U_0}$$

$$t_2 = \sqrt{3} + \sqrt{2+U_0}$$

$$k_1 = F(\sqrt{3} - \sqrt{2}) \qquad \text{(A. 37)}$$

$$k_2 = F(\sqrt{3} + \sqrt{2})$$

$$k_3 = -\frac{2}{5}\left[\sqrt{6} - \tanh^{-1}\sqrt{\frac{2}{3}}\right]$$

$$C_1 = \text{arbitrary constant of integration} \quad .$$

The constant C_1 can be determined from the boundary condition $\lim_{U_0 \to 1} (1-U_0)\lambda(U_0) = 0$. As $U_0 \to 1$,

$$\frac{d\lambda}{dU_0} \sim \frac{1}{\sqrt{6}} \frac{1}{(1-U_0)^3}\left\{F(2\sqrt{3}) + \frac{7}{6}\sqrt{3} + 6k_3(\sqrt{3} - \sqrt{2}) - (k_1+k_2) + C_1\right\}$$

$$+ \alpha_1 \frac{\ell n(1-U_0)}{1-U_0} + \frac{\alpha_2}{1-U_0} + \cdots$$

therefore, the boundary condition is satisfied if the bracketed term is required to vanish since then

$$\lambda \sim \beta_1 [\ell n(1-U_0)]^2 + \beta_2 \ell n(1-U_0)$$

and $(1-U_0)\lambda(U_0) \to 0$. Hence C_1 is

$$C_1 = k_1 + k_2 - \left[F(2\sqrt{3}) + \frac{7}{6}\sqrt{3} + 6k_3(\sqrt{3} - \sqrt{2})\right] \quad . \qquad \text{(A. 38)}$$

Now the value of $D = 4/(3I_1)(d\lambda/dU_0)_{U_0=0}$ is simply C_1/I_1 and the integral Q_2 is easily determined. The solution for $d\lambda/dU_0$ is complete and Q_3 can be determined.

If we return to the original objective of writing the functions

$\mathcal{N}$, J, R, P, etc. as series in $1/\beta$, it is now possible to evaluate

$$\int_0^\infty \left(\frac{\partial u}{\partial \zeta}\right)^2 d\zeta = \frac{4}{5} I_1 \left[1 + \frac{1}{\beta}\left(1 - 5\,\frac{Q_3}{I_1}\right) + \cdots\right]$$

$$\left(\frac{\partial u}{\partial \zeta}\right)_{\zeta=0} = \frac{2}{\sqrt{3}} \left[1 + \frac{1}{\beta}\left(\frac{\sqrt{3}}{2} I_1 D\right) + \cdots\right] . \qquad \text{(A. 39)}$$

With the use of Equations (A. 33) and (A. 39), one can write the profile functions as series in $1/\beta$:

$$\mathcal{N} = \mathcal{N}_0 + \frac{1}{\beta}\mathcal{N}_2 + \cdots = \mathcal{N}_{AL} + \frac{1}{\beta}\mathcal{N}_2 + \cdots$$

$$J = J_0 + \frac{1}{\beta} J_2 + \cdots = J_{AL} + \frac{1}{\beta} J_2 + \cdots \qquad \text{(A. 40)}$$

etc.

where the zeroth order functions are those previously determined and the second order functions are:

$$\mathcal{N}_2 = 1 + D - Q\left(\frac{3}{5} + \frac{Q_3}{I_1}\right)$$

$$J_2 = \frac{3}{5}\left(\frac{6}{5} - 8\,\frac{Q_3}{I_1}\right)$$

$$R_2 = \frac{32}{5} I_1^2 \left(\frac{3}{20} - \frac{Q_3}{I_1}\right)$$

$$P_2 = I_1^2\left[D - Q\left(\frac{2}{5} - \frac{Q_3}{I_1}\right)\right] .$$

The quantities D and Q_3/I_1 were determined numerically and the values are:

$$D = .0958$$

$$\frac{Q_3}{I_1} = .1694 .$$

These solutions, Equations (A. 40), are compared with the numerical solutions obtained by Klineberg in Figures (A. 3) and (A. 4).

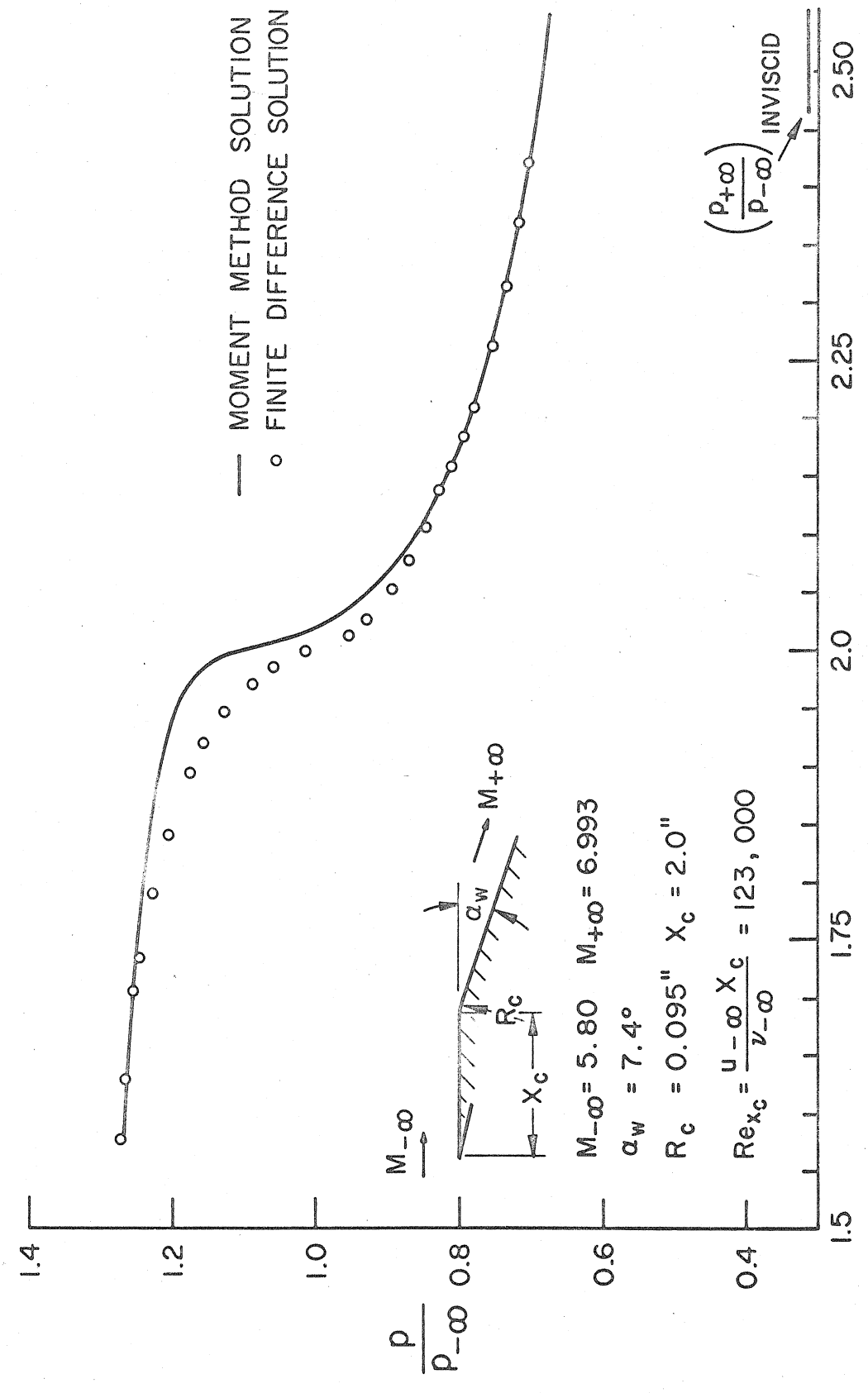

FIG. I COMPARISON OF MOMENT METHOD AND FINITE DIFFERENCE SOLUTION

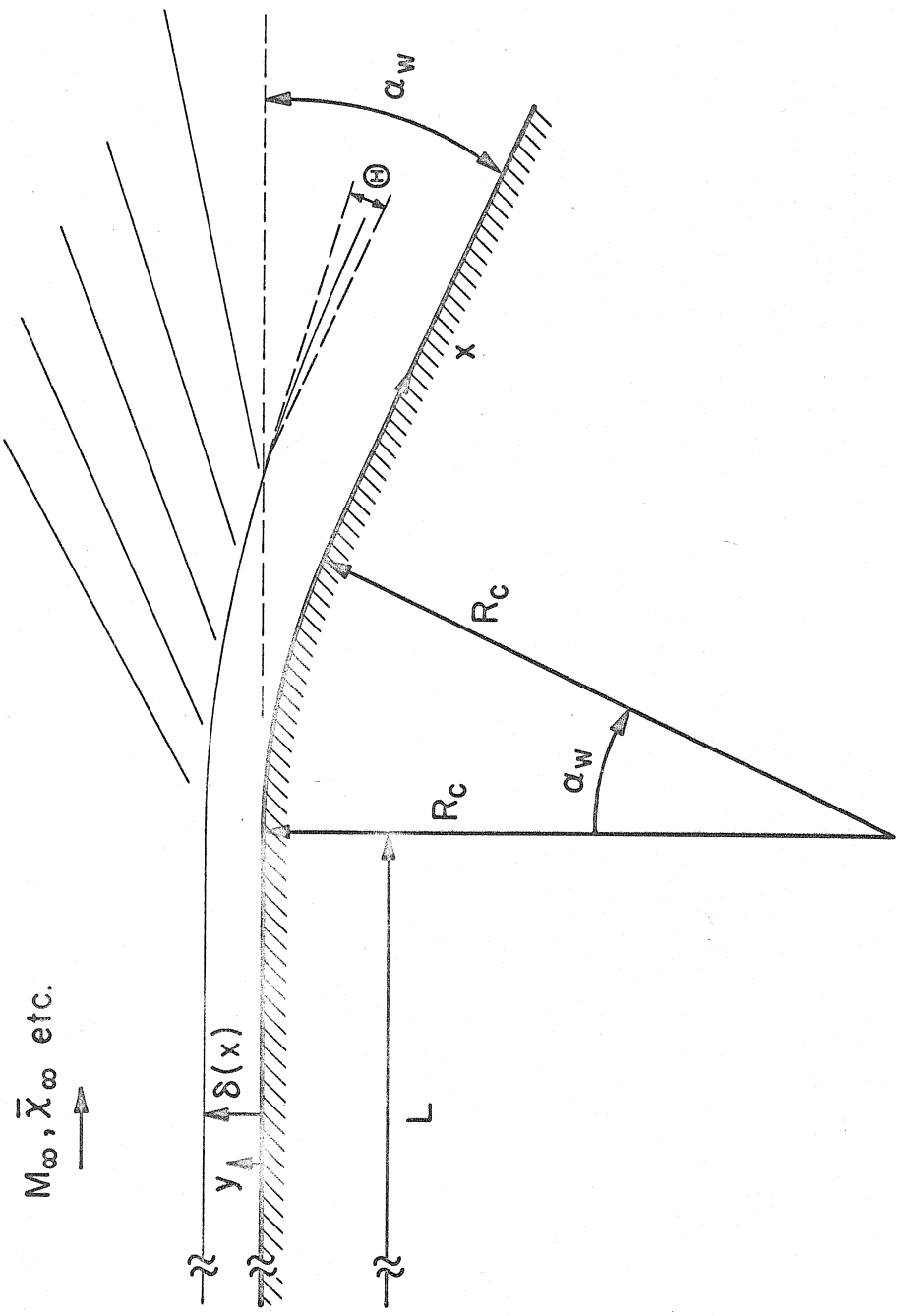

FIG. 2 SKETCH OF INDUCED ANGLE DOWNSTREAM OF EXPANSION CORNER

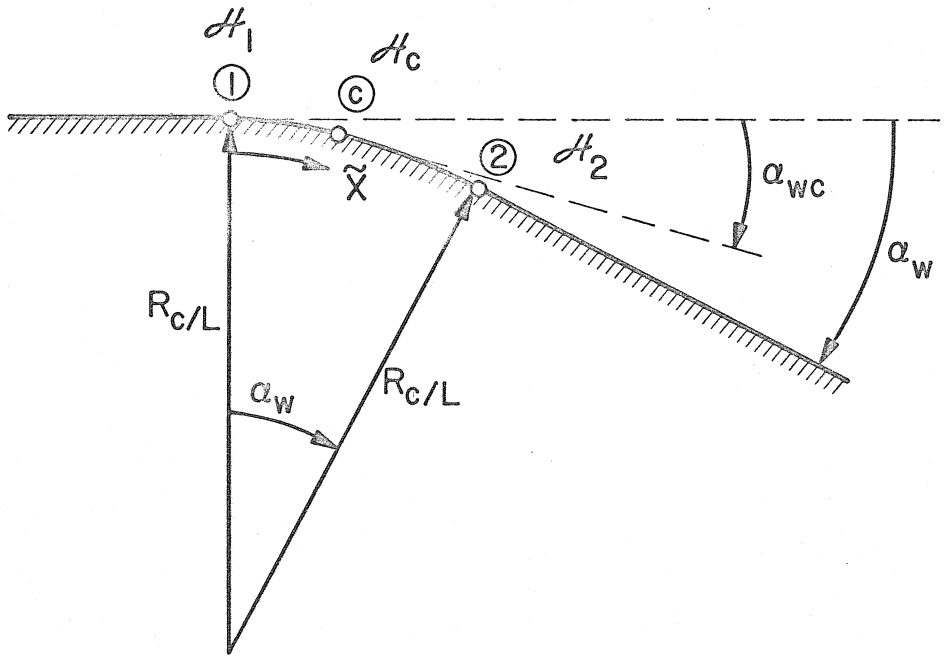

$$\frac{\Delta \mathcal{H}_{①,②}}{\Delta \tilde{X}_{①,②}} = \frac{(\mathcal{H}_2 - \mathcal{H}_c) + (\mathcal{H}_c - \mathcal{H}_1)}{(\tilde{X}_2 - \tilde{X}_c) + (\tilde{X}_c - \tilde{X}_1)} = \frac{\mathcal{H}_2 - \mathcal{H}_1}{\tilde{X}_2 - \tilde{X}_1} \sim \frac{1}{\sqrt{R_{c/L}}}$$

$$\Delta \mathcal{H}_{①,②} \sim \sqrt{R_{c/L}}$$

FIG. 3 SKETCH OF GEOMETRY FOR CRITICAL POINT ANALYSIS

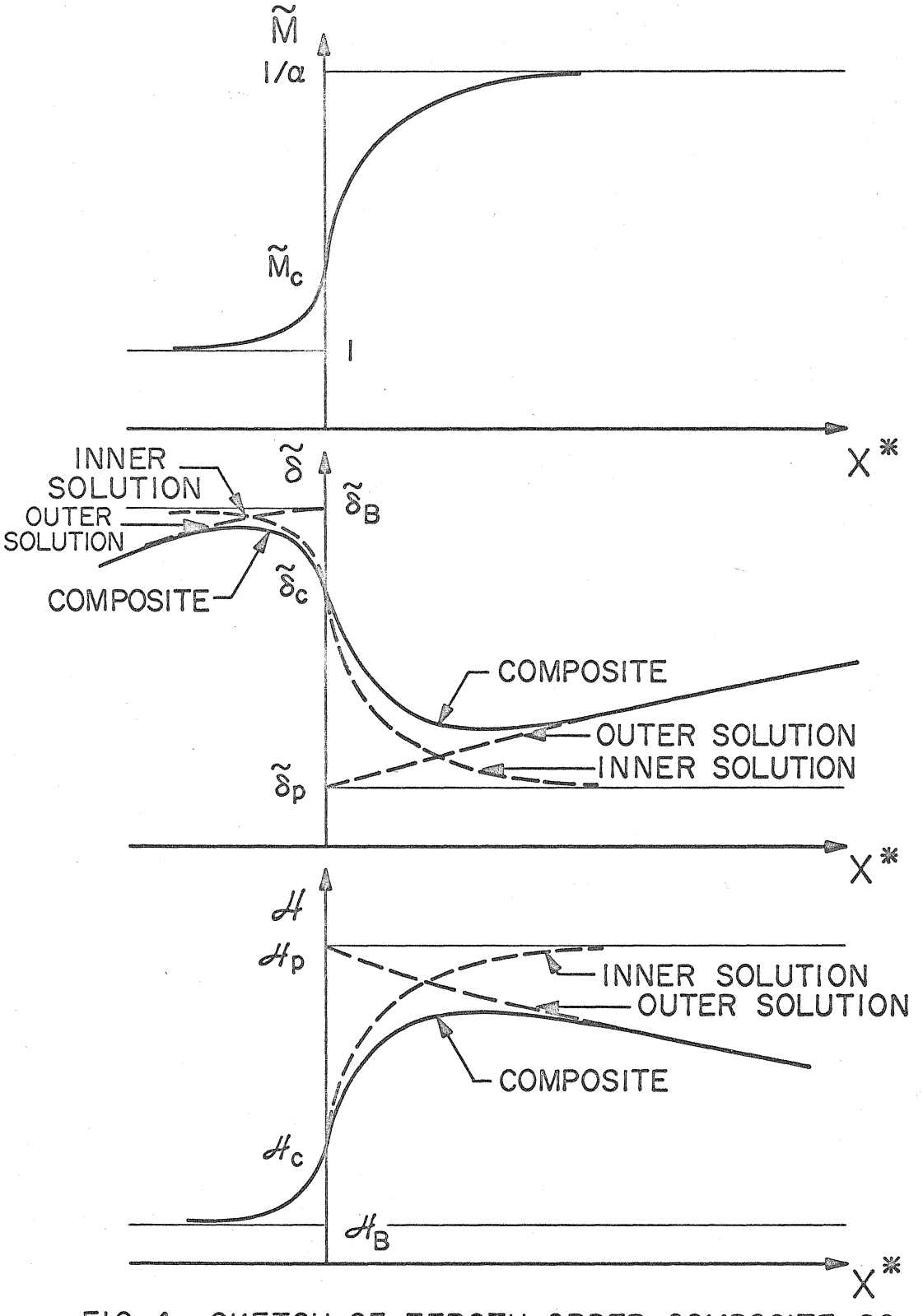

FIG. 4 SKETCH OF ZEROTH ORDER COMPOSITE SOLUTIONS FOR SHARP EXPANSION CORNER

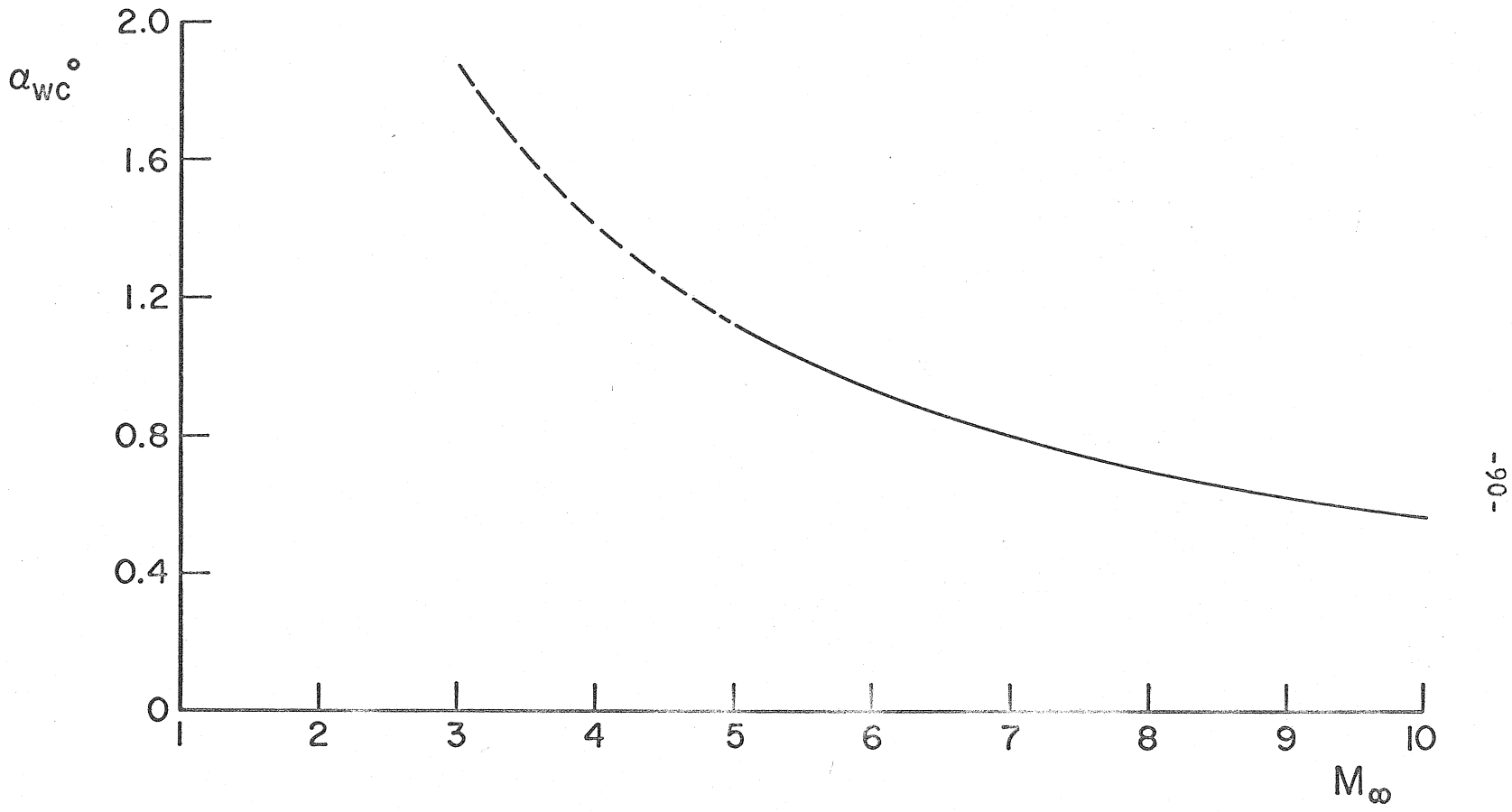

FIG. 5 MINIMUM EXPANSION ANGLE REQUIRED FOR SUBCRITICAL – SUPERCRITICAL TRANSITION

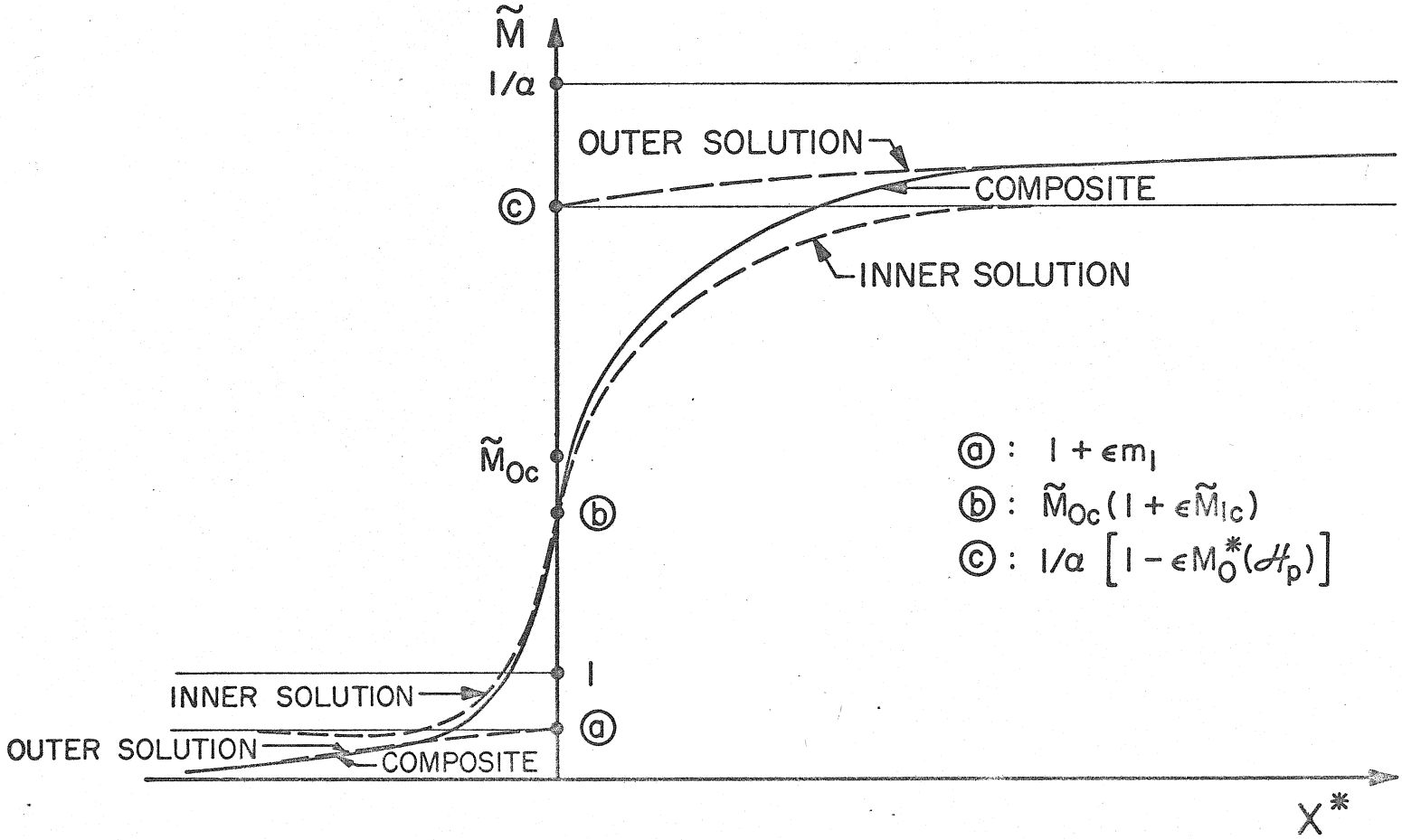

FIG.6 SKETCH OF FIRST ORDER COMPOSITE SOLUTION FOR SHARP EXPANSION CORNER

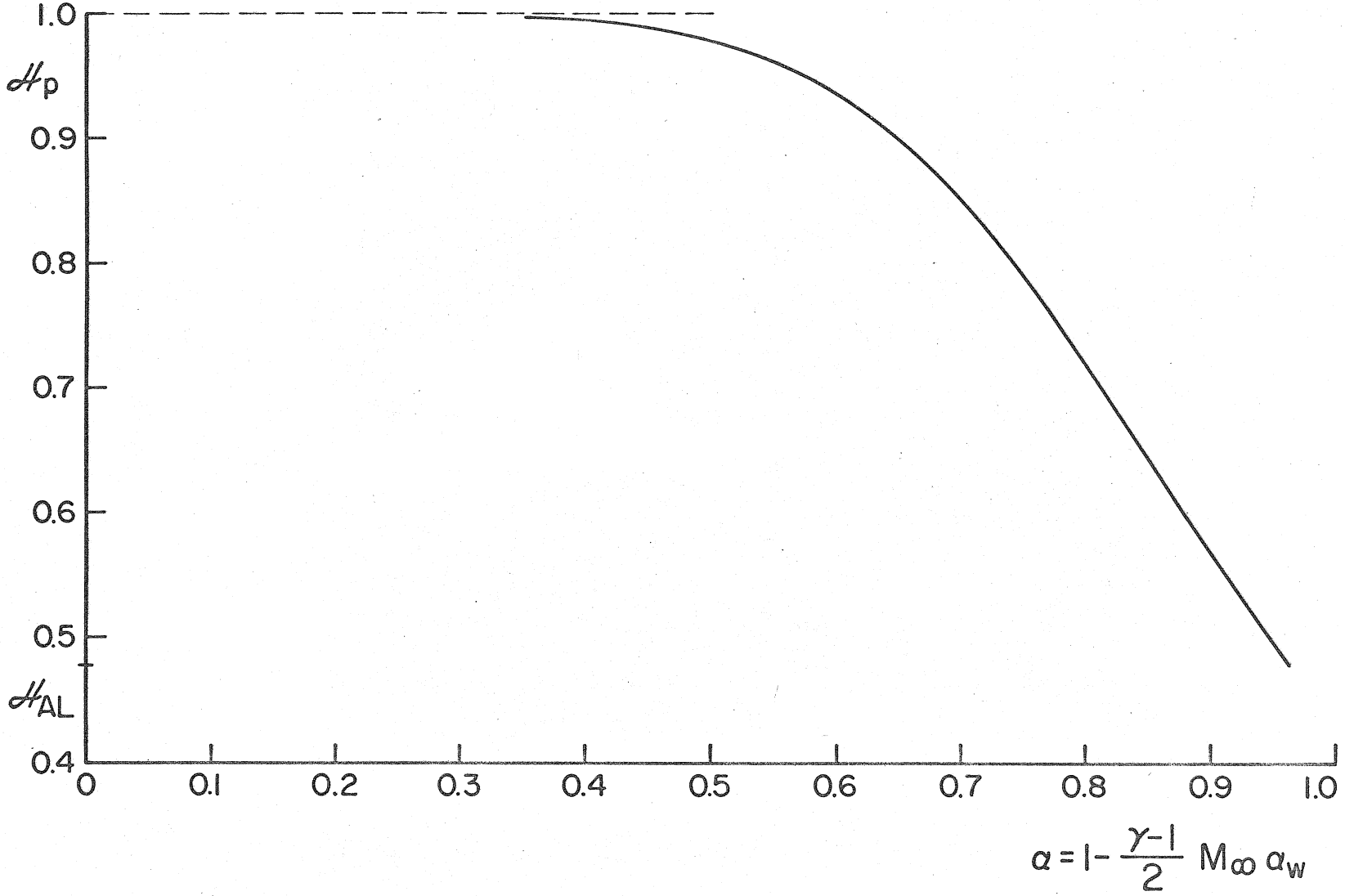

FIG. 7 MAXIMUM VALUE OF $\mathscr{H}_0$ FOR A GIVEN $M_\infty \alpha_w$

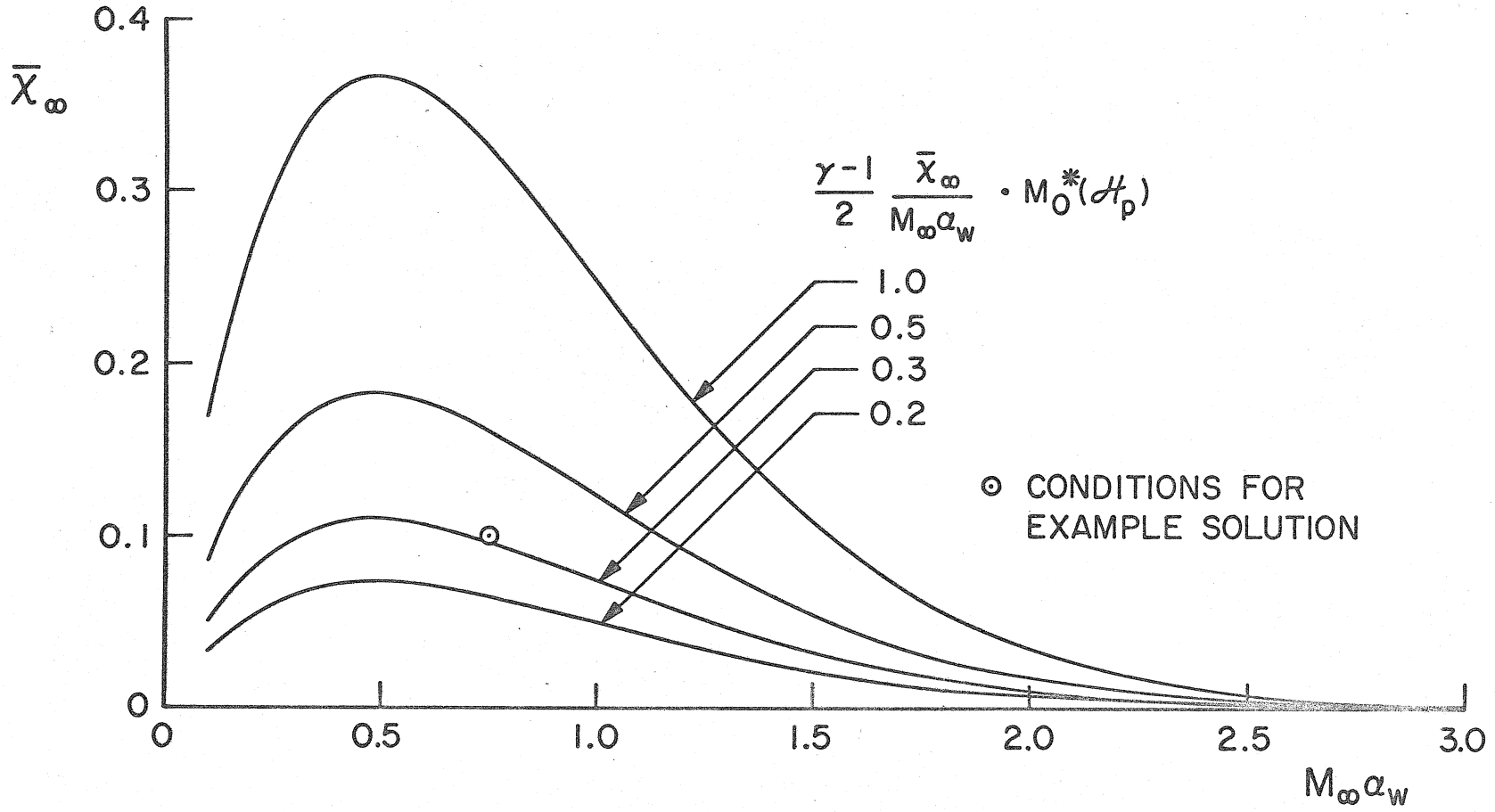

FIG. 8 PARAMETER BOUNDARIES FOR CLOSED FORM SOLUTIONS

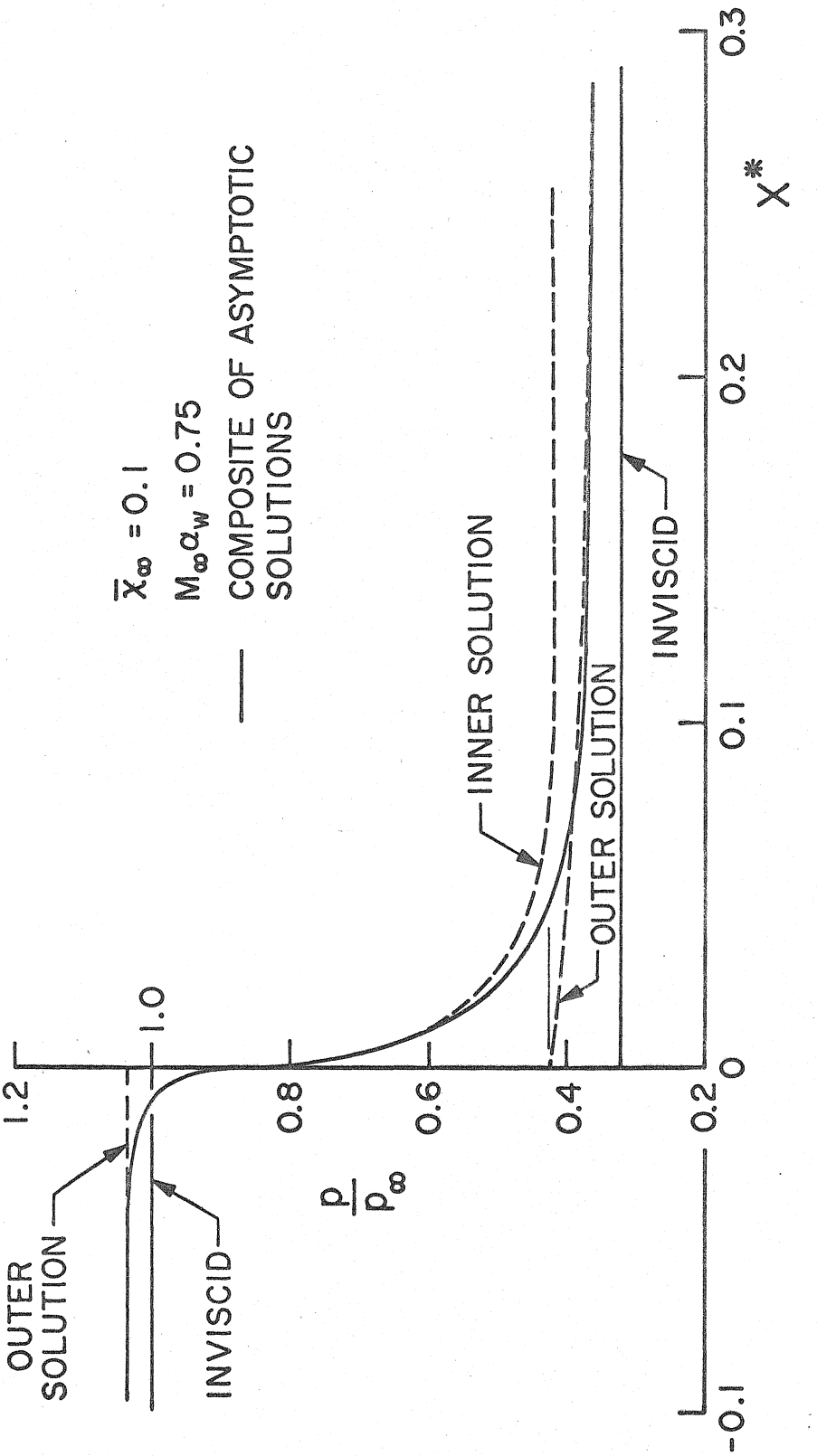

FIG. 9 ASYMPTOTIC SOLUTIONS FOR PRESSURE DISTRIBUTION

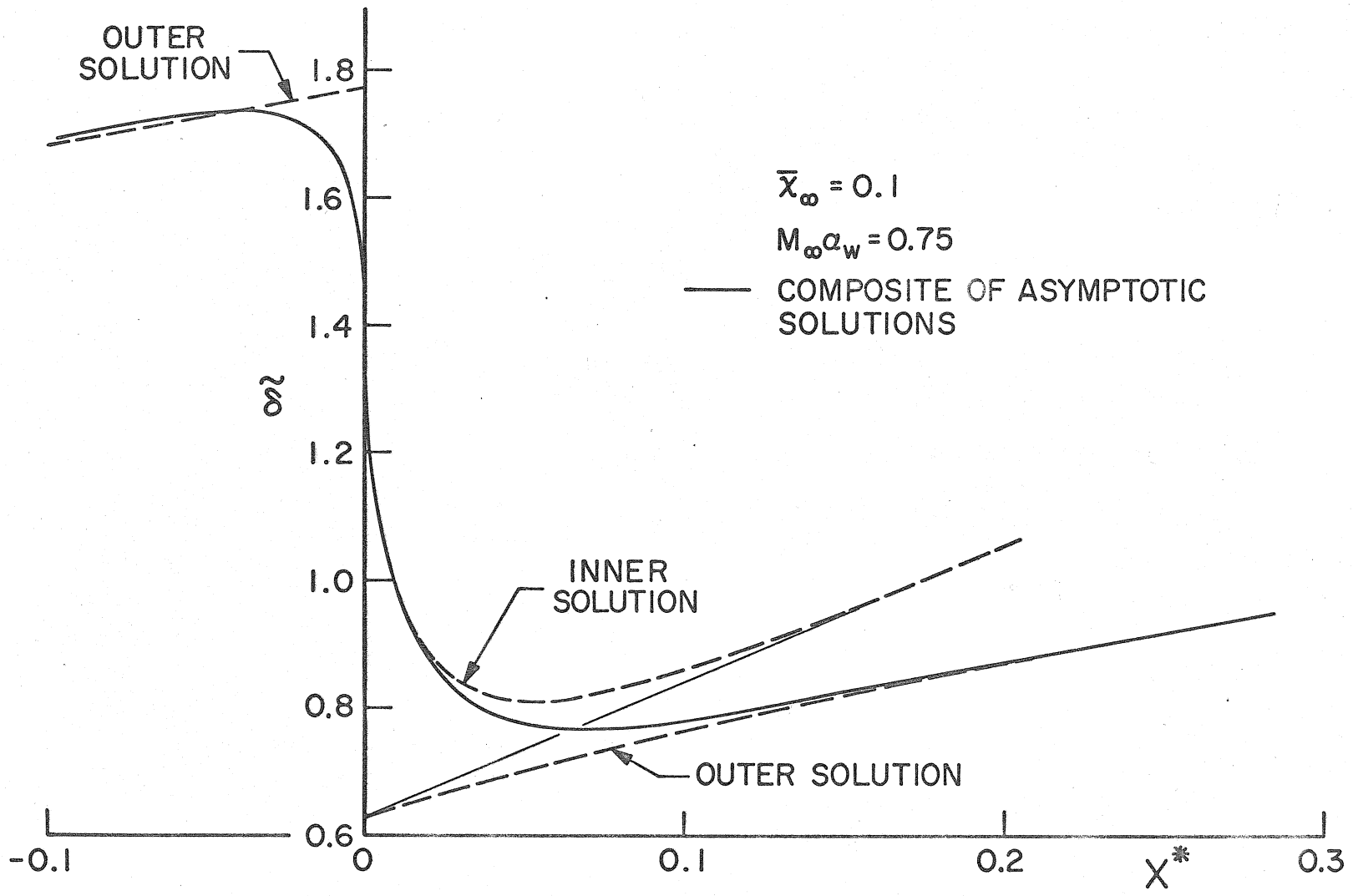

FIG. 10 ASYMPTOTIC SOLUTIONS FOR INCOMPRESSIBLE DISPLACEMENT THICKNESS DISTRIBUTION

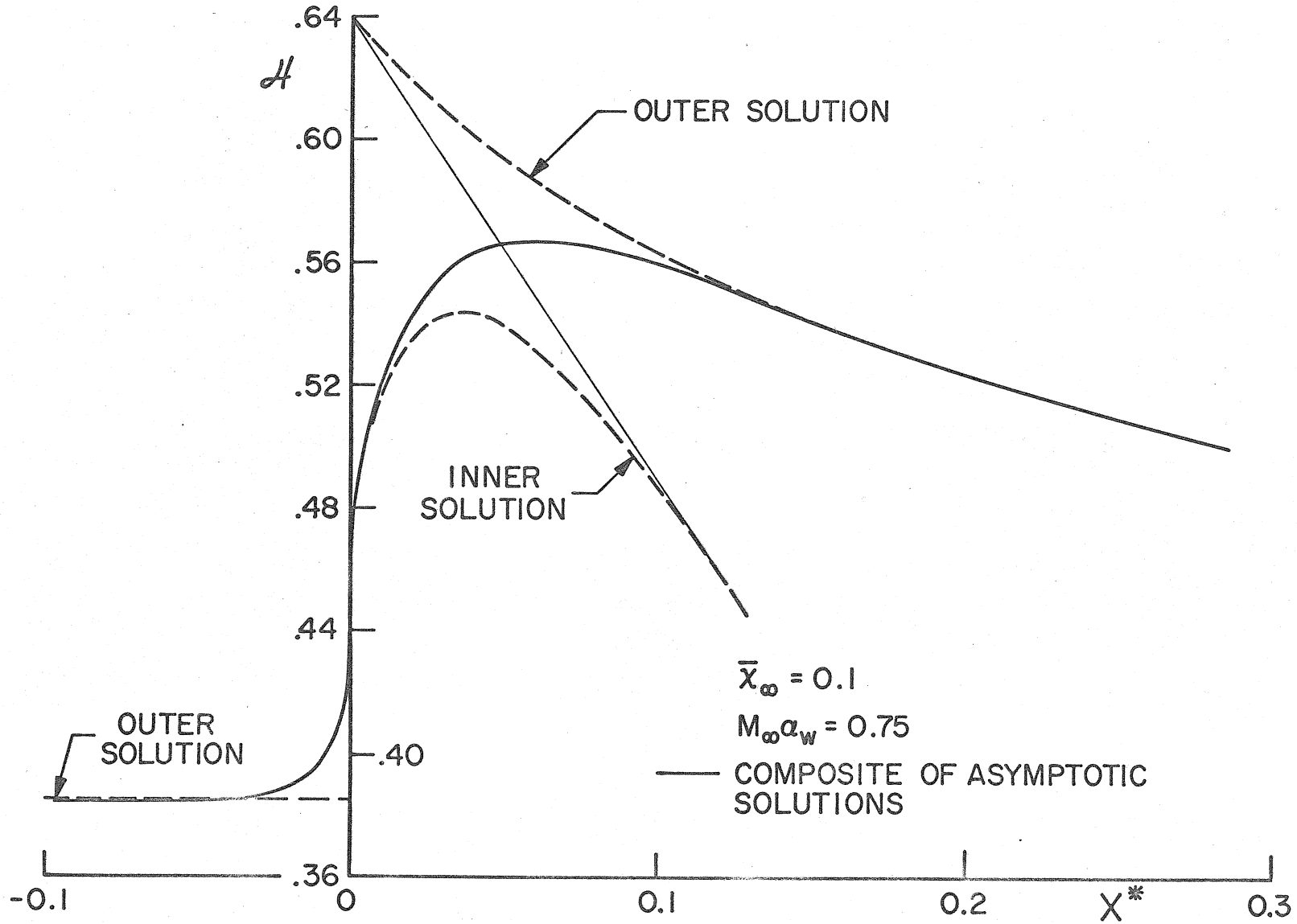

FIG. 11 ASYMPTOTIC SOLUTIONS FOR $\mathcal{H}$ DISTRIBUTION

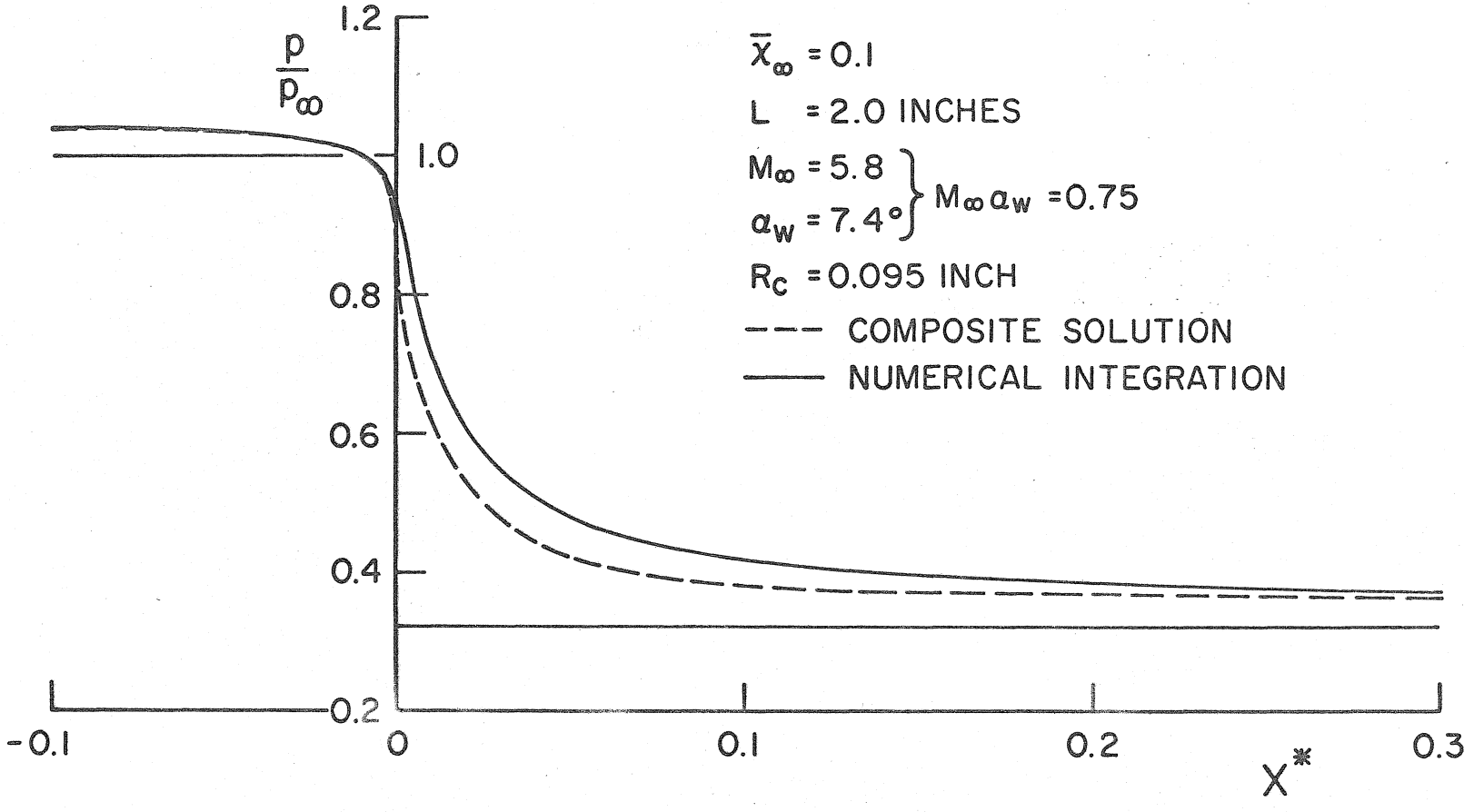

FIG. 12 COMPARISON OF COMPOSITE SOLUTION WITH "EXACT" RESULT

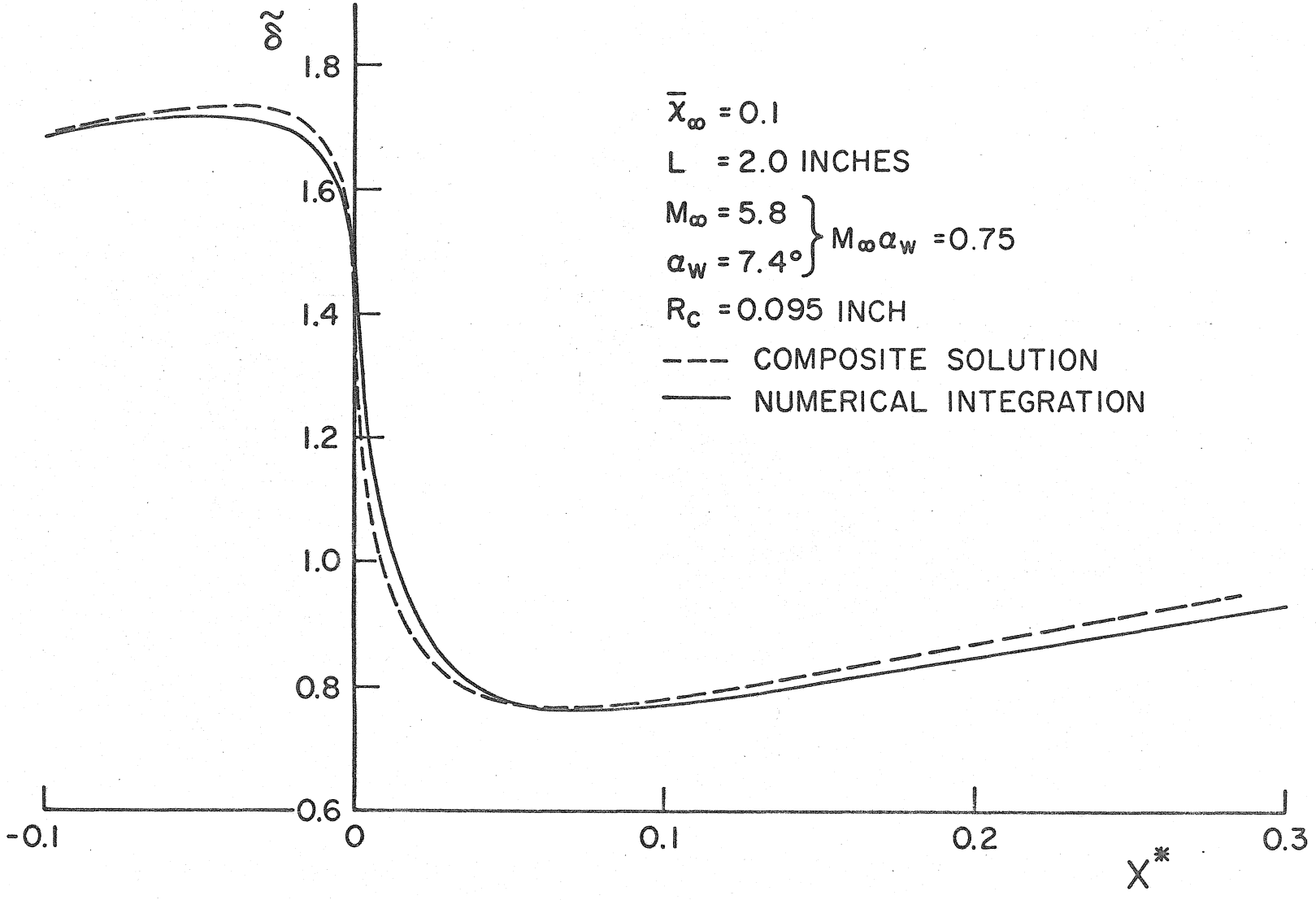

FIG. 13 COMPARISON OF COMPOSITE SOLUTION WITH "EXACT" RESULT

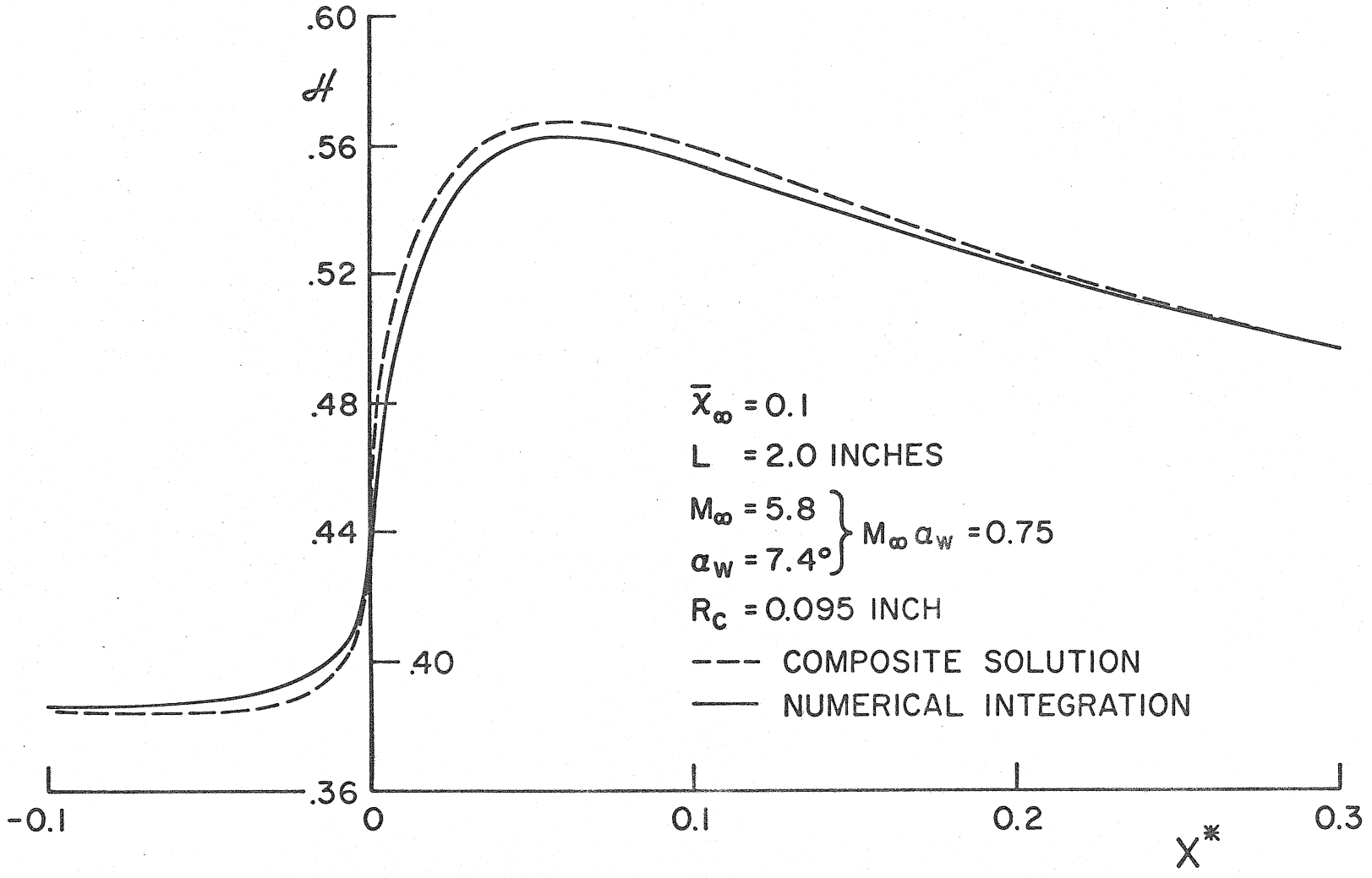

FIG. 14 COMPARISON OF COMPOSITE SOLUTION WITH "EXACT" RESULT

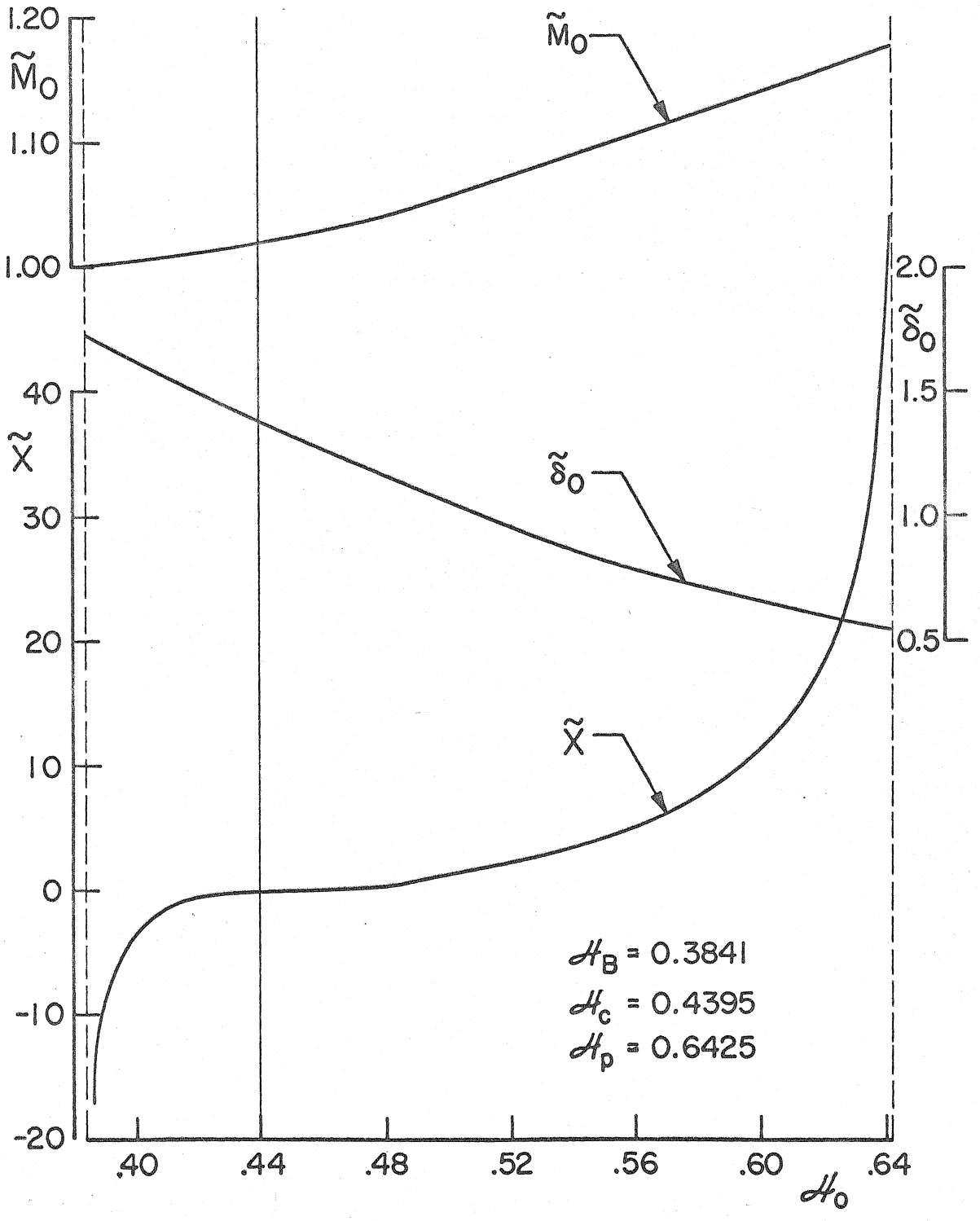

FIG. 15 ZEROTH ORDER FUNCTIONS OF $\mathcal{H}_0$ FOR $\alpha = 0.85$

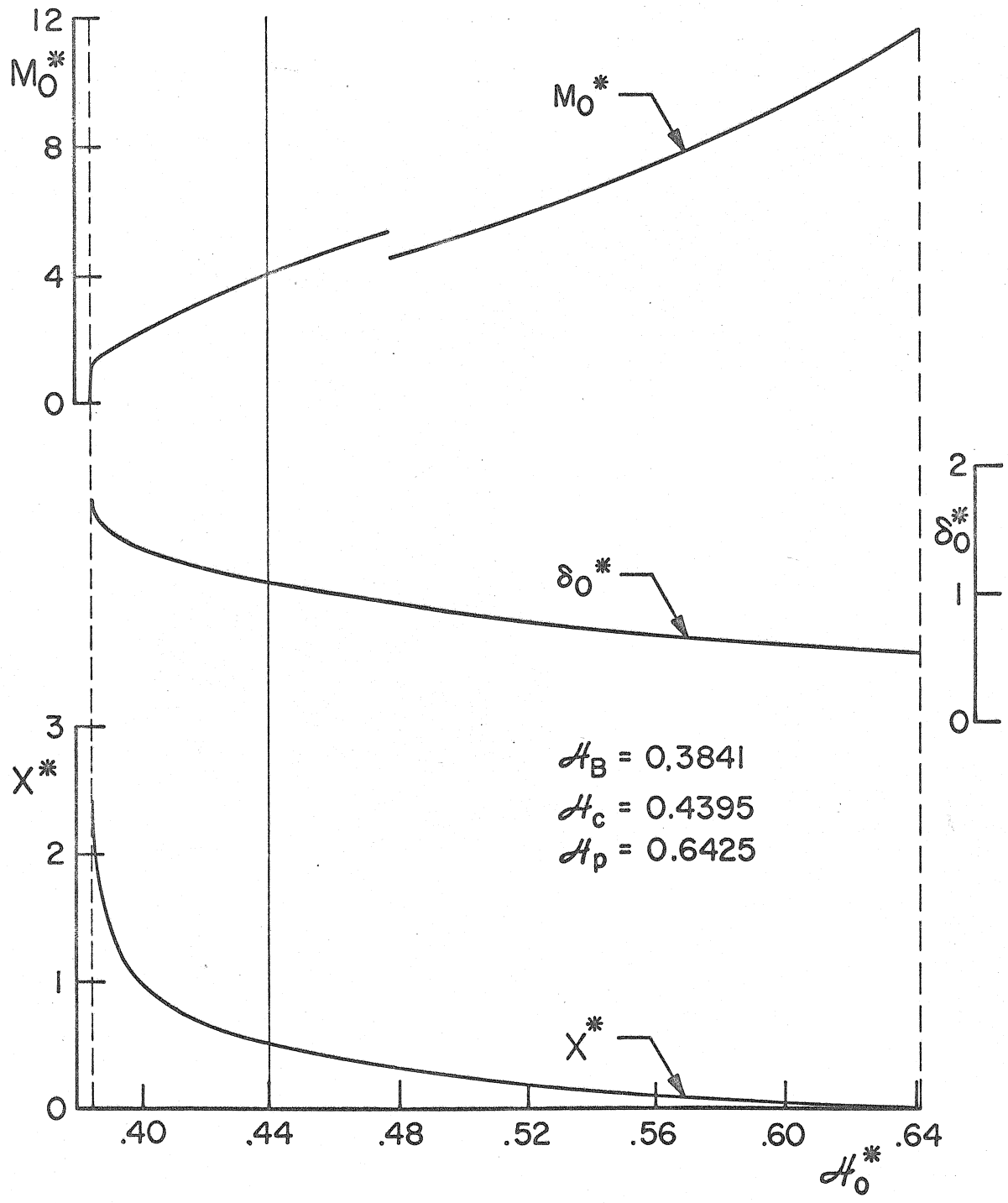

FIG. 16 ZEROTH ORDER FUNCTIONS OF $\mathcal{H}_0^*$ FOR $\alpha = 0.85$

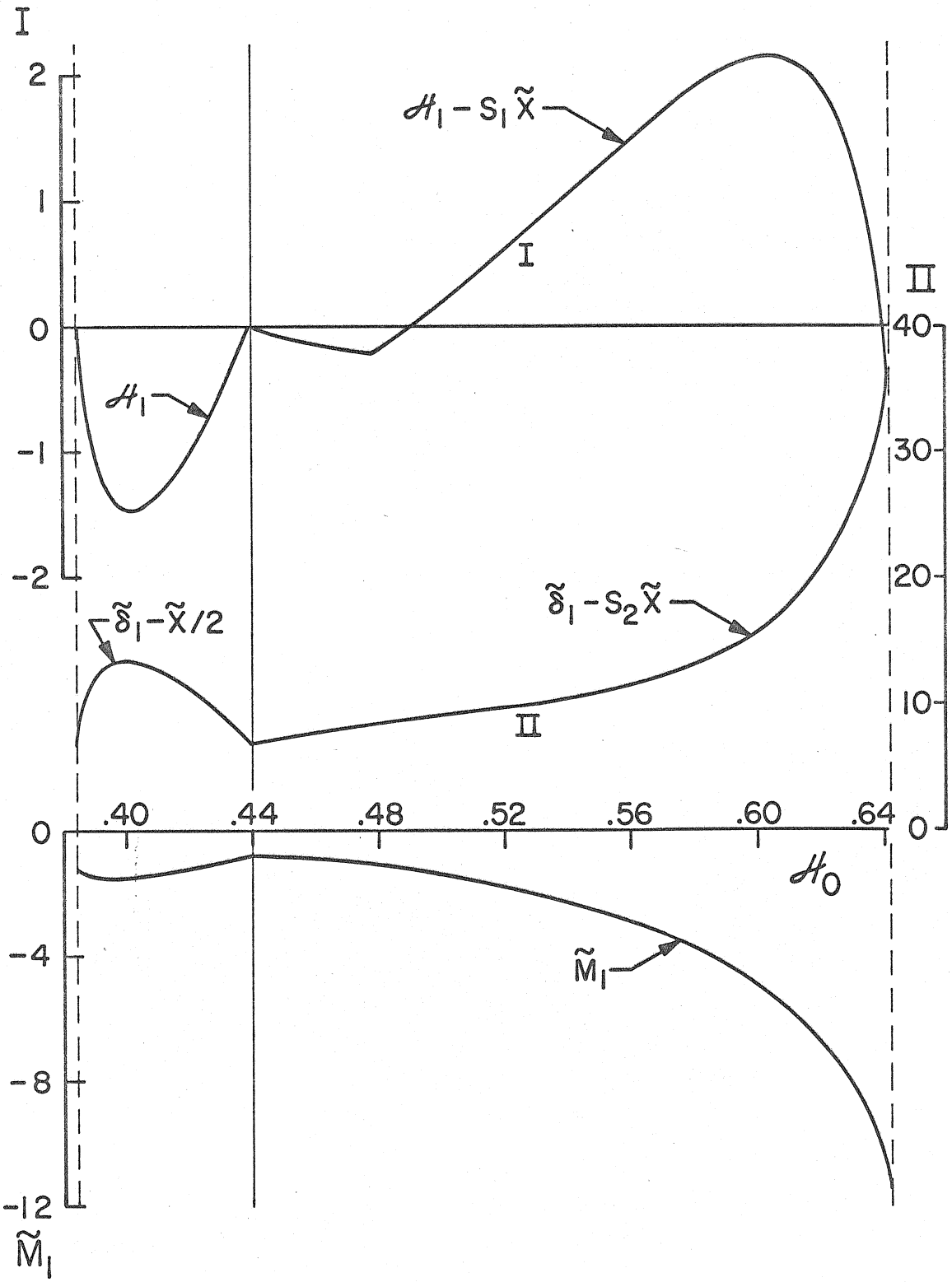

FIG. 17 FIRST ORDER FUNCTIONS OF $\mathcal{H}_0$ FOR $\alpha = 0.85$

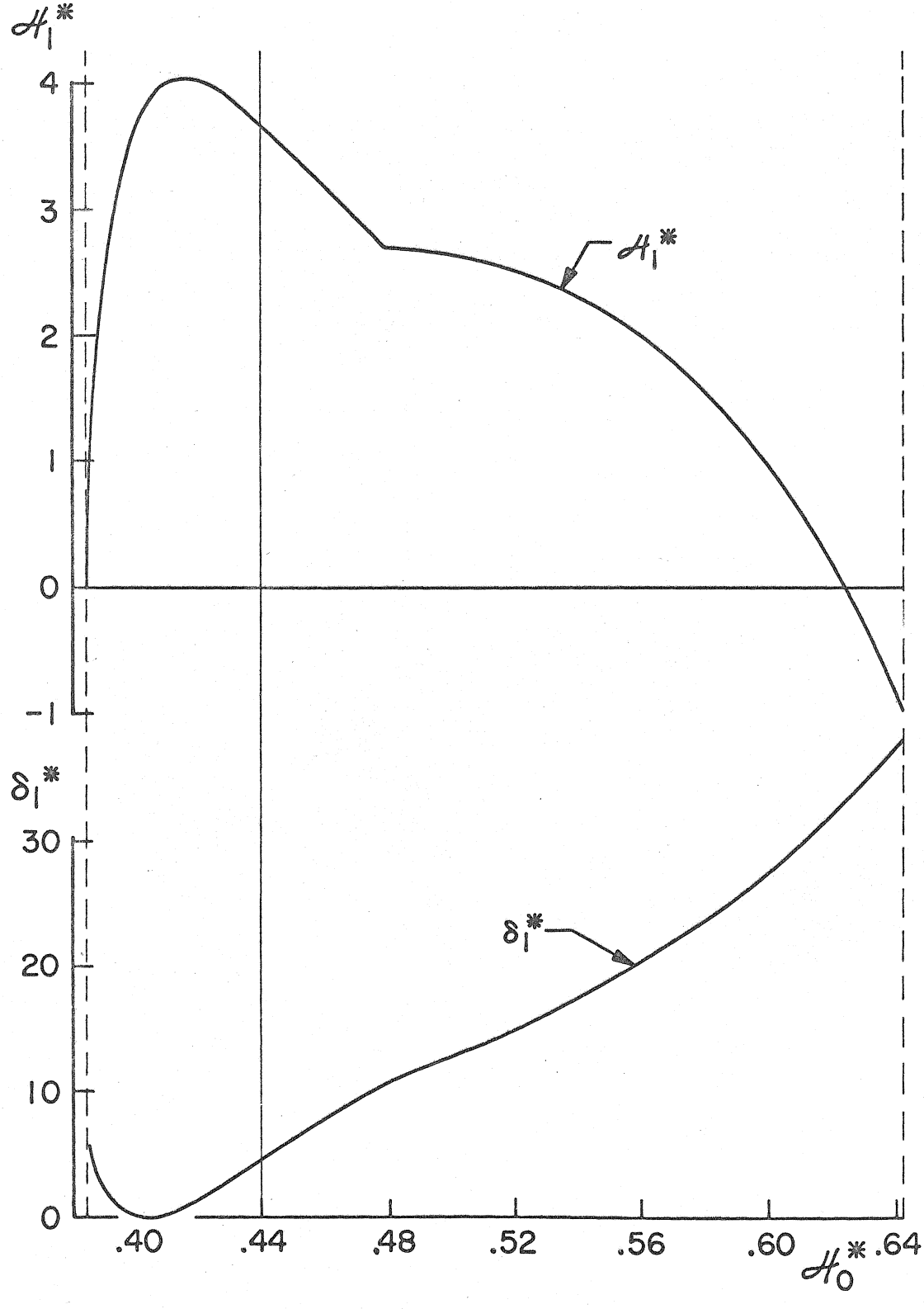

FIG. 18 FIRST ORDER FUNCTIONS OF $\mathcal{H}_0^*$ FOR $\alpha = 0.85$

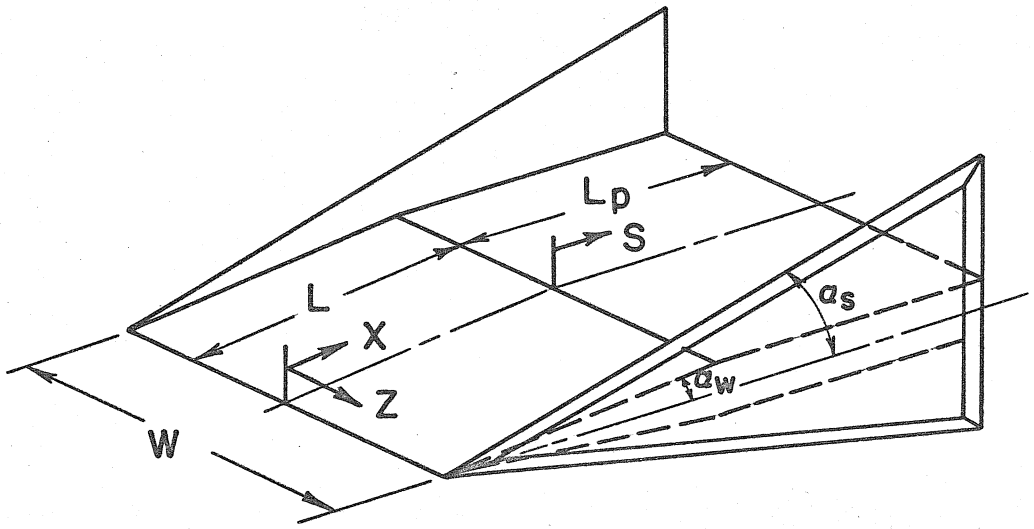

$L = 4.173"$ $\alpha_w = 5°$

$L_p = 4.006"$ $\alpha_s = 14°$

$W = 5.000"$

FIG. 19 WIND TUNNEL MODEL S-1

Model S-1
℄ Static Pressure Orifices

X	S
2.674"	- 1.498"
3.420	- 0.752
3.663	- 0.509
3.851	- 0.321
4.013	- 0.160
4.089	- 0.084
4.131	- 0.042
4.153	- 0.020
	0.023
	0.038
	0.080
	0.161
	0.321
	0.501
	0.649
	0.800
	1.000
	1.197
	1.400
	1.600
	1.802
	2.400
	3.000

Upper and Lower Surfaces

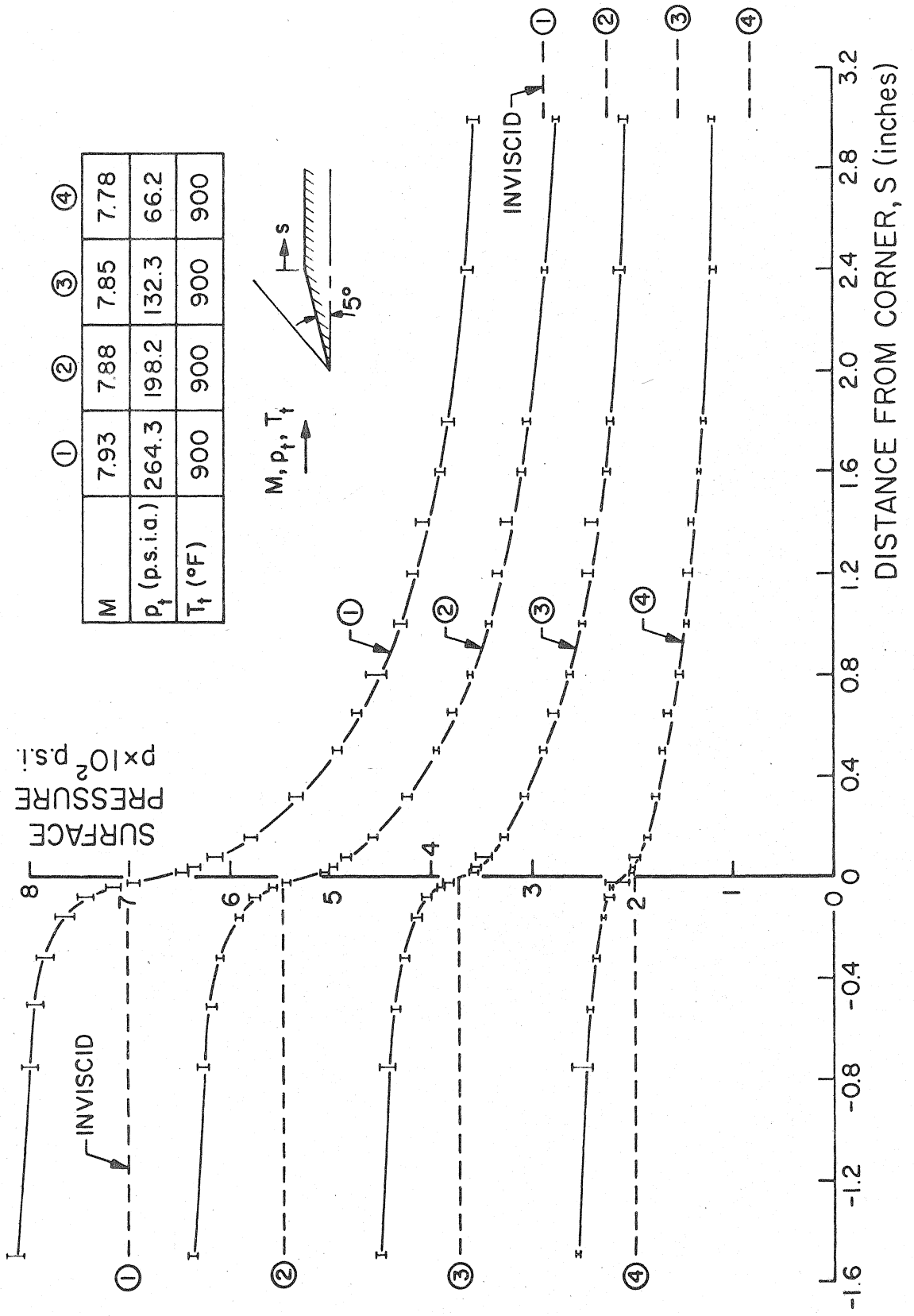

FIG. 20 EXPERIMENTAL SURFACE PRESSURE DISTRIBUTIONS

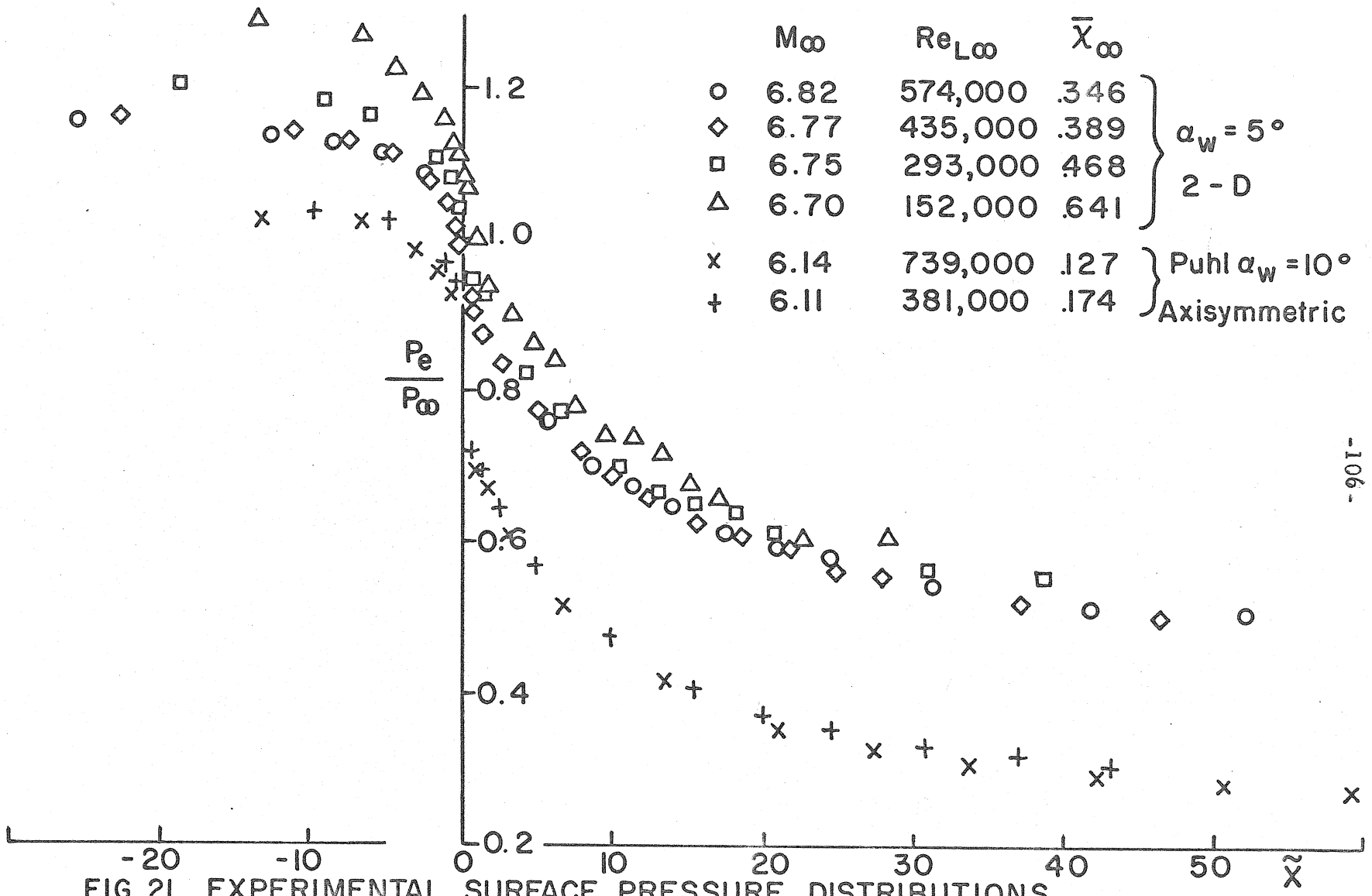

FIG. 21 EXPERIMENTAL SURFACE PRESSURE DISTRIBUTIONS

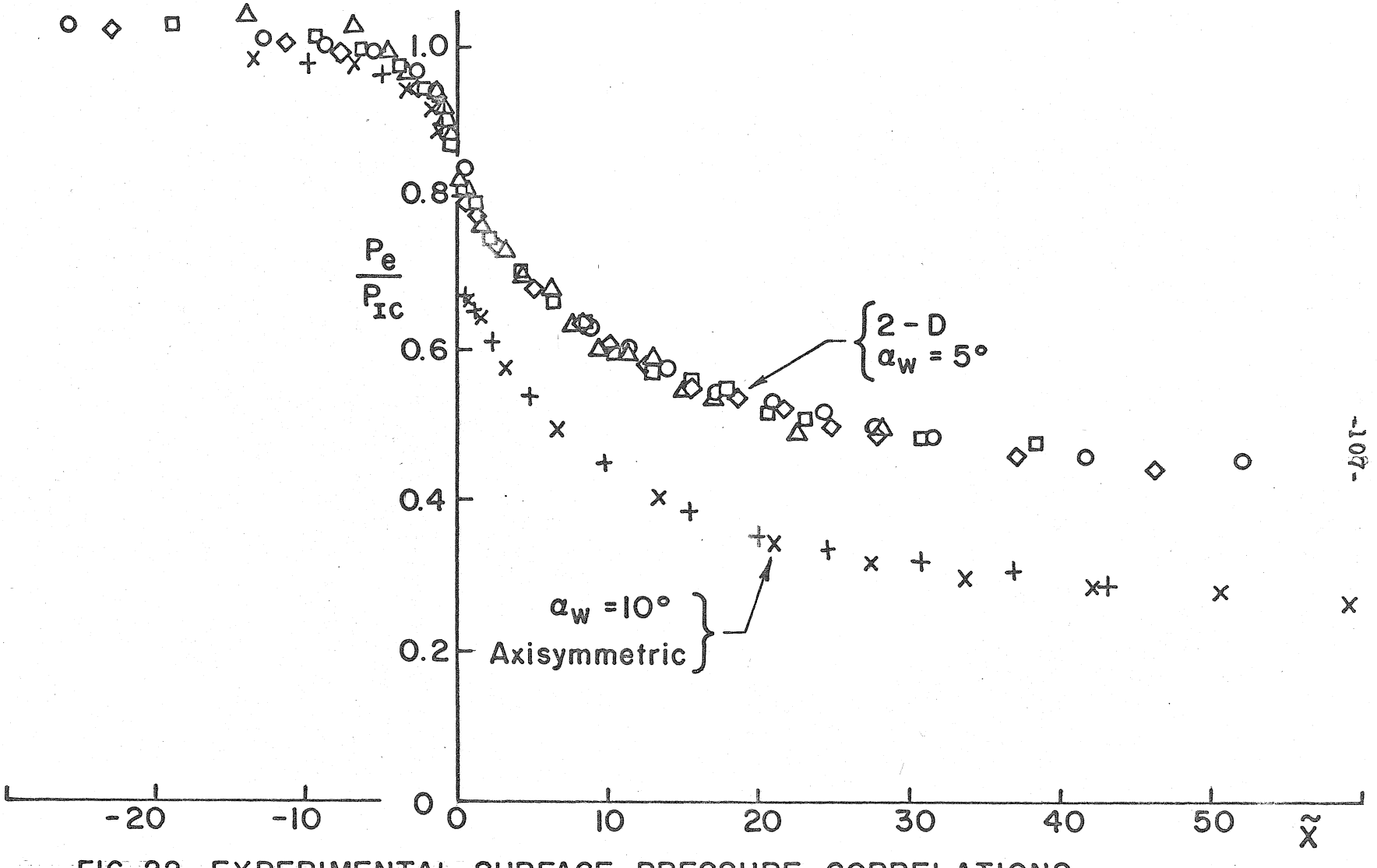

FIG. 22 EXPERIMENTAL SURFACE PRESSURE CORRELATIONS

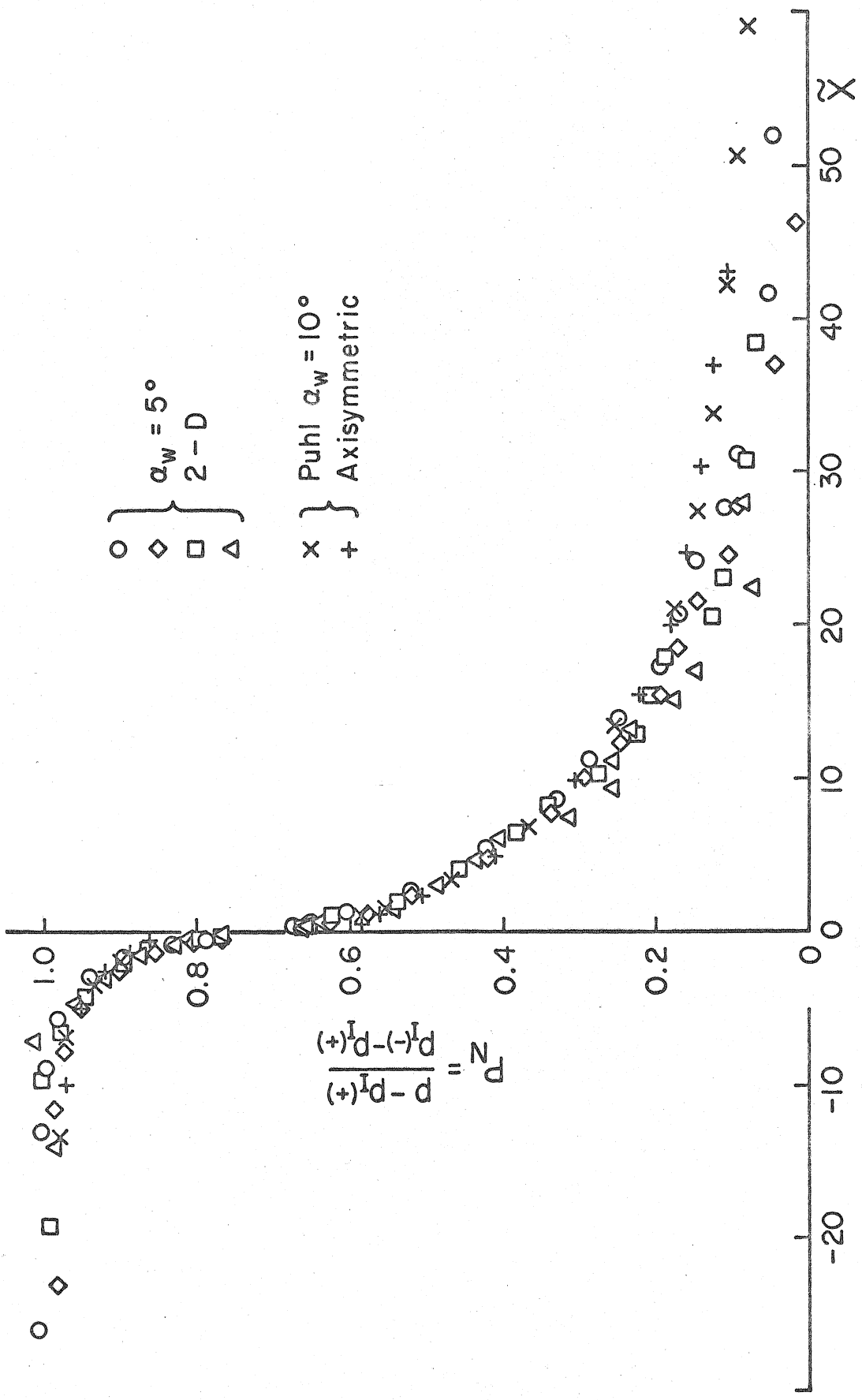

FIG. 23 EXPERIMENTAL SURFACE PRESSURE CORRELATION

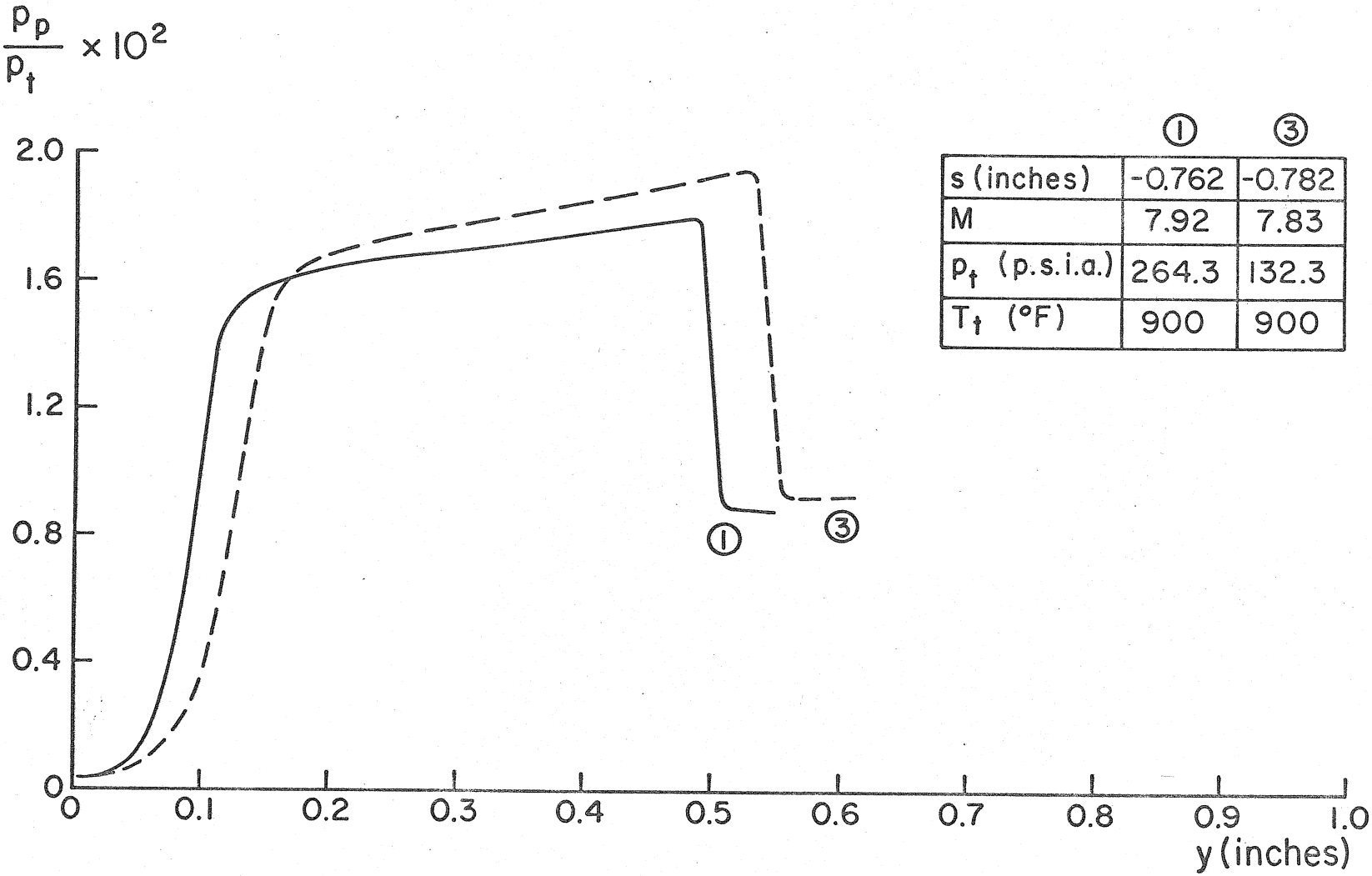

	①	③
s (inches)	-0.762	-0.782
M	7.92	7.83
p_t (p.s.i.a.)	264.3	132.3
T_t (°F)	900	900

FIG. 24 PITOT PRESSURE PROFILES UPSTREAM OF CORNER

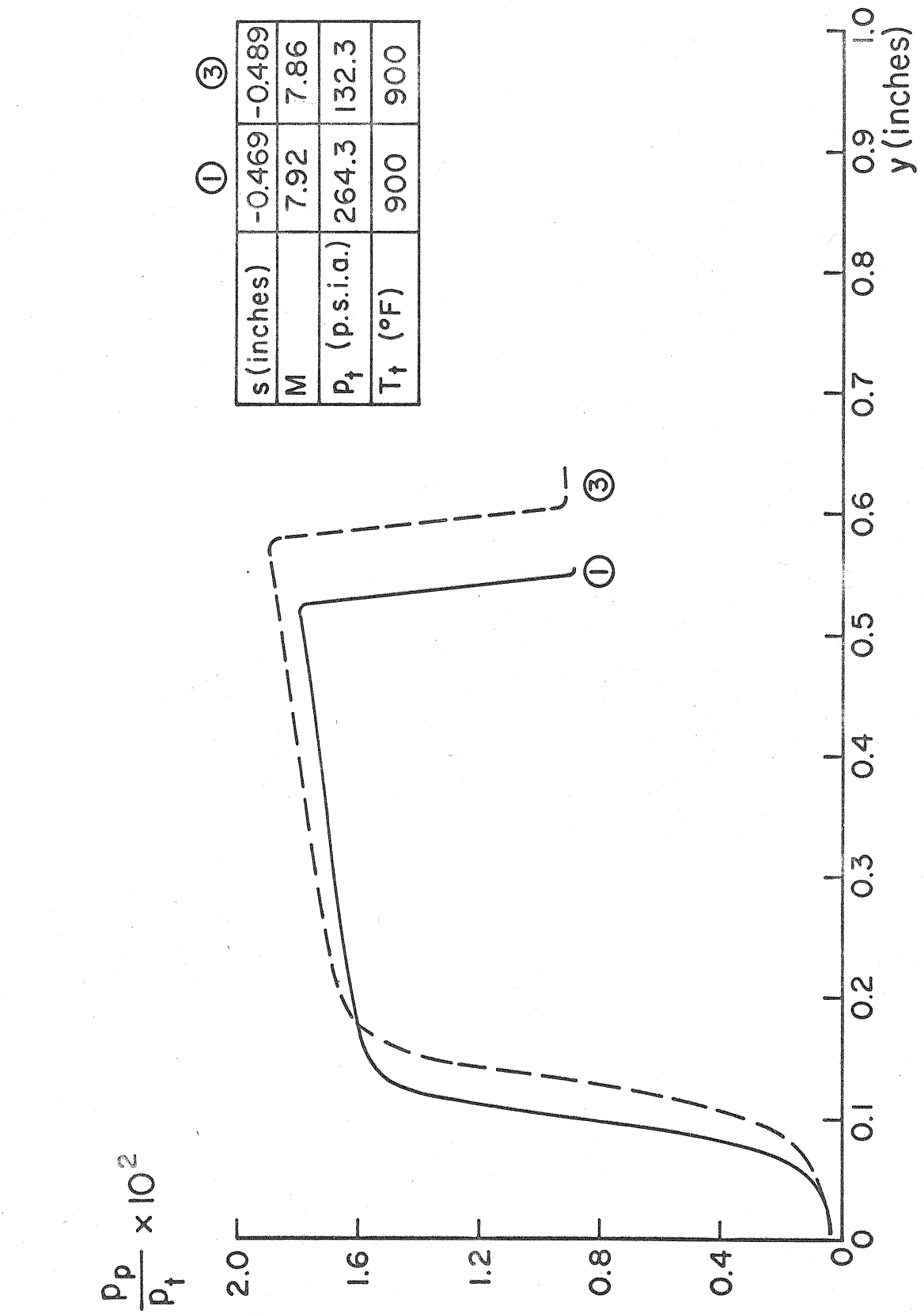

FIG. 25 PITOT PRESSURE PROFILES UPSTREAM OF CORNER

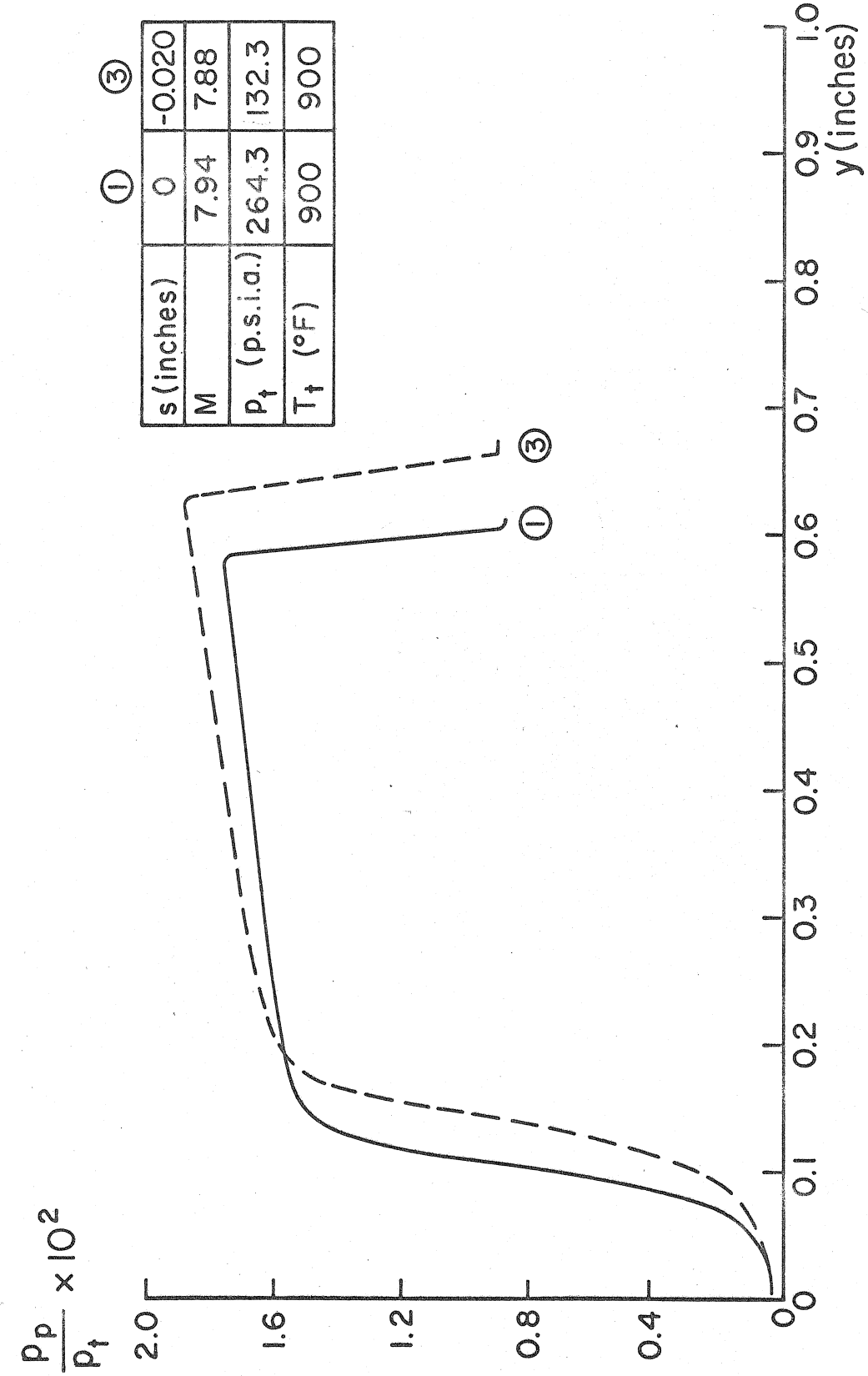

FIG. 26 PITOT PRESSURE PROFILES UPSTREAM OF CORNER

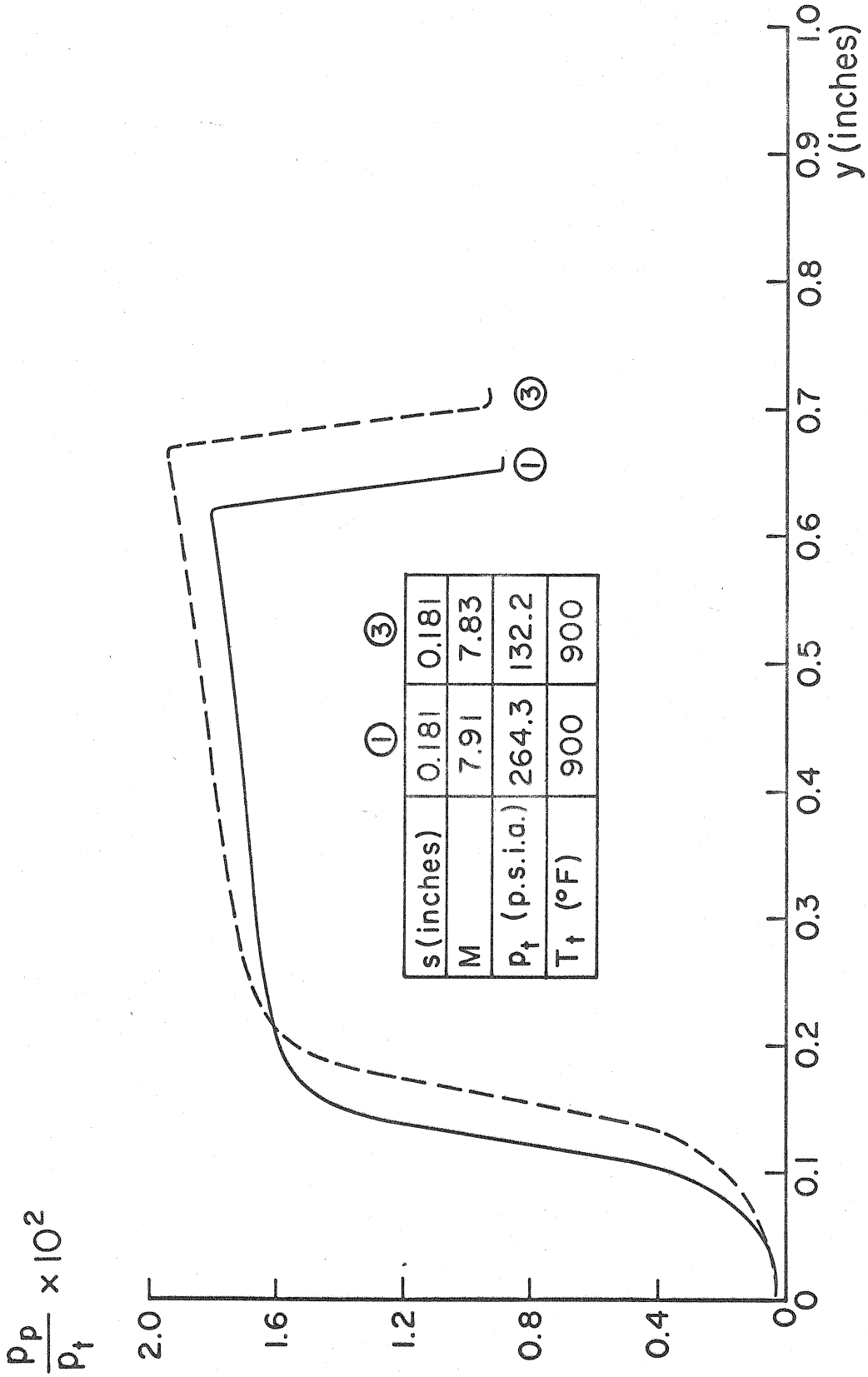

FIG. 27 PITOT PRESSURE PROFILES DOWNSTREAM OF CORNER

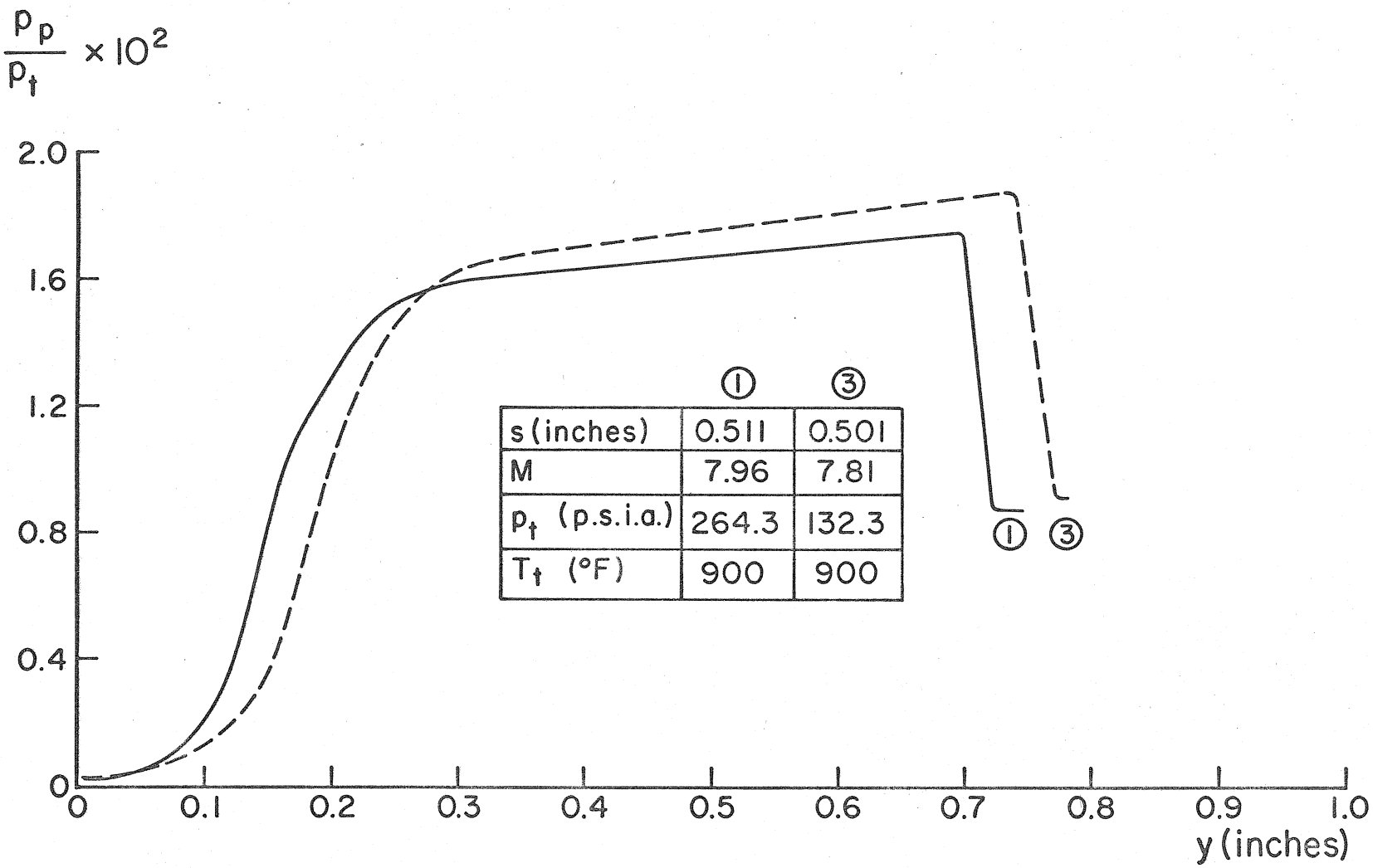

FIG. 28 PITOT PRESSURE PROFILES DOWNSTREAM OF CORNER

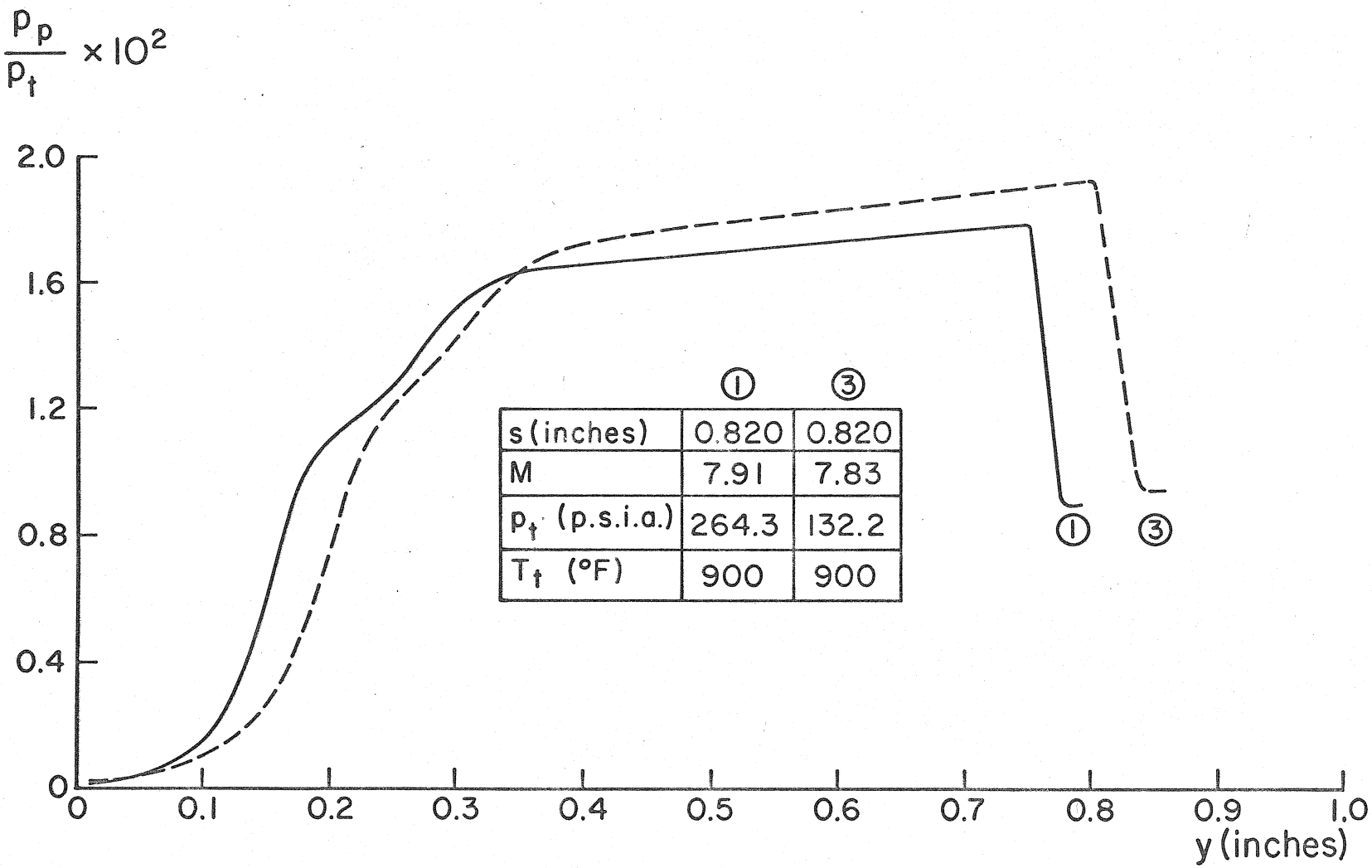

FIG. 29 PITOT PRESSURE PROFILES DOWNSTREAM OF CORNER

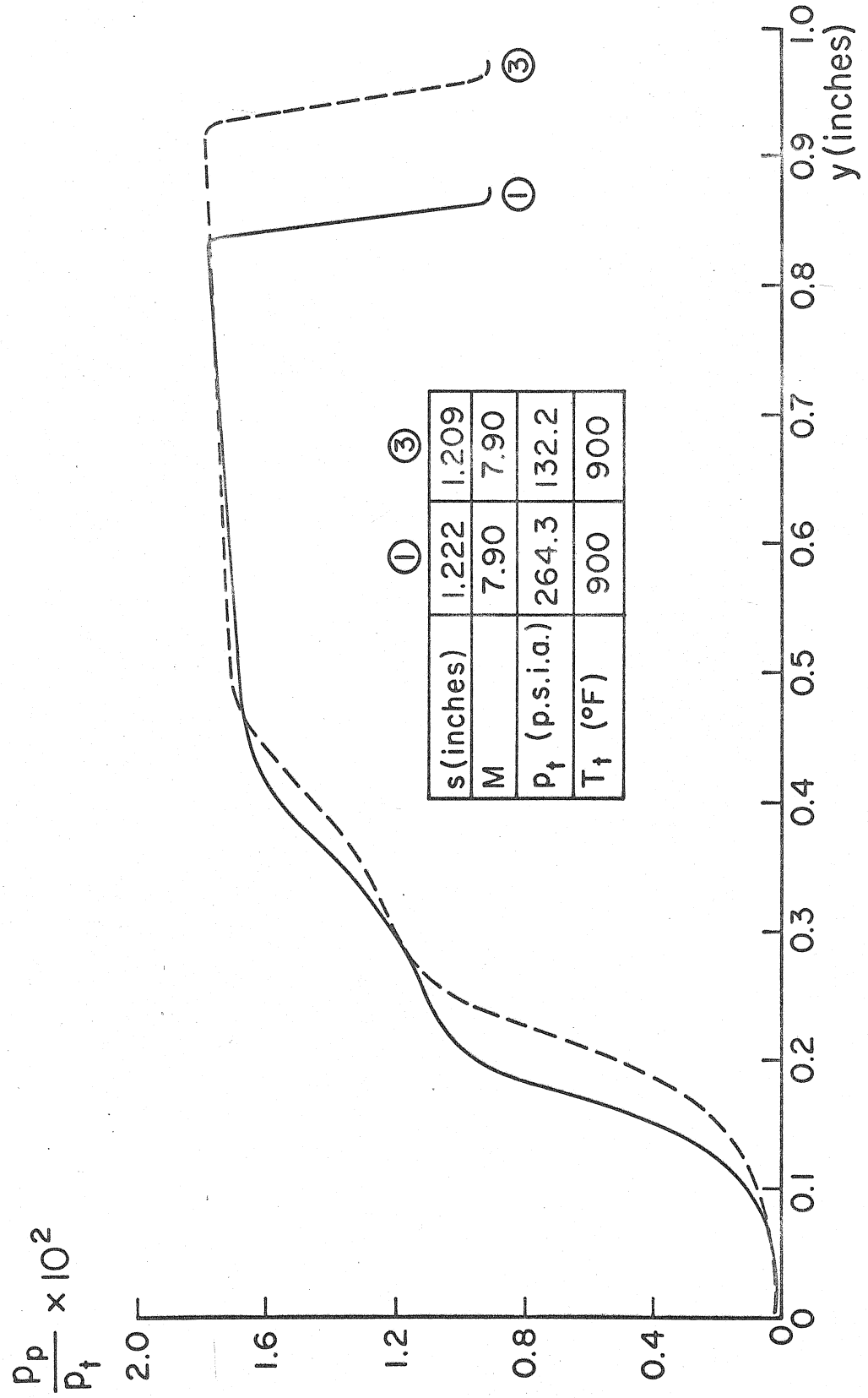

FIG. 30 PITOT PRESSURE PROFILES DOWNSTREAM OF CORNER

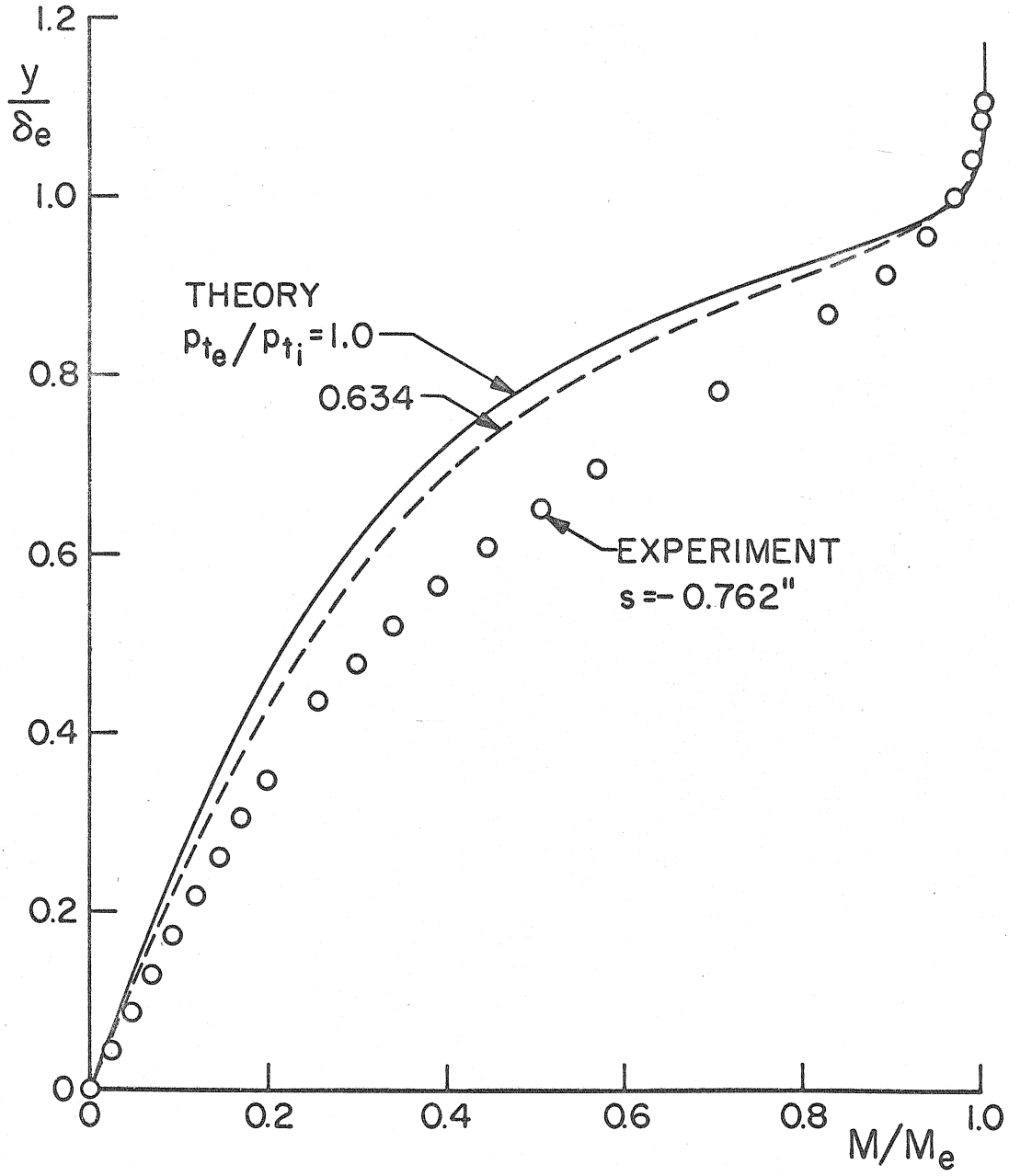

FIG. 31 EFFECT OF REDUCTION OF EDGE TOTAL PRESSURE

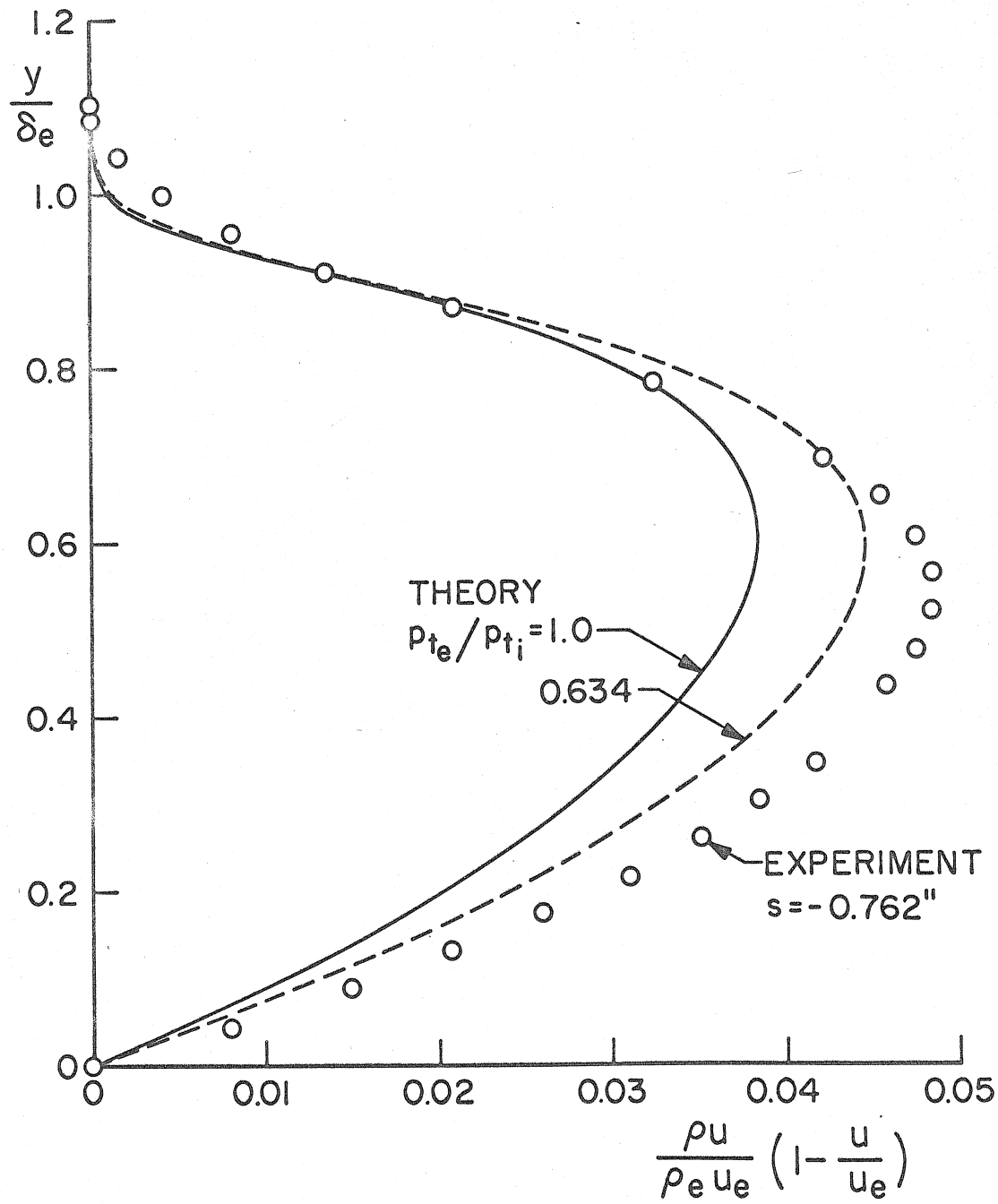

FIG. 32 EFFECT OF REDUCTION OF EDGE TOTAL PRESSURE

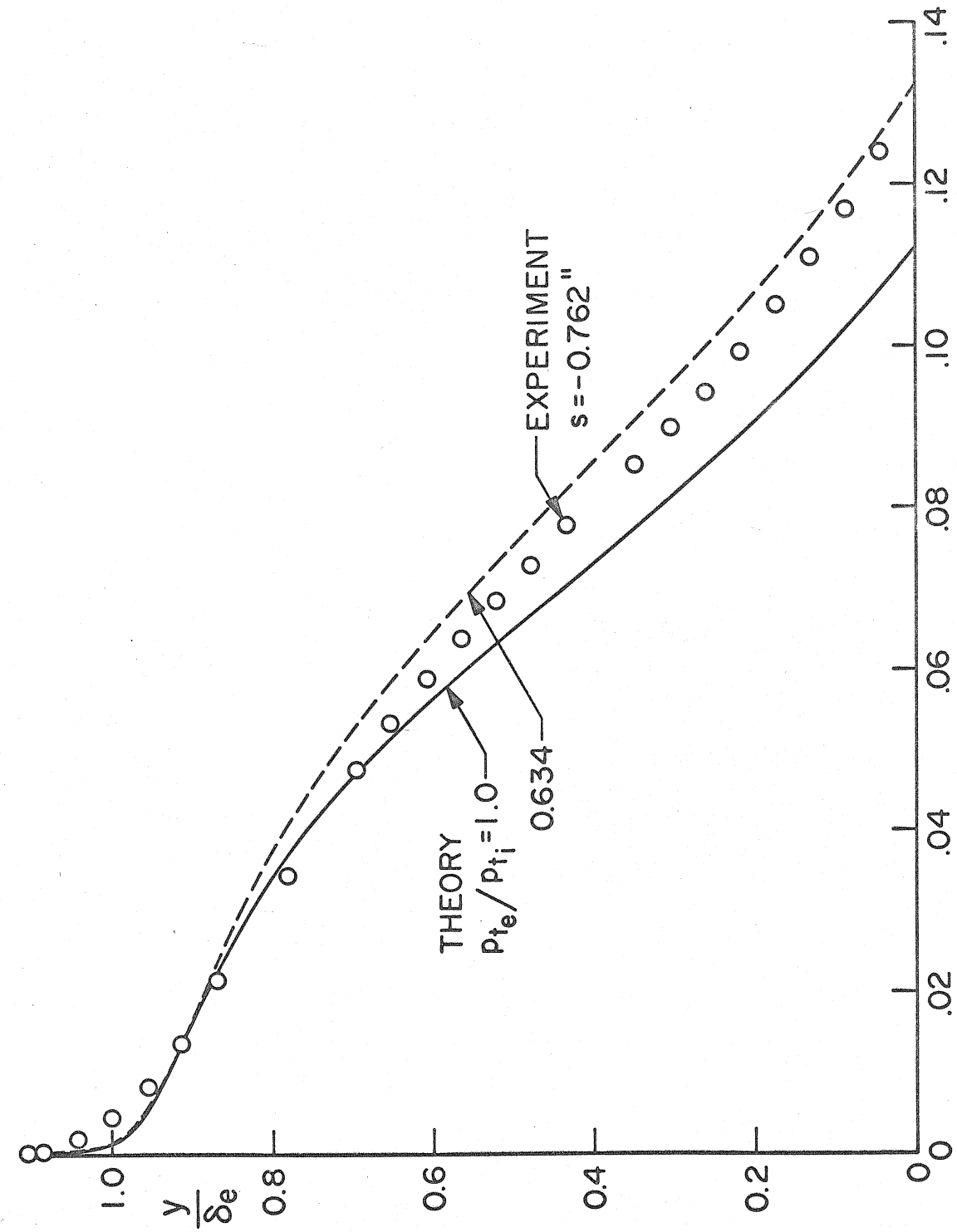

FIG. 33 EFFECT OF REDUCTION OF EDGE TOTAL PRESSURE

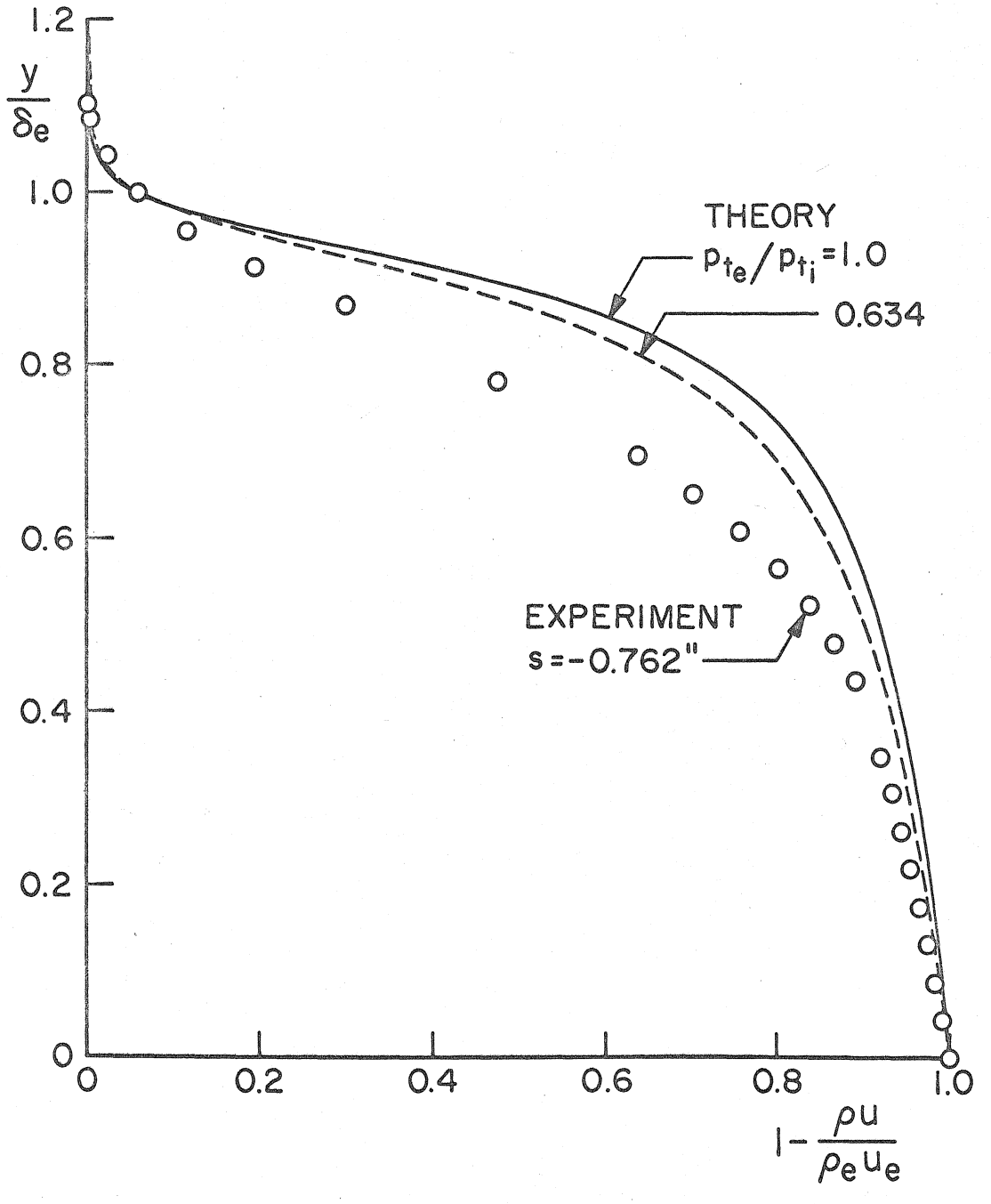

FIG. 34 EFFECT OF REDUCTION OF EDGE TOTAL PRESSURE

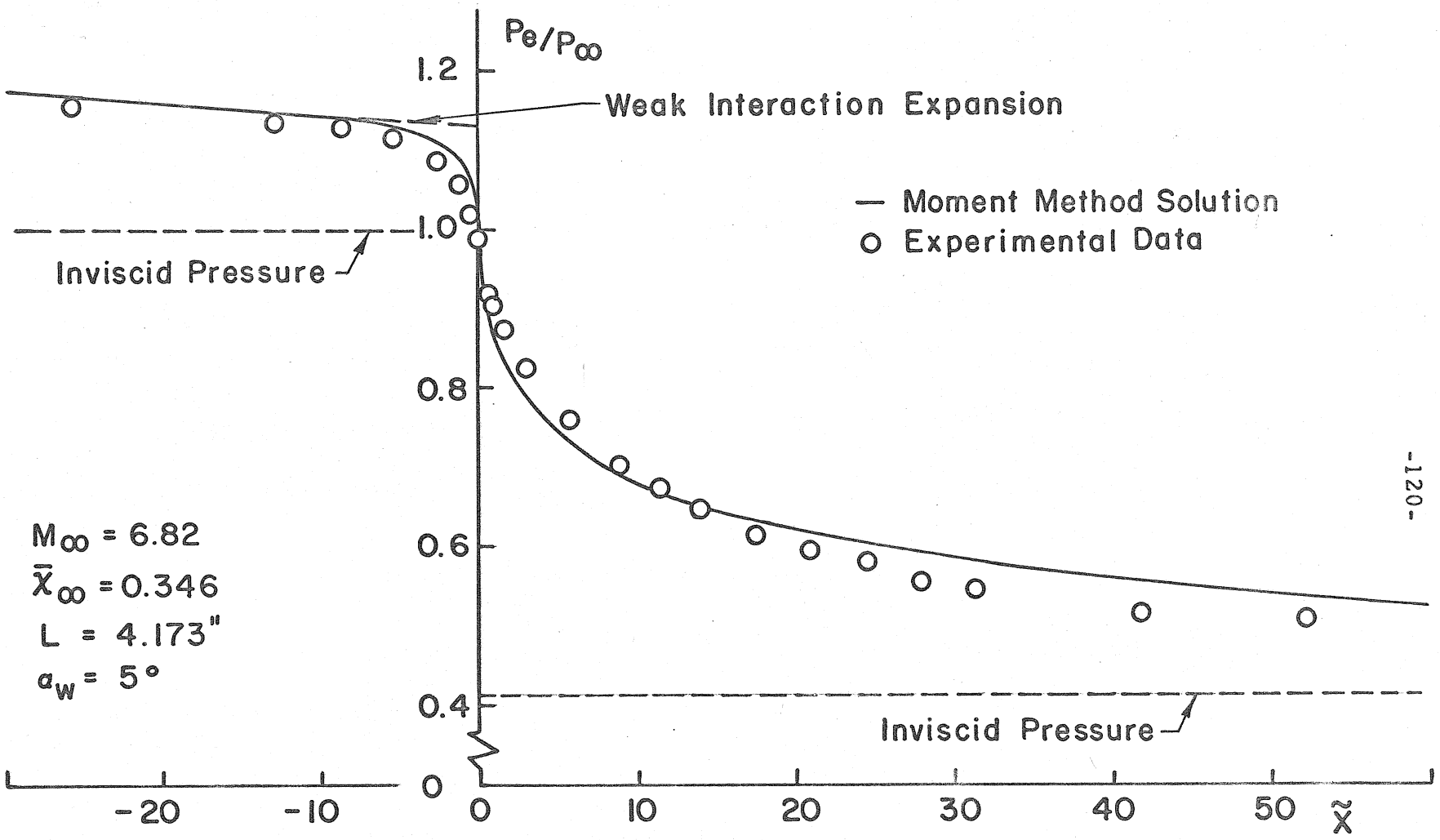

FIG. 35 EXPERIMENTAL AND THEORETICAL SURFACE PRESSURE DISTRIBUTIONS

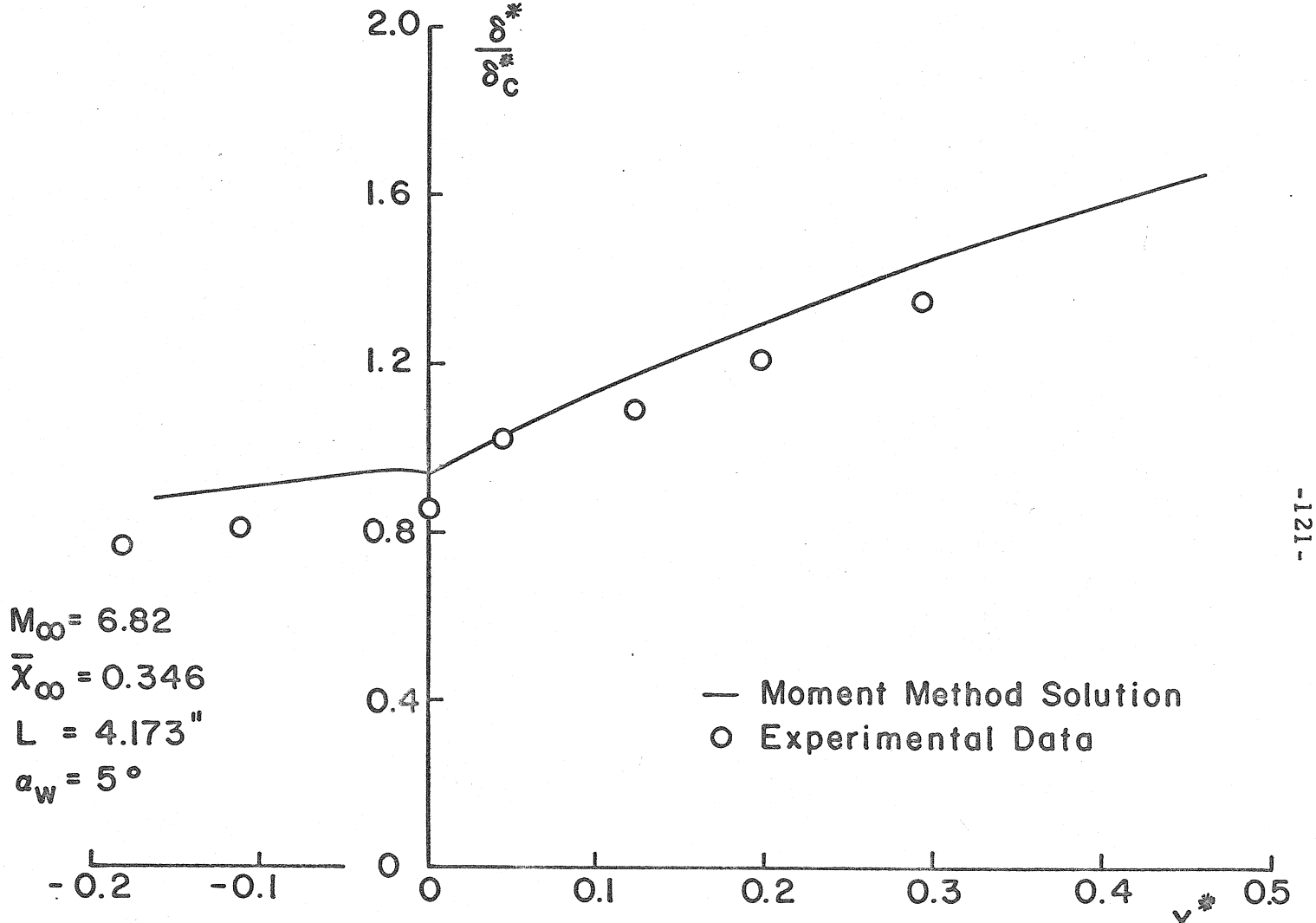

FIG. 36 EXPERIMENTAL AND THEORETICAL DISPLACEMENT THICKNESS DISTRIBUTION

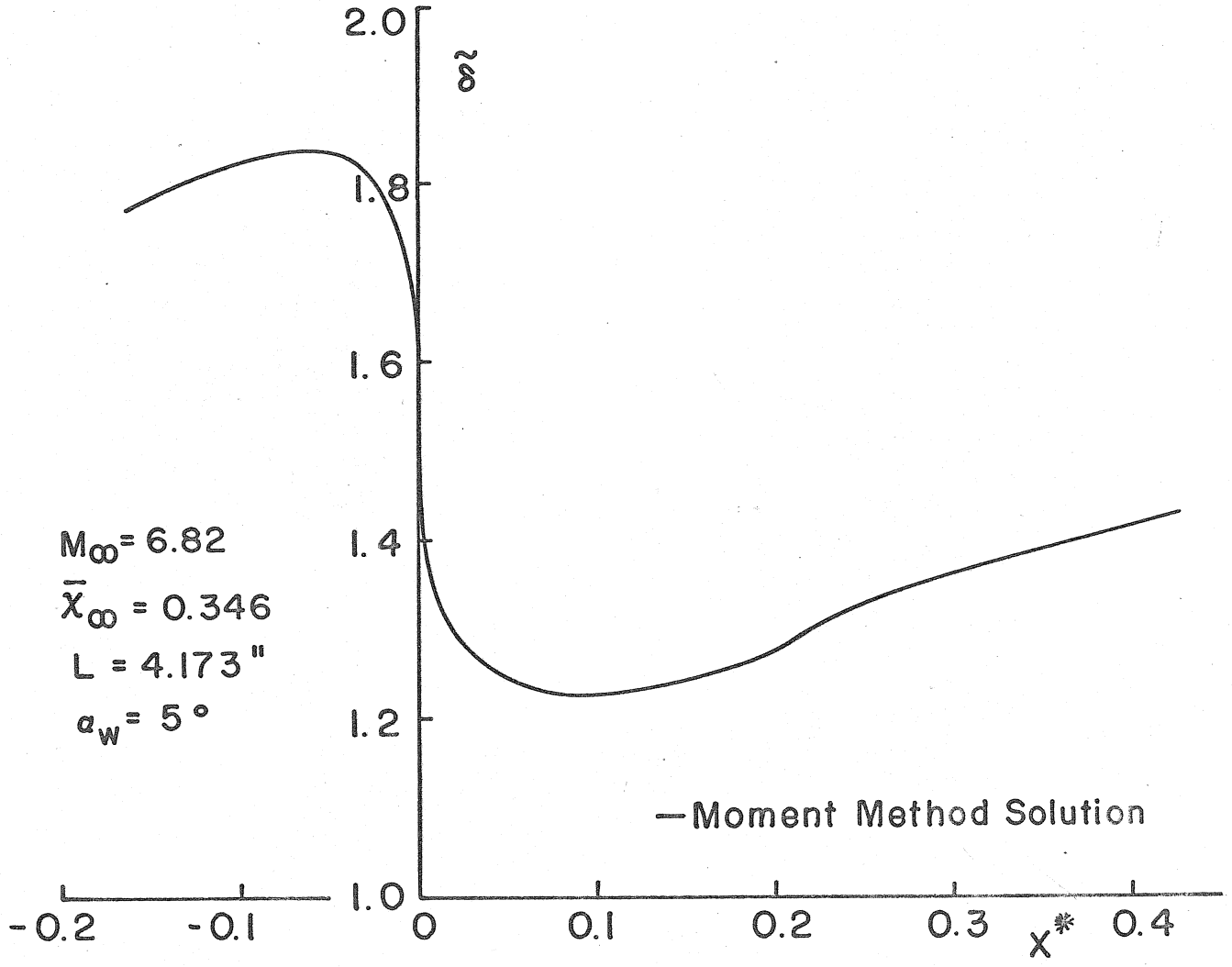

FIG. 37 THEORETICAL INCOMPRESSIBLE DISPLACEMENT THICKNESS DISTRIBUTION

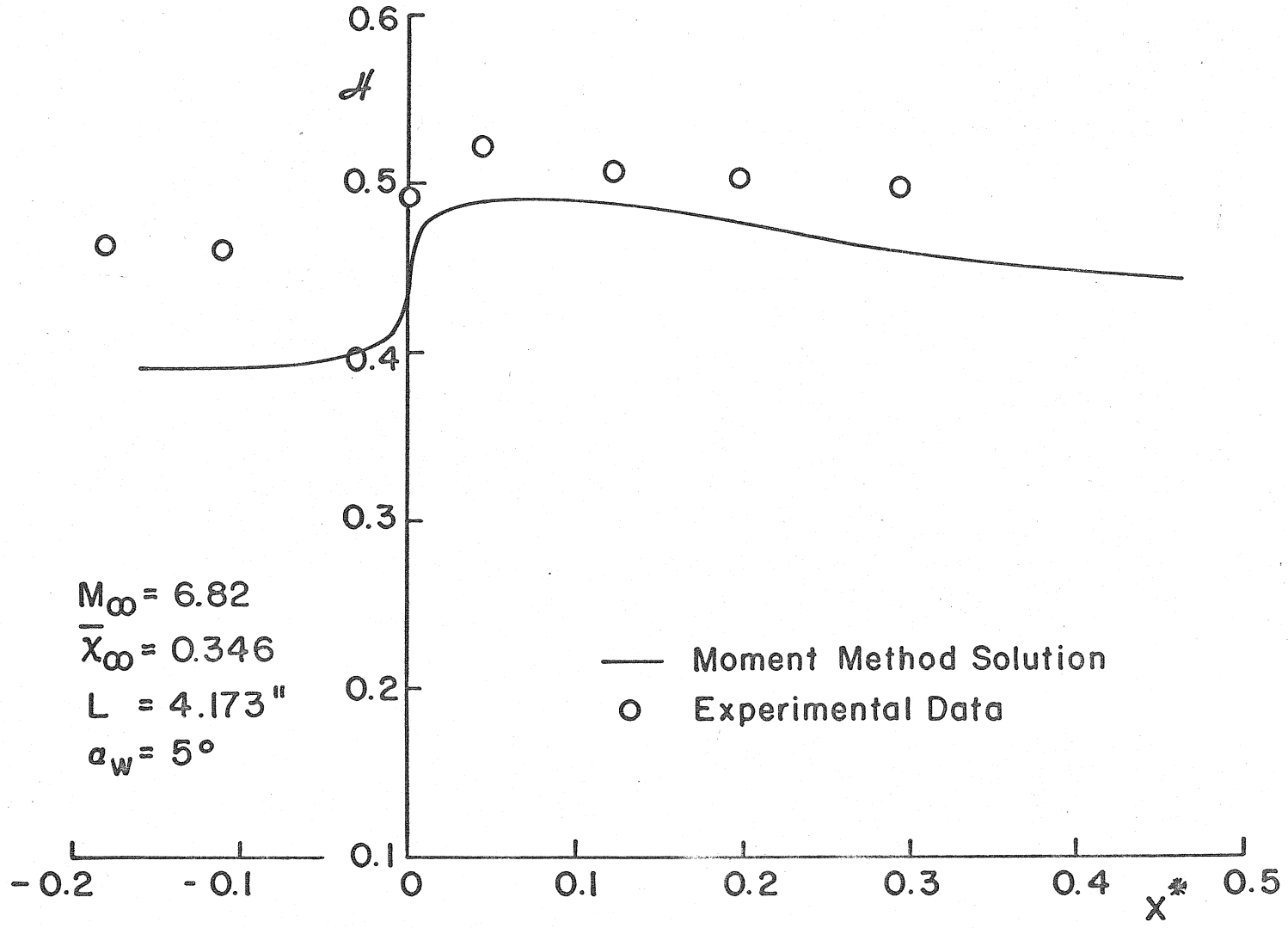

FIG. 38 EXPERIMENTAL AND THEORETICAL $\mathcal{H}$ DISTRIBUTIONS

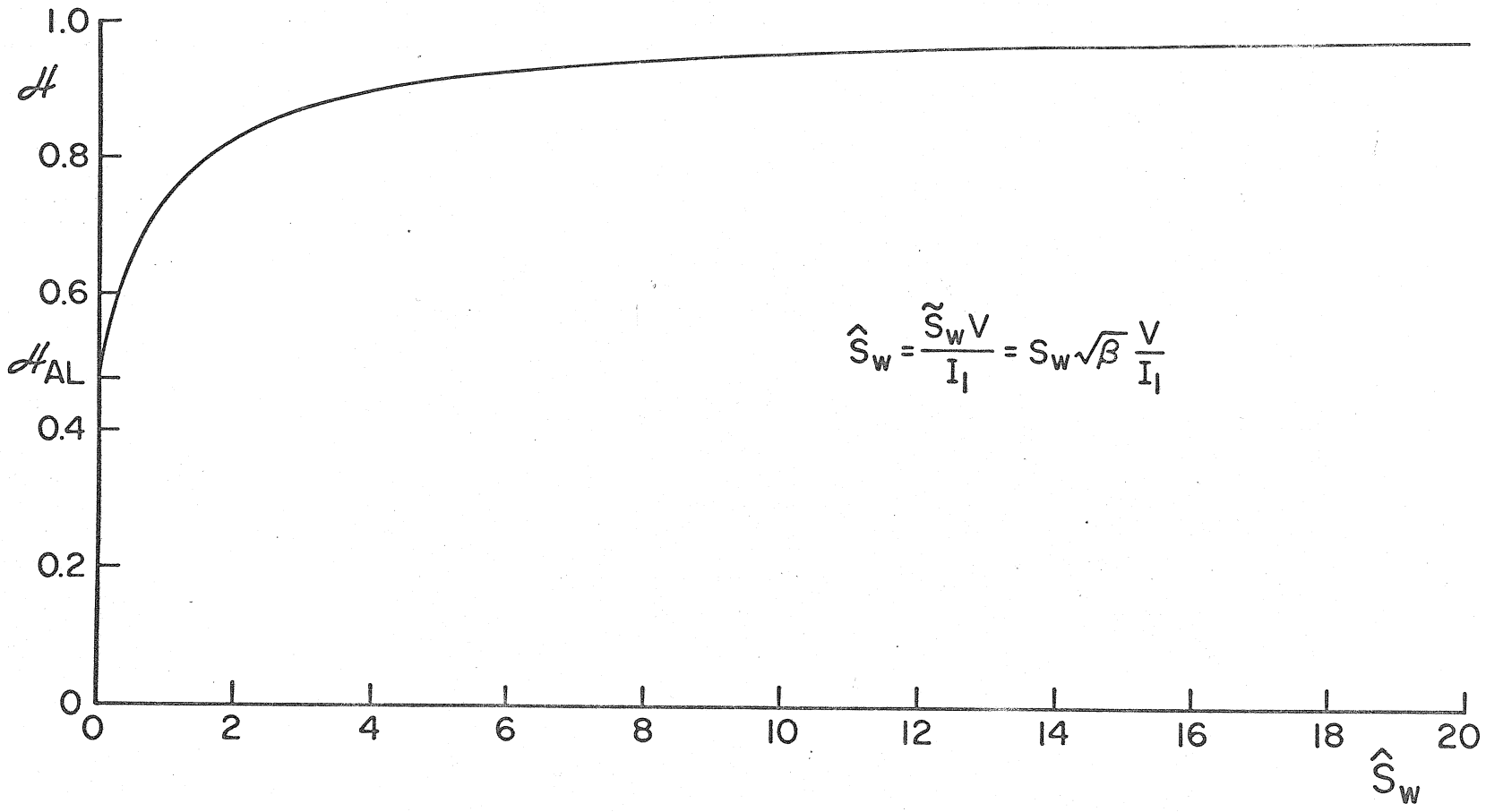

FIG. A.I EXTENSION OF $\mathcal{H}$ BEYOND THE ADIABATIC LIMIT

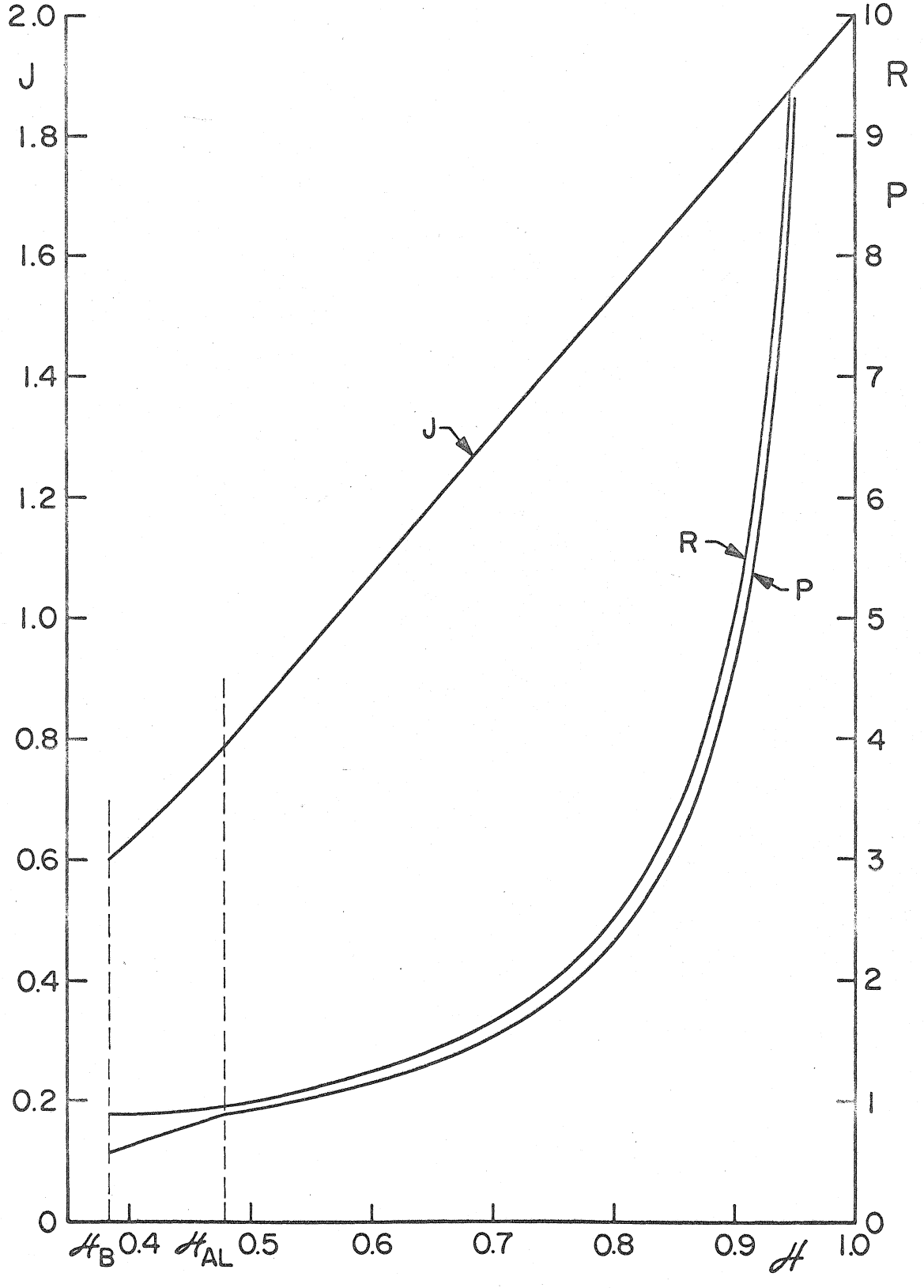

FIG. A.2 EXTENSION OF PROFILE FUNCTIONS OF $\mathcal{H}$

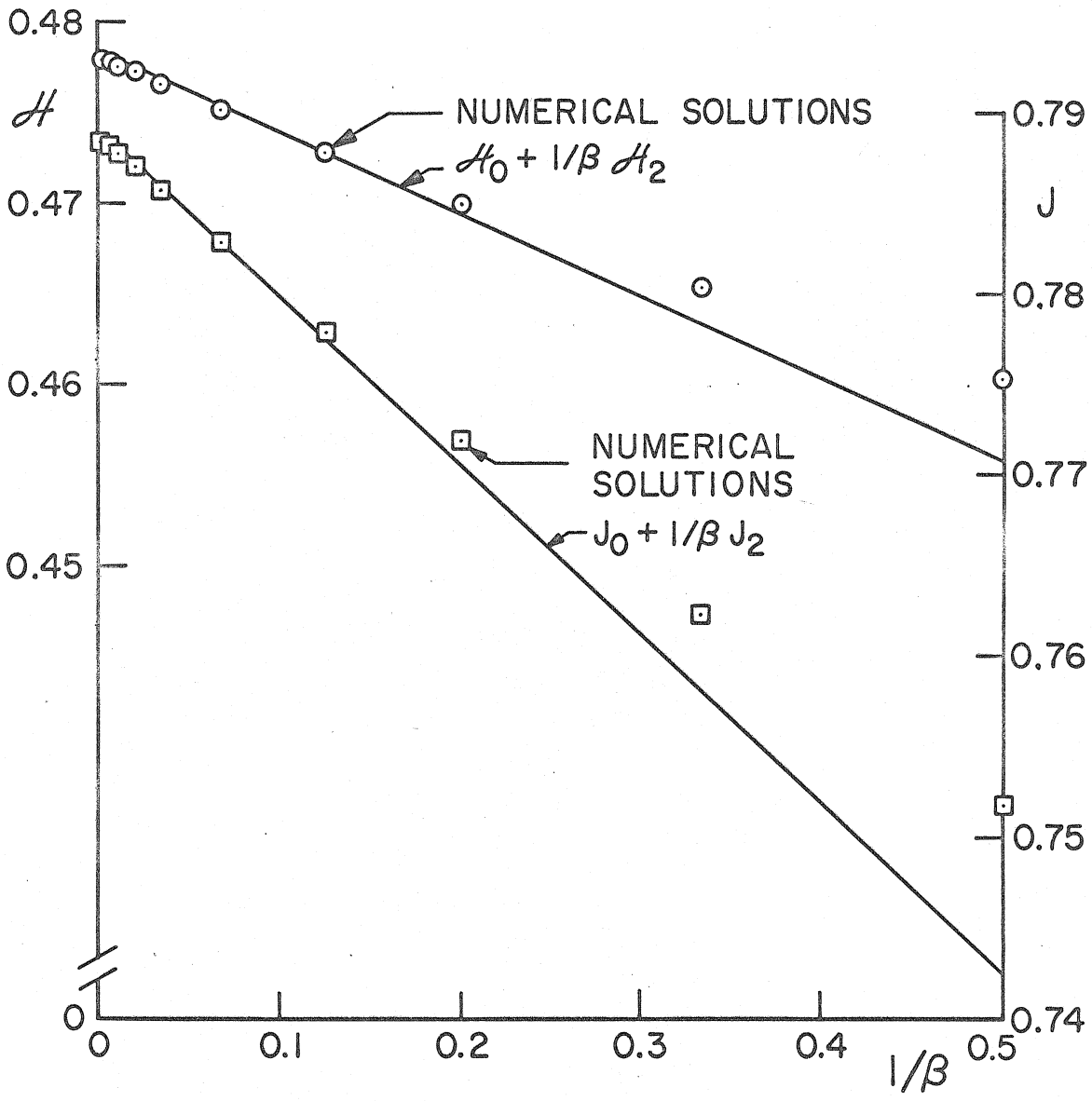

FIG. A.3 LIMITING SOLUTIONS OF ADIABATIC EQUATIONS

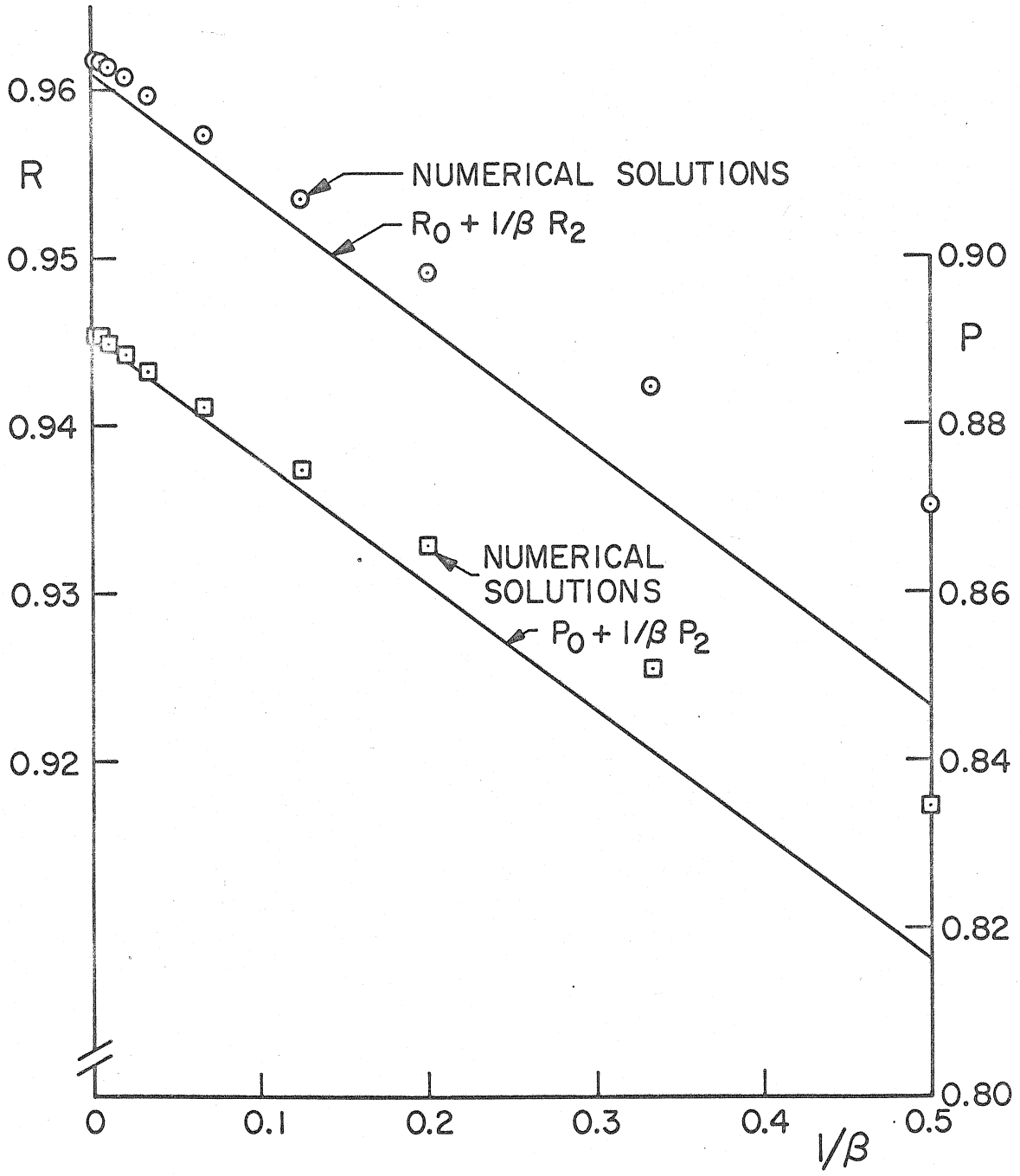

FIG. A.4 LIMITING SOLUTIONS OF ADIABATIC EQUATIONS